


RNI - No. MAHENG/2017/74063
VOLUME 2 (Issue 2) January - June 2019

ISSN No. 2581-5911
BI-ANNUAL SUBSCRIPTION : Rs. 2000/-

G P GLOBALIZE RESEARCH JOURNAL OF CHEMISTRY

**Abstracted in Chemical Abstracts (CAS), USA
International Scientific Indexing (ISI)
Impact Factor 0.883 (2018)**

The background of the cover is a complex, abstract design. It features a grid of squares in various shades of blue and cyan. Overlaid on this grid are several glowing, curved lines that create a sense of depth and movement, resembling a molecular structure or a data visualization. The overall aesthetic is clean, modern, and scientific.

RNI No. MAHENG/2017/74063

ISSN (Print) No. 2581-5911

Volume 2 Issue 2 ❖ January – June 2019

G P GLOBALIZE RESEARCH JOURNAL OF CHEMISTRY

**Abstracted in Chemical Abstracts (CAS), USA
International Scientific Indexing (ISI) Impact Factor 0.883 (2018)**

Supported by **ASSOCIATION OF CHEMISTRY TEACHERS**, the National Registered
Organisation of Chemistry Educators of India
Registration No. Maharashtra Government, Mumbai, 922, 2010 G.B.B.S.D. dated 08.04.2010.
Website: www.associationofchemistryteachers.org



GAURANG PUBLISHING GLOBALIZE PRIVATE LIMITED, MUMBAI

CIN No. U22130MH2016PTC287238

UAN - MH19D0008178

Published by:

Gaurang Publishing Globalize Private Limited, Mumbai

1, Plot 72, Pandit M.M.M. Marg, Tardeo, Mumbai 400 034.

Email: gpglobalize@gmail.com

Tel: +91 9969392245

CIN No. U22130MH2016PTC287238

ISSN (Print) No: 2581-5911

Disclaimer: Please be informed that the author and the published have put in their best efforts in producing this book. Every care has been taken to ensure the accuracy of the contents. However, we make no warranties for the same and therefore shall not be responsible or liable for any loss or any commercial damages accruing thereof. Neither the publisher nor the author is engaged in providing services of any professional nature and shall therefore not be responsible for any incidental, consequential, special or any other damages. Please do consult a professional where appropriate.

All rights reserved. No part of this book may be reproduced in any form including photocopying, microfilms, photoprints, storage in any retrieval systems, transmission in any permanent or temporary form, without the prior written consent of the publisher.

GP GLOBALIZE RESEARCH JOURNAL OF CHEMISTRY

An International Peer Reviewed Journal of Chemistry

RNI No: MAHENG/2017/74063
ISI Impact Factor: 0.883 (2018)

ISSN (Print) No: 2581-5911

Editor-in-Chief

Dr. D.V. Prabhu

Adjunct Professor and Former Head,
Department of Chemistry, Wilson College, Mumbai - 400 007, India
E-mail : dvprabhu48@gmail.com
Contact: +91 9870 22 68 99

Consulting Editors

Prof. Dr. S.M. Khopkar

Professor Emeritus
Department of Chemistry,
IIT-Bombay, Mumbai - 400 076, India
Email: drsmkhopkar@gmail.com

Prof. Dr. Tulsi Mukherjee

Former Group Director, Chemistry Group,
BARC, Mumbai.
Professor, Homi Bhabha National Institute,
BARC, Mumbai, India
Email: tulsi.mukherjee@gmail.com

Prof. Dr. Irena Kostova

Department of Chemistry,
Faculty of Pharmacy, Medical University,
Sofia, Bulgaria
E-mail : irenakostova@yahoo.com

Publishing Co-ordinator

Mr. Rajan Pendurkar

Gaurang Publishing Globalize Private Limited, Mumbai.
Email: gpglobalize@gmail.com
Contact: +91 9969 392 245

Printed and Published by Gaurang Rajan Pendurkar on behalf of Gaurang Publishing Globalize Private Limited and printed at NIL CREATION, Shop No. 7, 35/55, Bandu Gokhale Path, Mughat Cross Lane, Jivanji Maharaj Chawl (Shree Swami Samarth Nagar), Girgaon, Mumbai 400004 and published at Gaurang Publishing Globalize Private Limited 1, Plot 72, P M M M Marg, Tardeo, Mumbai-400034.
Editor-in-Chief Dr. D.V. Prabhu.



Editorial Board

1. Dr. S.K. Aggarwal
Associate Director, Radiochemistry and Isotope Group,
BARC, Mumbai, India
2. Prof. Ram K. Agarwal
Editor-in-Chief, Asian Journal of Chemistry,
Sahibabad, Ghaziabad, India
3. Prof. Amani S. Awaad
Department of Chemistry,
King Saud University, Riyadh, Saudi Arabia
4. Prof. Sultan T. Abuorabi
Department of Chemistry,
Yarmouk University, Jordan
Secretary General, Association of Arab Universities, Jubeyha, Amman, Jordan
5. Dr. Mahmood M. Barbooti
Department of Applied Sciences,
University of Technology, Baghdad, Iraq
6. Prof. Dr. Satish A. Bhalerao
Former Head, Department of Botany and Environment, Wilson College, Mumbai, India
7. Prof. Kamala N. Bhat
Department of Chemistry,
Alabama A&M University, Alabama, USA
8. Prof. C.P. Bhasin
Department of Chemistry, Hem. North Gujarat University, Patan, Gujarat, India
9. Dr. Sheshanath V. Bhosale,
ARC Future Fellow, School of Applied Sciences, RMIT University, Melbourne, Australia
UGC Professor, Department of Chemistry, Goa University Goa, India
10. Prof. Zhigang Chen,
Director, Jiangsu Key Laboratory of Environment Functional Materials, School of Chemistry, Biology and Materials, Suzhou University of Science and Technology, Suzhou, Jiangsu, China
11. Dr. Prabodh Chobe
Former Senior General Manager-Development and Head, R&D Centre, BASF India Limited, Mumbai, India
12. Prof. Eva Chmiedewska
Department of Environmental Ecology, Faculty of Natural Sciences, Comenius University, Bratislava, Slovak Republic
13. Prof. Abdalla M. Darwish
School of STEM, Department of Physics, Dillard University, New Orleans, Louisiana, USA
14. Dr. Ajit Datar
Advisor, Shimadzu Analytical (India) Private Limited, Mumbai, India
15. Dr. Ravindra G. Deshmukh
Associate Dean, Faculty of Science, University of Mumbai, Mumbai,
Principal, Konkan Gyanapeeth Karjat College of Arts, Science and Commerce, Karjat, Raigad District, India.
16. Prof. K.R. Desai
Director, Department of Chemistry
Director, C.G. Bhakta Institute of Biotechnology,
Uka Tarsadia University, Surat, India
17. Dr. Shivani S. Dhage
Vice President, Aquara Labs., Mumbai, India



Editorial Board

- Former Deputy Director, CSIR National Environmental Engineering Research Institute, Mumbai, India
18. Prof. E.S. Dragan
Petruoni Institute of Macromolecular Chemistry, Aleea Grigore Voda, Iasi, Romania
19. Dr. Priy Brat Dwivedi
Faculty-Chemical Sciences, College of Engineering, National University of Science and Technology, Muscat, Oman
20. Dr Chandrakant Gadipelly
The Wolfson Department of Chemical Engineering, Technion-Israel Institute of Technology, Haifa, Israel
21. Prof. Shankar Lal Garg,
Director, World Research Journals Group, Patron, World Researchers Associations, Indore, India
22. Prof. Kallol K. Ghosh
Head, Department of Chemistry, Pandit Ravi Shankar Shukla University, Raipur, India
23. Dr. Pushpito Ghosh
K.V. Mariwala-J.B. Joshi Distinguished Professor, Institute of Chemical Technology, Mumbai, India
Former Director, CSIR Central Salt and Marine Chemical Research Institute, Bhavnagar, India
24. Prof. Falah H. Hussein
Professor of Physical Chemistry, College of Science, University of Babylon, Babylon, Iraq
25. Prof. Sudha Jain
Former Head, Department of Chemistry, University of Lucknow, Lucknow, India
26. Prof. Shehdeh Jodeh
Department of Chemistry, Najah National University, Nablus, Palestine
27. Prof. S.B. Jonnalagadda
Department of Chemistry, University of Kwazulu – Natal, Durban, South Africa
28. Dr. Hidemitsu Katsura
University of Tsukuba, Sakado, Japan, Universiti Kuala Lumpur IPROM, Kuala Lumpur, Malaysia
29. Prof. Olga Kovalchukova
Department of General Chemistry, People's Friendship University of Russia, Moscow, Russia
30. Dr. Sudhir Kapoor
Head, Nanochemistry Section, Radiation and Photochemistry Division, BARC, Mumbai, India
Professor, Homi Bhabha National Institute, BARC, Mumbai, India
31. Dr. Anna D. Kudryavtseva
P.N. Lebedev Physical Institute, Russian Academy of Sciences, Moscow, Russia
32. Prof. R.S. Lokhande
Head, Department of Chemistry
Director, University Research Cell, Jaipur National University, Jaipur, India
33. Prof. Mahendra Mahanti
Visiting Professor, School of Chemical



Editorial Board

- Sciences, NISER, Bhubaneswar, India
Retired Professor, Department of Chemistry,
North Eastern University, Shillong,
Meghalaya, India
34. Prof. Jyotsna Meshram
Head, Department of Organic Chemistry,
School of Chemical Sciences, North
Maharashtra University, Jalgaon, India
35. Dr. Seema Mishra
Director, SIES Indian Institute of
Environment, Navi Mumbai, India
36. Prof. Jose R. Mora
Universidad San Francisco de Quito, Ecuador
Venezuelan Institute for Science Research,
Centre of Chemistry, Caracas, Miranda,
Venezuela
37. Prof. Subhash C. Mojumdar
External Faculty, Trecin University of
A Dubcek, Serbia (SR), EU
38. Prof. Gurunath Mukherjee
Sir Rashbehary Ghosh Professor (Retired),
University of Calcutta, Kolkata, India
39. Dr. D.B. Naik
Radiation and Photochemistry Division,
BARC, Mumbai, India
40. Dr. Reji Nair
Staff Scientist,
The Scripps Research Institute La Jolla, CA,
USA.
41. Dr. Venkat Narayan
Anthara Technologies Consulting, Texas,
USA
Formerly Polymer Research Group,
De Puy Orthopaedics Inc., Johnson &
Johnson, Warsaw, IN, USA
42. Dr. R. Nagaraj
NASI Senior Scientist and J.C. Bose Fellow,
CSIR Centre for Cellular and Molecular
Biology, Hyderabad, India
43. Dr. Sunil S. Patil
Head, Department of Chemistry, CKT
College, Panvel, India
44. Dr. Harichandra A. Parbat
Department of Chemistry, Wilson College,
Mumbai, India
45. Prof. Sourav Pal
Director, IISER-Kolkata, Kolkata, India
Former Director, CSIR National Chemical
Laboratory, Pune, India
46. Dr. Pradnya J Prabhu
Principal, K.J. Somaiya College of Science
and Commerce, Mumbai, India
47. Prof. Surendra Prasad
School of Biological and Chemical
Sciences, University of South Pacific,
Suva, Fiji
48. Dr. G. Ramakrishnan
Director, SIES Institute of Chromatography
and Spectroscopy, Navi Mumbai, India
President, Chromatographic Society of India
49. Dr. A.V.R. Reddy
Former Head, Analytical Chemistry
Division, BARC, Mumbai, India
Professor, Homi Bhabha National Institute,
BARC, Mumbai, India
50. Prof. C. Suresh Reddy
Department of Chemistry, S.V. University,
Tirupati, India



Editorial Board

- | | |
|---|--|
| <p>51. Prof. Genserik Reniers
Department of Chemistry, University of Antwerpen, Antwerp, Belgium</p> <p>52. Prof. Anil Kumar Singh
Department of Chemistry, IIT-Bombay, Mumbai, India
Former Vice-Chancellor, University of Allahabad, Allahabad, India</p> <p>53. Prof. A.D. Sawant
Department of Chemistry, Institute of Science, Mumbai, India
Former Vice-Chancellor, University of Rajasthan, Jaipur, India</p> <p>54. Prof. M.S. Sadjadi,
Professor of Chemistry, Tehran Science and Research Branch, Islamic Azad University, Tehran, Iran</p> <p>55. Prof. Sri Juari Santosa
Department of Chemistry, Faculty of Mathematics and Natural Sciences, Gadjah Mada University, Yogyakarta, Indonesia</p> <p>56. Prof. Pradeep K. Sharma
Head, Department of Chemistry, J.N.V. University, Jodhpur, India</p> <p>57. Prof. R.K. Sharma
Coordinator, Green Chemistry Network Centre, Department of Chemistry, University of Delhi, Delhi, India</p> <p>58. Dr. S. Sivaram
INSA Senior Scientist, IISER – Pune
Former Director, CSIR National Chemical Laboratory, Pune, India</p> | <p>59. Dr. B. Sreedhar
Senior Principal Scientist-Analytical Division, CSIR Indian Institute of Chemical Technology, Hyderabad, India</p> <p>60. Prof. Alok Srivastava
Head, Department of Chemistry, Panjab University, Chandigarh, India</p> <p>61. Prof. Toyohide Takeuchi
Department of Chemistry, Faculty of Engineering, Gifu University, Gifu, Japan</p> <p>62. Prof. Sunil Kumar Talapatra
Former Head, Department of Chemistry, University of Calcutta, Kolkata, India</p> <p>63. Dr. S. Vasudevan
Principal Scientist, Electroinorganics Division, CSIR-Central Electrochemical Research Institute, Karaikudi, India</p> <p>64. Prof. Suresh Valiyaveetil
Materials Research Laboratory, Department of Chemistry, National University of Singapore, Singapore</p> <p>65. Prof. Shuli You
Shanghai Institute of Organic Chemistry, Chinese Academy of Sciences, China</p> |
|---|--|

GUIDELINES TO AUTHORS

GP Globalize Research Journal of Chemistry is an international peer reviewed journal which publishes full length research papers, short communications, review articles and book reviews covering all areas of Chemistry including Environmental Chemistry. GP Globalize Research Journal of Chemistry is a biannual journal published in English in print and online versions.

(1) Manuscript preparation

- a) Page Layout: A4 (21 cm x 29.7 cm) leaving 2.5 cm margin on all sides of the text. All the text should be in Times New Roman font, double spaced and pages should be numbered consecutively.
- b) Use MS word (2003-2007) for text and TIFF, JPEG or Paint for figures.
- c) The first page should contain title in bold, 14 point size, name/s of author/s in bold, 12 point size, affiliation/s-address, email id and contact number in 11 point size, abstract-up to 200 words in 11 point size, keywords-between 5 to 10 keywords in 11 point size.
- d) Main Text- The paper should be divided into the following sections:

Introduction, Materials and Methods, Results and Discussion, Conclusions, Acknowledgement and References.

Tables and Figures of good resolution (600 dpi) should be numbered consecutively and given in the order of their appearance in the text and should not be given on separate pages.

- e) References- References should be cited in the text as superscript numbers in order of appearance.

References at the end of the paper should be listed in serial order to match their order of appearance in the text. Names of journals should be in italics and volume number should be in bold.

Reference to papers e.g. Ganesh R.S., Pravin S. and Rao T.P., 2005, *Talanta*, **66**, 513.

Reference to books e.g. Lee J.D., 1984, A New Course in Inorganic Chemistry, 3rd ed., ELBS and Van Nostrand Reinhold (UK) Co. Ltd., p.268-269.

GUIDELINES TO AUTHORS

- f) Abbreviations should be explained at first appearance in the text.
- g) Nomenclature should be as per **IUPAC** guidelines.
- h) SI units should be used throughout.

(2) Manuscript Submission

Manuscripts should be submitted online at dvprabhu48@gmail.com. The paper will be accepted for publication after review. All correspondence should be made to the Editor-in-Chief at dvprabhu48@gmail.com.

(3) Proofs

Galley proofs will be sent online to the corresponding author on request and should be returned to the Editorial office within seven working days.

(4) Plagiarism

GP Globalize Research Journal of Chemistry is committed to avoid plagiarism and ensure that only original research work is published.

The Editorial Board and panel of reviewers will check and prevent plagiarism in the manuscripts submitted for publication.

(5) Copyright

Publication of a paper in GP Globalize Research Journal of Chemistry automatically transfers copyright to the publisher. Authors can share free eprints of their published papers with fellow researchers.

(6) Circulation and Subscription rates

The Journal is published twice a year - January and July

Subscription rates are as follows:

Library/Institutional charges (In India)	₹ 2000/-
Individual charges (In India)	₹ 2000/-
Library/Institutional charges (Outside India)	US \$ 100
Individual charges (Outside India)	US \$ 100

Subscription charges:

Review of Research papers is done free of charge. Subscription to the Journal is expected.

GUIDELINES TO AUTHORS

Mode of Payment:

Demand draft/Multicity cheque payable at Mumbai in favour of
“Gaurang Publishing Globalize Pvt. Ltd. Mumbai”

For Online Payment:

Name of the Bank: Axis Bank
Branch Name: Tardeo, Mumbai (MH)
Account No. 916020066451552
IFSC Code: UTIB0001345

For further details please contact:

Dr. D.V. Prabhu, Editor-in-Chief,
Email: dvprabhu48@gmail.com
Mobile: 09870 226 899

Mr. Rajan Pendurkar, Publishing Co-ordinator,
Email: gpglobalize@gmail.com
Mobile: 09969 392 245

A Request to Authors

X f!uibol!zpv!gps!tfoejch!zpv!s ftfbs di!qoqfs!up!H!Q!Hmpclmj {f!S ftfbs di!Kpvsolm
pg!Di.fnjtusz! (RNI No. MAHENG/2017/74063 ISSN No. (Print): 2581-5911)

Zpv!bs fs frvftufe!up!tfoe!b!EE0Nmujdjuz!Di frvf!gps! a!31110.!jo!gwpvs!pg! **"Gaurang
Publishing Globalize Pvt. Ltd., Mumbai"**! qozbamf! bu! Nmcbj/! Jg! uif! Fejupsjlm
Cpbose!bddfqt!zpv!qoqfs!gps!qvanjdaujpo!bgufs!s fwj fx-! uifo!zpv!EE0di frvf!xjrm
cf!efqptjufe!boe!b!s fdfjqu!xjrm!cf!tfou!gps!uif!tbnf-!pui fsxjtf! uif! EE0Di frvf
xjrm!cf!s fuvsofe!up!zpv!bu! uif! fbsmjftu/

X f!xpvme!bqqs fdjbuf!jg!zpv!ifrq!vt!jo!pvs!fggpsut!up!qspnpuf!bdlbe fnjd!fydfirmfodf/

Volume 2 Issue 2 * January-June 2019

CONTENTS

Papers

1. Synthesis and Vibrational Characterization of New Er(III) Complex with Hepatoprotective and Antioxidant Activity 1 - 16
I. Kostova, V. Atanasova, M. S. Kondeva-Burdina and V. I. Tzankova
2. Ru(III) Catalysed Oxidation of Glucitol and Osmitrol with Chloramine T in Alkaline medium 17 - 23
Swarn Lata Bansal and Amrita Srivastava
3. Physiochemical Properties of Kappa-Carrageenan Packed with Zinc Oxide Nanoparticles Biocomposite Films 24 - 29
Flyndon Mark S. Dagalea and Karina Milagros R. Cui-Lim
4. Synthesis and Diagnosis of Heterogeneous Compounds, Pyrimidine and Oxazepine from Alcofenac Drug and Evaluation of their Biological Activity 30 - 38
Fatimah Ali Hussein, Hala Shkyiar Lihimes, Luma Ahmed Mohammed Ali and Sana Hitur Awad
5. Effects of Salinity and Temperature on the Rate of Biodegradation of Domestic Waste Released into the Marine Waters around Mumbai City, India 39 - 42
Shivani S Dhage, D V Prabhu and Prakash S Kelkar
6. Physicochemical and Phytochemical Analysis of some Selected Herbal Medicinal Products Consumed in Wukari, Taraba State, Nigeria 43 - 48
Odoh Raphael and Ajiboye O. Emmanuel
7. Detection of Organochlorine Pesticides in *Typhadomingensis* in Euphrates River, Iraq 49 - 57
Amerah Imran. H. AL-Janabi
8. Antimicrobial Property of Kappa-Carrageenan Filled with Zinc Oxide Nanoparticles (ZNONPS) in Textile Fabrics 58 - 61
Judy Ann H. Brensis and Karina Milagros R. Cui-Lim

Invited Article

9. Historical Landmarks in the Development of the Periodic Table 62 - 73
S. Vasudevan
10. Book Review 74 - 75
- Conference Alerts 76 - 77



Synthesis and Vibrational Characterization of New Er(III) Complex with Hepatoprotective and Antioxidant Activity

I. Kostova^{1*}, V. Atanasova¹, M. S. Kondeva-Burdina² and V. I. Tzankova²

¹Department of Chemistry, Faculty of Pharmacy, Medical University, 2 Dunav Str., Sofia 1000, Bulgaria

²Laboratory of Drug Metabolism and Drug Toxicity, Department of Pharmacology, Pharmacotherapy and Toxicology, Faculty of Pharmacy, Medical University, 2 Dunav Str., Sofia 1000, Bulgaria

E-mail: irenakostova@yahoo.com

Abstract

The Erbium(III) complex was synthesized and its structure was determined by means of elemental analysis, FTIR and FT-Raman spectroscopies. Detailed comparative vibrational analysis of the IR and Raman spectra of the complex with that of the free ligand (HAOA) allowed a straightforward assignment of the vibrations of the ligand groups involved in coordination. The binding mode in the complex was elucidated. The compounds HAOA and ErAOA were investigated for possible antioxidant activity in a model of non-enzyme-induced lipid peroxidation on isolated rat microsomes and for cytotoxicity on isolated rat hepatocytes. On isolated rat microsomes, administered alone, HAOA and ErAOA did not reveal pro-oxidant effects, but in conditions of non-enzyme-induced lipid peroxidation showed antioxidant activity, which was stronger for the complex ErAOA. On isolated rat hepatocytes, isolated by two-stepped collagenase perfusion, both HAOA and ErAOA showed cytotoxicity, but the complex ErAOA was with lower cytotoxicity than the ligand HAOA. We suggest that lower hepatotoxicity and higher antioxidant activity of the complex ErAOA, might be due to the presence of Er(III) ion in the structure of the complex.

Keywords: Erbium(III) Complex, 5-aminoorotic acid, Vibrational Spectroscopy, Hepatoprotective and Antioxidant Activity

Introduction

5-Aminoorotic acid is the amino-derivative of naturally occurring orotic acid (vitamin B₁₃), which is a key intermediate in the biosynthesis of the pyrimidine nucleotides of DNA and RNA. Orotic acid and its metal complexes have attracted growing attention in medicine¹⁻⁵. Because of the importance of orotic acid and its complexes in living systems, a reliable assignment of their vibrational spectra is a useful basis in the study of their interactions with other chemical species present in the biological milieu. In our previous work, we per-

formed comprehensive experimental and theoretical studies of the structural and spectroscopic properties of orotic acid and its metal complexes^{6, 7}. The orotic acid molecule is related to the molecules of uracil or thymine. Various theoretical studies on these types of molecules have been reported⁸⁻¹⁰ and these results are very helpful in the assignment of the vibrational spectra of orotic acid.

Coordination compounds of orotic acid and its substituted derivatives continue to attract attention because of its multidentate functionality and its role in bioinorganic



chemistry. Orotic acid is an interesting multidentate ligand capable of coordinating to metal ions through the pyrimidine nitrogen atoms, the two carbonyl oxygens and the carboxylate oxygens¹¹⁻¹⁶. The equilibrium composition of the reactant mixture and thus the solution pH are critical factors which determine the mode of coordination. The literature lists many reports on the coordinating preferences of the orotate moiety in metal complexes¹¹⁻¹⁷.

Despite the interest in orotate metal complexes, the coordination chemistry of the derivatives of orotic acid has received rather scant attention. One of these derivatives is 5-aminoorotic acid (5-amino-2,6-dioxo-1,2,3,6-tetrahydropyrimidine-4-carboxylic acid, HAOA, Fig. 1) which has relatively unknown coordination chemistry¹⁸⁻²⁰. 5-Aminoorotic acid has demonstrated flexible coordination modes during the formation of coordination frameworks, that is why it was a challenge for us to obtain new lanthanide(III) coordination complexes with HAOA, especially in view of their application as antioxidant agents. In order to estimate the most preferred reactive sites for electrophilic attack and metal binding, the geometry of HAOA was calculated and optimized by us on the basis of DFT calculations¹⁸.

The present work can be regarded as a continuation of our efforts in the bioinorganic chemistry of lanthanide(III) complexes with a number of biologically active ligands. We have reported promising results on their significant cytotoxic activity in different human cell lines²¹⁻²⁵, which encouraged us to search for new lanthanide complexes.

The coordination chemistry of lanthanides, relevant to the biological, biochemical and medical aspects, makes a significant contribution to understanding the basis of application of lanthanides, particularly in biological and medical systems. The lability of lanthanide complexes, strong oxyphilicity, very fast water exchange reaction, nondirectionality of lanthanide ligand bond and varying coordination number, all contribute towards lanthanide interaction with biomolecules. The ionic size of Ln(III)

varies from one lanthanide to another lanthanide; in addition, the ionic size of a particular lanthanide also varies significantly with the coordination number. The smaller size of chelating biologically active ligand can even suit larger lanthanides with lowered coordination number. Similarly small lanthanides can expand their coordination number and can form stable chelates with larger biomolecules. This can explain the different coordinating potential and biological behaviour of different lanthanides under different physiological conditions. It has been reported by us earlier that Ln(III) ions attack cancer cells and induce apoptosis, considered as the core of the lanthanide potential as anticancer activity²¹⁻²⁵. Along with apoptosis, there are several synergic related effects, ROS scavenging, cell protection, cytoskeleton stabilization and also immunologic enhancement²⁶⁻³⁵. Reactive oxygen species (ROS) are the mediators of a number of degenerative diseases. The antioxidants are excellent substances used as drugs for the treatment of degenerative diseases. Lanthanides are considered of high potential because of their inherent antioxidant properties²⁷⁻²⁹. Recently the antioxidant activity of Ln(III) complexes was determined by DPPH radical scavenging method, which indicated that the Ln(III) complexes exhibited more effective antioxidant activity than the respective ligands^{28,29,34,35}. It was shown that metal complexes exhibited considerable scavenging activity due to the chelation of organic molecules to rare earth ions and rare earth ions such as La(III), Sm(III), Eu(III) and Dy(III) exerted differential and selective effects on scavenging radicals of the biological system. Therefore, the studied Ln(III) complexes of biologically active derivatives of orotic acid deserve to be further researched.

Therefore, the aim of this work was to synthesize and characterize new erbium(III) complex of 5-aminoorotic acid and to evaluate its activity. In the present study 5-aminoorotic acid (HAOA) and its erbium(III) complex (HoAOA) were investigated for possible hepatotoxicity on rat hepatocytes, isolated by two-stepped, collagenase perfusion, and for possible antioxidant activity in a model of non-enzyme-induced lipid

Synthesis and Vibrational Characterization of New Er(III) Complex with Hepatoprotective and Antioxidant Activity

peroxidation on isolated rat liver microsomes, model of lipid membrane.

Materials and Methods

Chemicals and Reagents

The compounds used for preparing the solutions required for the synthesis were Sigma-Aldrich products, p.a. grade: $\text{Er}(\text{NO}_3)_3 \cdot 6\text{H}_2\text{O}$ and 5-aminoorotic acid. 5-Aminoorotic acid (Fig. 1) was used as a ligand for the preparation of the metal complex.

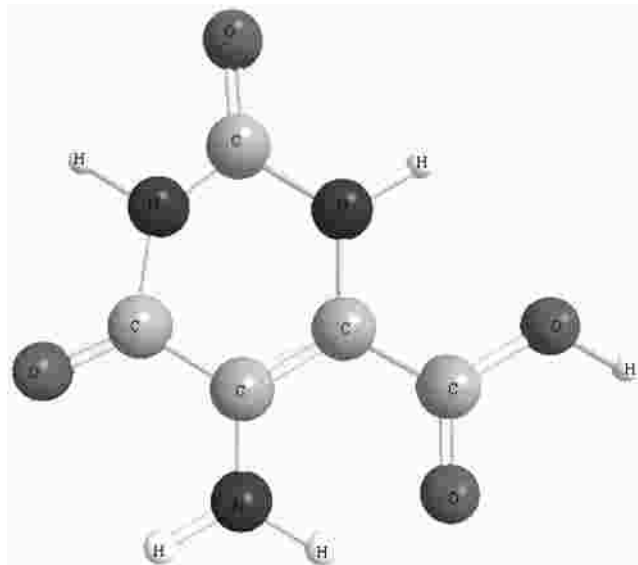


Fig. 1: Molecular structure of the ligand 5-aminoorotic acid (HAOA)

The carbon, hydrogen and nitrogen contents of the compound were determined by elemental analysis.

The solid-state infrared spectra of the ligand and its Er(III) complex were recorded in KBr in the 4000-400 cm^{-1} frequency range by FT-IR 113V Bruker spectrometer.

The Raman spectra of HAOA and its new Er(III) complex were recorded with a Dilor microspectrometer (Horiba-Jobin-Yvon, model LabRam) equipped with a 1800 grooves/mm holographic grating. The 514.5 nm line of an argon ion laser (Spectra Physics, model 2016)

was used for the excitation of probes. The spectra were collected in a backscattering geometry with a confocal Raman microscope equipped with an Olympus LMPlanFL 50x objective and with a resolution of 2 cm^{-1} . The detection of Raman signal was carried out with a Peltier-cooled CCD camera. The laser power of 100 mW was used in our measurements.

In our experiments, pentobarbital sodium (Sanofi, France), HEPES (Sigma Aldrich, Germany), NaCl (Merck, Germany), KCl (Merck), D-glucose (Merck), NaHCO_3 (Merck), KH_2PO_4 (Scharlau Chemie SA, Spain), $\text{CaCl}_2 \cdot 2\text{H}_2\text{O}$ (Merck), $\text{MgSO}_4 \cdot 7\text{H}_2\text{O}$ (Fluka AG, Germany), collagenase from *Clostridium histolyticum* type IV (Sigma Aldrich), albumin, bovine serum fraction V, minimum 98% (Sigma Aldrich), EGTA (Sigma Aldrich), 2-thiobarbituric acid (4,6-dihydroxypyrimidine-2-thiol; TBA) (Sigma Aldrich), trichloroacetic acid (TCA) (Valerus, Bulgaria), 2,2'-dinitro-5,5'-dithiodibenzoic acid (DTNB) (Merck), lactate dehydrogenase (LDH) kit (Randox, UK), FeSO_4 (Merck) and Ascorbinic acid (Valerus, Bulgaria), Glycerol (Valerus, Bulgaria) were used.

Animals

Male Wistar rats (body weight 200-250 g) were used. The rats were housed in plexiglass cages (3 per cage) in a 12/12 light/dark cycle, under standard laboratory conditions (ambient temperature 20 ± 2 °C and humidity $72 \pm 4\%$) with free access to water and standard pelleted rat food 53-3, produced according to ISO 9001:2008.

Animals were purchased from the National Breeding Centre, Sofia, Bulgaria. At least 7 days of acclimatization was allowed before the commencement of the study. The health was monitored regularly by a veterinary physician. The vivarium (certificate of registration of farm¹ 0072/01.08.2007) was inspected by the Bulgarian Drug Agency in order to check the husbandry conditions (¹ A-11-1081/03.11.2011). All performed procedures were approved by the Institutional Animal Care Committee and made according Ordinance¹ 15/2006 for



humaneness behaviour to experimental animals. The principles stated in the European Convention for the Protection of Vertebrate Animals used for Experiments and other Scientific Purposes (ETS 123) (Council of Europe, 1991) were strictly followed throughout the experiment.

Isolation of liver microsomes

Liver is perfused with 1.15% KCl and homogenized with four volumes of ice-cold 0.1 M potassium phosphate buffer, pH=7.4. The liver homogenate was centrifuged at 9 000 x g for 30 min at 4°C and the resulting post-mitochondrial fraction (S9) was centrifuged again at 105 000 x g for 60 min at 4°C. The microsomal pellets were re-suspended in 0.1 M potassium phosphate buffer, pH=7.4, containing 20 % Glycerol. Aliquots of liver microsomes were stored at -70°C until use³⁶. The content of microsomal protein was determined according to the method of Lowry using bovine serum albumin as a standard³⁷.

FeSO₄/Ascorbinic acid-induced lipid peroxidation in vitro

As a system, in which metabolic activation may not be required in the production of lipid peroxide, 20 μM FeSO₄ and 500 μM Ascorbinic acid were added directly into rat liver microsomes and incubated for 20 min at 37°C³⁸.

Lipid peroxidation in microsomes

After incubation of microsomes (1 mg/ml) with the compounds, we added to the microsomes 1 ml 25% (w/v) trichloroacetic acid (TCA) and 1 ml 0.67% 2-Thiobarbituric acid (TBA). The mixture is heated at 100°C for 20 min. The absorbance was measured at 535 nm, and the amount of MDA was calculated using a molar extinction coefficient of $1.56 \times 10^5 \text{ M}^{-1}\text{cm}^{-1}$ ³⁸.

Isolation and incubation of hepatocytes

Rats were anesthetized with sodium pentobarbital (0.2 ml/100 g). An optimized *in situ* liver perfusion using less reagents and shorter time of cell isolation was performed. The method provided in higher amount of live

and metabolically active hepatocytes³⁹.

After portal catheterization, the liver was perfused with HEPES buffer (pH = 7.85) + 0.6 mM EDTA (pH = 7.85), followed by HEPES buffer (pH = 7.85) and finally HEPES buffer containing collagenase type IV (50 mg/200 ml) and 7 mM CaCl₂ (pH = 7.85). The liver was excised, minced into small pieces, and hepatocytes were dispersed in Krebs-Ringer-bicarbonate (KRB) buffer (pH = 7.35) + 1% bovine serum albumin.

Cells were counted under the microscope and the viability was assessed by Trypan blue exclusion (0.05%)⁴⁰. Initial viability averaged 89%.

Cells were diluted with KRB to make a suspension of about 3×10^6 hepatocytes/ml. Incubations were carried out in flasks containing 3 ml of the cell suspension (i.e. 9×10^6 hepatocytes) and were performed in a 5% CO₂ + 95% O₂ atmosphere⁴⁰.

Cell incubation with HAOA and ErAOA

Cells were incubated with concentration 100 iM of the compounds⁴¹.

Lactate dehydrogenase (LDH) release

LDH release in isolated rat hepatocytes was measured spectrophotometrically using a LDH kit⁴⁰.

Reduced glutathione (GSH) depletion

At the end of the incubation, isolated rat hepatocytes were recovered by centrifugation at 4°C, and used to measure intracellular GSH, which was assessed by measuring non-protein sulfhydryls after precipitation of proteins with trichloroacetic acid (TCA), followed by measurement of thiols in the supernatant with DTNB. The absorbance was measured at 412 nm⁴⁰.

Malondialdehyde (MDA) assay

Hepatocyte suspension (1 ml) was taken and added to 0.67 ml of 20% (w/v) TCA. After centrifugation, 1 ml of the supernatant was added to 0.33 ml of 0.67% (w/v) 2-thiobarbituric acid (TBA) and heated at 100°C

Synthesis and Vibrational Characterization of New Er(III) Complex with Hepatoprotective and Antioxidant Activity

for 30 min. The absorbance was measured at 535 nm, and the amount of TBA-reactants was calculated using a molar extinction coefficient of MDA $1.56 \times 10^5 \text{ M}^{-1} \text{ cm}^{-1}$ ⁴⁰.

Statistical analysis

Statistical analysis was performed using statistical programme 'MEDCALC'. Results are expressed as mean \pm SEM for 6 experiments. The significance of the data was assessed using the nonparametric Mann-Whitney test. A level of $P < 0.05$ was considered significant. Three parallel samples were used.

Results and Discussion

Chemistry

The complex was synthesized by reaction of Er(III) salt and the ligand, in amounts equal to metal: ligand molar ratio of 1: 3. The synthesis was made in different ratio (1:1, 1:2, 1:3) but in all the cases the final product was with the composition 1:3. The complex was prepared by adding an aqueous solution of Er(III) salt to an aqueous solution of the ligand subsequently raising the pH of the mixture gradually to ca. 5.0 by adding dilute solution of sodium hydroxide. The reaction mixture was stirred with an electromagnetic stirrer at 25°C for one hour. At the moment of mixing of the solutions, precipitate was obtained. The precipitate was filtered (pH of the filtrate was 5.0), washed several times with water and dried in a desiccator to constant weight. The obtained complex was insoluble in water, methanol and ethanol, but well soluble in DMSO.

Reaction of Er(III) and 5-aminoorotic acid afforded a complex which was found to be quite stable both in solid state and in solution. The new Er(III) complex was characterized by elemental analysis. The content of the metal ion was determined after mineralization. The used spectral analyses confirmed the nature of the complex.

The data of the elemental analysis of the Er(III) complex serve as a basis for the determination of its empiri-

cal formula and the results are presented below. The founded elemental analysis of Er(III) complex of HAOA ($\text{Er}(\text{AOA})_3 \cdot 2\text{H}_2\text{O}$) are shown as % calculated/found: C = 25.24/25.63; H = 2.24/2.49; N = 17.67/17.82; H_2O = 5.05/5.34; Er = 23.42/23.10, where HAOA = $\text{C}_5\text{N}_3\text{O}_4\text{H}_5$ and AOA = $\text{C}_5\text{N}_3\text{O}_4\text{H}_4$.

In our previous work the geometry of 5-aminoorotic acid was computed and optimized with the Gaussian 03 program employing the B3PW91 and B3LYP methods with the 6-311++G** and LANL2DZ basis sets¹⁸. In the present study the binding mode of the HAOA ligand to Er(III) ions is elucidated by recording the IR and Raman spectra of the complex in comparison with those of the free ligand. It was found that the density functional theory (DFT) calculated geometries, harmonic vibrational wavenumbers including IR and Raman scattering activities for the ligand and its complex were in good agreement with the experimental data, a complete vibrational assignment being proposed.

Vibrational spectroscopy

Because no crystal structure data are available for HAOA, its structure was optimized at different levels of theory¹⁸ and compared with literature data for compounds containing identical or similar functional groups⁴²⁻⁴⁸. Previously published X-Ray diffraction data about orotic acid^{42, 44} helped us to get better inside. The HAOA molecule has a planar structure which is very similar to the structure of orotic acid obtained by X-Ray diffraction^{18, 42}. In the calculated solid state conformation of HAOA, the existence of the intramolecular hydrogen bondings is highly probable¹⁸. The HAOA has a good ability to adopt several modes of intramolecular hydrogen bonding^{43, 47}, which take place between the coordinated carboxylate O1 and one of the protons of amino group, between the pyrimidine carbonyl oxygens O4 and the other one of the protons of amino group, and between the carboxylate O3 and the imido N1-H1 group. Taking into account the average calculated hydrogen bonds lengths, the latter being particularly strong. The intramolecular hydrogen bonds play an important function in the crystal packing and have influence on the



respective vibrational spectra. Additionally, the geometry of La(III) complex of 5-aminoorotic acid was computed and optimized by us with B3PW91/LANL2DZ and B3LYP/LANL2DZ methods¹⁸. Through the DFT calculations with different bases, HAOA coordinated to the lanthanum ion as a dianion and the complex contained three HAOA ligands. It has been found that 5-aminoorotic acid binds to the La(III) ion through both oxygen atoms of the carboxylic group from all three ligands; the central atom La(III) is six-coordinated and form together with the ligands a trigonal prismatic structure¹⁸. It should be mentioned that different kinds of hydrogen bonds were observed in the La(III) complex of 5-aminoorotic acid¹⁸: hydrogen bonding of coordinated carboxylic oxygen and the proton of the nitrogen atom; hydrogen bonding of uncoordinated carbonylic oxygen from the pyrimidine rings and one of the protons of the amino group, and hydrogen bonding of the coordinated carboxylic oxygen and the other proton of the amino group. The theoretical study performed by us earlier has helped us to interpret properly the vibrational IR and Raman spectra of the newly synthesized Er(III) complex.

The vibrational fundamentals from the IR and Raman spectra, presented in Figures 2 and 3, were analyzed by comparing these modes with those from the

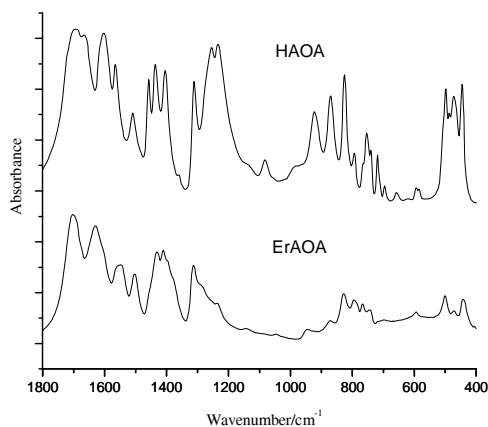


Fig. 2: IR spectra of 5-aminoorotic acid (HAOA) and its Er(III) complex

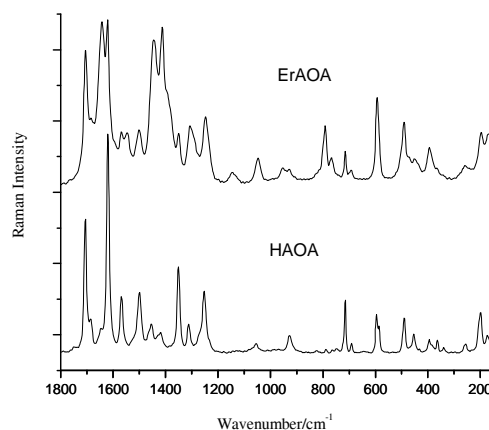


Fig. 3: Raman spectra of the solid state of 5-aminoorotic acid (HAOA) and its Er(III) complex. Excitation: 514.5 nm, 100 mW

literature^{42-44, 49-58} and in combination with the results of our DFT calculations (i.e., harmonic vibrational wavenumbers and their Raman scattering activities)¹⁸. The selected experimental IR and Raman data of the ligand and the newly synthesized Er(III) complex together with their tentative assignments are given in Table 1. The vibrational spectra of HAOA and its Er(III) complex are relatively complex (Figs. 2 and 3). Several contributions of relatively high IR intensity were found, corresponding to carbonyl, carboxylic and C=C stretching, and amino bending vibrations, which appear strongly coupled. The assignment of the bands is quite difficult because they are overlapped in the same spectral region, and the involvement of these groups in hydrogen bonds affects their wavenumbers and produces a relevant band broadening^{43, 49-53}.

N-H modes

The $\nu(\text{N1-H1})$ and $\nu(\text{N3-H3})$ stretching wavenumbers in HAOA appear little affected due to the intermolecular H-bonds. In the IR spectra, the strong band at 3457 cm^{-1} (HAOA) and the band at 3448 cm^{-1} (Er(III) complex of HAOA) were assigned to the N1-H1 stretching modes from the pyrimidine rings (Table 1)^{46, 48, 59}, while the bands at 3333 cm^{-1} in the IR spectrum of HAOA as well as the band at 3332 cm^{-1} from the IR spectrum of Er(III) complex of HAOA were attributed

Synthesis and Vibrational Characterization of New Er(III) Complex with Hepatoprotective and Antioxidant Activity

to the N3-H3 stretching modes^{42, 48, 60} (Fig. 2, Table 1). In the Raman spectra, the N3-H3 stretching vibrations are present for the ligand and for the complex (Table 1, Fig. 3). The observed experimental IR bands at 3044 and 3011 cm^{-1} could be tentatively ascribed to intermolecular H-bonds. The experimental IR bands at 2850 cm^{-1} (HAOA) and at 2831 cm^{-1} (Er(III) complex of HAOA) correspond also to these H-bonds. In the in-plane N-H bending modes the main contributions correspond to the modes $\delta(\text{N1-H1})$ and $\delta(\text{N3-H3})$ which appear as IR bands with medium intensity at 1405 and 1436 cm^{-1} (HAOA) and at 1379 and 1409 cm^{-1} (Er(III) complex). The experimental Raman band corresponding to $\delta(\text{N1-H1})$ mode was not detected in the Raman spectrum of the ligand. These modes appear strongly coupled with $\delta(\text{ring})$ mode. In general, all the vibrations in the 1500–950 cm^{-1} range have significant contributions of $\delta(\text{N-H})$ modes. In the out-of-plane N-H bending modes the main contribution corresponds to the $\gamma(\text{N3-H3})$ mode with weak IR intensity and null Raman intensity. It appears as IR band at 871 cm^{-1} (HAOA) and at 874 cm^{-1} (Er(III) complex). The $\gamma(\text{N1-H1})$ mode possesses almost null IR and Raman intensity and has not been detected in the experimental spectra.

NH₂ group vibrations

The NH₂ asymmetrical stretching mode that is absent in the IR and Raman spectra of the ligand can be seen in the IR and Raman spectra of the complex at 3355 cm^{-1} as a medium band (IR) and 3357 cm^{-1} as a weak band (Raman), whereas the symmetrical NH₂ stretch is present in both IR spectra by bands with medium relative intensity at 3196 and 3170 cm^{-1} and in Raman spectrum⁶⁰ of the ligand as a very weak band at 3166 cm^{-1} . Moreover, the wavenumber region 2700–3000 cm^{-1} in the IR spectra of HAOA and its Er(III) complex is typical of strongly hydrogen bonded intermolecular complexes due to a strong anharmonic coupling (Fermi resonance) of the N-H stretching vibrations with overtones and combinations of lower frequency modes of the bonded molecules⁶⁰⁻⁶². The β_s scissors deformation appears strongly coupled with $\nu(\text{C-C=C})$ mode, which is in excellent agreement with the experimental IR bands detected at

1566 cm^{-1} (HAOA) and at 1550 cm^{-1} (Er(III) complex). The rocking mode, denoted as r or β_{as} , appears strongly coupled with $\nu(\text{COO})$ vibrations in HAOA and it is assigned to the experimental IR band at 1083 cm^{-1} and to the Raman band at 1047 cm^{-1} (HAOA), which shifted in the complex. In the solid state, due to NH₂ group appears strongly H-bonded with the C=O group, it is expected an increment in the N-H bond lengths, and consequently, an increase in the wavenumber of the wagging mode. The value of the torsional mode $\tau(\text{NH}_2)$ in HAOA is due to an almost planar NH₂ group and a nearly pure sp² hybridization.

C=O modes

The C=O groups are very important as they take part in hydrogen bonding, especially in nucleic acid base derivatives. When the carbonyl is hydrogen bonded but not dimerized, a band active in the IR spectra appears at about 2700–3000 cm^{-1} and also another band active in both IR and Raman spectra appears at 1730–1705 cm^{-1} ⁵⁹. In our IR spectra these bands with medium and weak intensities for the ligand and the complex, respectively, can be observed at 2850 and 2831 cm^{-1} . Besides, one very strong band can be observed in 1730–1690 cm^{-1} region at 1691 cm^{-1} in the IR spectrum of the ligand and one medium band at 1704 cm^{-1} in the IR spectrum of the complex, which were assigned to the symmetrical stretching mode of C2=O2 (Fig. 2). Opposite to the IR spectra, in this region of the Raman spectra only a medium band at 1699 cm^{-1} for the free ligand was observed. It is detected that the $\nu(\text{C2=O2})$ band's position remains almost unaffected by changes in the molecular structure of the uracil ring. This is caused by the fact that the C2=O2 group is quite distanced from the COOH and NH₂ groups and, moreover, it is surrounded by the two N-H groups, which buffer it from influences of the remaining molecular moieties⁵⁸. On the other hand, the C4=O4 moiety is nearer to the NH₂ group, and due to an intramolecular contact between both, the N-H and C4=O4 bonds appear slightly lengthened⁵⁸. The dimer form is best characterized by the Raman bands in the 1680–1640 cm^{-1} range⁵⁴⁻⁵⁶ and by IR bands, around 1290 cm^{-1} and between 1440 cm^{-1} and



Table 1: Selected experimental IR and Raman wavenumbers (cm⁻¹) of 5-aminoorotic acid (HAOA) and its Er(III) complex and their tentative assignment

IR		Raman solid		Vibrational assignment
HAOA	ErAOA	HAOA	ErAOA	
3457 s	3448 w	3456 vw		$\nu(\text{N1H1})^{46, 48, 58, 59}$
	3355 m		3357 w	$\nu_{\text{as}}(\text{NH}_2)^{60}$
3333 s	3332 m	3323 m	3333 w	$\nu(\text{N3H3})^{58}$
3196 m	3170 m	3166 vw		$\nu_{\text{s}}(\text{NH}_2)^{60}$
2850 w	2831 w/m			Bonded $\text{NH}\cdots\text{O}^{60}$
1691 vs	1704 m	1699 m		$\delta(\text{NH})^{58}$; $\nu_{\text{s}}(\text{C2=O})^{44, 59}$; $\nu(\text{N1-C6})^{58}$
	1699 vs			$\nu_{\text{s}}(\text{C4=O4})$
1667 s	1630 vs	1678 sh	1705 m	$\nu_{\text{s}}(\text{C4=O4})^{66}$; $\nu(\text{COO}^-)^{45, 59}$; $\nu(\text{C5=C6})$; $\delta(\text{N3-H3})^{58}$
1604 s	1610 vs	1612 vs	1621, 1642 vs	$\nu(\text{C5=C6})^{44, 60}$; $\beta(\text{NH}_2)$; $\nu(\text{COO}^-)^{58}$
1566 m	1550 m	1560 m	1567 m	$\delta_{\text{ip}}(\text{N1H1}, \text{N5H5})$; $\nu(\text{C5C6})^{59}$; $\beta_{\text{s}}(\text{NH}_2)^{58}$
1511 w	1504 m	1492 w/m	1501 w	$\delta(\text{NC})^{33}$; $\nu(\text{ring})^{42, 59}$; $\delta_{\text{ip}}(\text{N3H3})^{42}$
1457 m	1429	1447 w	1441 w	$\nu(\text{ring})$; $\beta_{\text{s}}(\text{NH}_2)$; $\delta(\text{N1-H1})^{42}$; $\nu(\text{COO}^-)^{58}$
1436 m	1409 s	1421 w	1412 vs	$\delta(\text{N3H3})$; $\delta(\text{ring})$; $\delta(\text{N1H1})^{58}$
1405 m	1379 s		1349 s	$\delta(\text{N3H3})$; $\delta(\text{ring})$; $\delta(\text{N1H1})^{58, 59}$; $\nu_{\text{s}}(\text{COO}^-)^{45}$
1312 m	1309 m	1301 w	1308 m/s	$\nu(\text{C5-N})$; $\nu(\text{C-N})$; $\delta(\text{OH})$; $\beta_{\text{s}}(\text{NH}_2)^{58}$
1255 m/s	1270 sh			$\nu(\text{C-N})$; $\delta(\text{N1H1})$; $r(\text{NH}_2)$; $\delta(\text{ring})^{58}$
1234 m/s	1236 w	1242 m	1248 m/s	$\nu(\text{C-N})$; $\delta(\text{N3H3})^{42, 59}$; $r(\text{NH}_2)$; $\delta(\text{N1H1})^{58}$
1140 sh	1132 vw		1122 vw	$\delta(\text{OH})^{58}$
1083 vw	1056	1047 vw	1050 w	$\nu(\text{C6-O}, \text{C6-C7})^{42}$; $\beta_{\text{as}}(\text{NH}_2)^{58}$
989 sh				$\nu(\text{NCN})$; $\delta(\text{N3H3})$; $r(\text{NH}_2)$; $\delta(\text{N1H1})^{58}$
924 w	946 sh	919 w/m	928 w/m	$\nu(\text{NCC})$; $\nu(\text{ring})$; $r(\text{NH}_2)$; $\nu(\text{COO}^-)^{58}$
871 w/m	874 vw			$\gamma(\text{N3-H3})$; $\gamma(\text{ring})^{58, 59}$
795 vw	829 m	809 vw	791 m	$\delta_{\text{op}}(\text{O3C7O1})^{43}$
767 vw	796 w		766 sh	$\gamma(\text{C4=O4})$; $\gamma(\text{C4-C=C6})$; $\gamma(\text{C6-C12})^{58}$
754 w	763 w	748 vw		$\gamma(\text{C6-C12})$; $\gamma(\text{C4=O4})$; $\gamma(\text{COOH})$; $\gamma(\text{N3-H})^{58}$
740 w	719 w		714 m	$\gamma(\text{C2=O2})$; $\gamma(\text{NC2N})$; $\gamma(\text{N3-H})^{58}$
696 vw	698 vw			$\delta(\text{ring})$; $\Delta_{\text{s}}(\text{COO})$; $r(\text{NH}_2)^{58}$
	611 vw			$\nu(\text{Er-O})$
584 vw	590 vw	582 w	593 w/m	$\delta(\text{ring})$; $\Delta_{\text{s}}(\text{COO})^{58}$
	501 m			$\nu(\text{Er-O})^{43}$
488 w	499 w	482 w/m	490 m	$\delta(\text{ring})$; $\delta(\text{NH}_2)$; $\Delta_{\text{s}}(\text{COO})^{58}$
446 m	441 m	445 w	450 m	$\delta(\text{OCNCO})$; $\delta(\text{COO}) + r(\text{NH}_2)^{42, 58}$
	424 sh	425 sh	442 w/sh	$\tau(\text{C2O2}, \text{ring})^{42}$; $\Delta_{\text{as}}(\text{COO})^{58}$
		381 vw	394 w	$\delta(\text{OCCN11})$; $\delta(\text{COO})$; $\delta(\text{C2=O})$; $r(\text{NH}_2)^{42, 58}$; $\nu(\text{Er-O})^{43}$
		249 w	255 w	$\tau(\text{NH}_2)^{42}$; $\Delta_{\text{s}}(\text{COO})^{58}$

Abbreviation: vw – very weak; w – weak; m – medium; ms – medium strong; s – strong; vs – very strong; sh – shoulder; ν – stretching; δ – bending; δ – torsion; s – symmetric; as – asymmetric; def. – deformation; ip – in plane; op – out of plane; ring – pyrimidine ring; sciss – scissoring

Synthesis and Vibrational Characterization of New Er(III) Complex with Hepatoprotective and Antioxidant Activity

1395 cm^{-1} (C-O stretching mode) (Figs. 2 and 3; Table 1)^{57, 59}. The strong band at 1667 cm^{-1} from the IR spectrum of HAOA and the two very strong bands at 1699 cm^{-1} and 1630 cm^{-1} from the IR spectrum of the complex, were assigned to the symmetrical stretching modes of C4=O4⁴⁴ and to the asymmetrical COO⁻ stretching modes^{45, 59}. In the Raman spectra, these vibrations can be observed as a shoulder at 1678 cm^{-1} for the ligand and as a medium band at 1705 cm^{-1} for its Er(III) complex (Table 1, Figs. 2 and 3). The in-plane bending modes appear strongly coupled with $\delta(\text{COO}^-)$ modes. The out-of-plane bending modes are also strongly coupled with ring modes⁵⁸. The $\gamma(\text{C4=O4})$ mode appears as a very weak experimental band at 767 cm^{-1} (IR spectrum of the ligand) and at 796 cm^{-1} (IR spectrum of Er(III) complex). The same band seems to be absent in the Raman spectrum of the ligand and appears in the Raman spectrum of the complex (at 766 cm^{-1}). The $\gamma(\text{C2=O2})$ mode appears at 740 cm^{-1} (IR spectrum of the ligand) and at 719 cm^{-1} (IR spectrum of Er(III) complex) with very weak IR intensity and null Raman intensity.

C-C and C-N ring modes

When the protons of $-\text{NH}_2$ group are engaged in intramolecular hydrogen bonding, the electron lone pair of the N atom is coupled more readily with the π -electrons of the C5=C6 bond. In the Raman spectra of HAOA and its Er(III) complex the C5=C6 stretching, NH_2 scissoring and $\nu(\text{COO}^-)$ vibrational modes are distinguish through the very strong bands at 1612 cm^{-1} for the ligand, and at 1621 and 1642 cm^{-1} for its Er(III) complex^{44, 59, 60}. An increase in the $\nu(\text{C=C})$ wavenumber in the ligand appears related to an increment in the negative charge on substituent in position 5. The medium bands from the IR spectra at 1566 cm^{-1} (ligand) and 1550 cm^{-1} (Er(III) complex), as well as the medium peaks from the Raman spectra at 1560 cm^{-1} (ligand) and 1567 cm^{-1} (Er(III) complex), were attributed to the C5=C6 stretching and in plane N-H bending modes (Table 1). The next pyrimidine ring vibrations, as N-C and N-H bending modes, can be observed in the 1520-1490 cm^{-1} wavenumber region (Table 1, Figs. 2 and 3).

In the IR spectra, the medium band at 1312 cm^{-1} for HAOA as well as the medium signal at 1309 cm^{-1} for the complex were attributed to the C5-N stretching modes (Fig. 2), while in the Raman spectra these vibrations can be observed as a weak peak at 1301 cm^{-1} for the ligand and as a medium/strong signal at 1308 cm^{-1} for the complex and they are shifted to lower wavenumbers (Table 1, Fig. 3).

The IR band at 1255 cm^{-1} was assigned as $\nu(\text{C-N})$. This mode was detected only in the IR spectra for the free ligand and blue shifted for the complex (1270 cm^{-1}). The experimental IR bands observed at 1234, 989 and 924 cm^{-1} in the spectrum of the ligand are also C-N stretchings. The last two bands were detected with weak intensity. Some of these modes appear in both IR and Raman spectra of the complex as well. In the IR spectra they can be seen at 1234 and 1236 cm^{-1} , while in the Raman spectra they are situated at 1242 and 1248 cm^{-1} , for HAOA and ErAOA respectively (Table 1). The very weak signal at 989 cm^{-1} in the IR spectrum of the ligand (absent in the IR spectrum of the complex), which was assigned to the trigonal pyrimidine ring breathing mode^{52, 69}, can not be observed in the corresponding Raman spectra.

COOH group vibrations

The $\nu(\text{O-H})$ and $\gamma(\text{O-H})$ modes are in general characterized as almost pure modes. The IR shoulder at 1140 cm^{-1} in the IR spectrum of the HAOA is assigned to the in-plane bending $\delta(\text{OH})$. This mode appears as a weak peak at 1132 cm^{-1} in the IR spectrum of Er(III) complex, whereas in the Raman spectra can be seen just for the complex as a very weak peak at 1122 cm^{-1} . The strong IR band at 1667 cm^{-1} is tentatively assigned to the $\nu(\text{C=O})$ mode of the carboxylic group of the ligand. It has to be mentioned that strong H-bonds are expected in the solid state through this group. The Raman bands at 425 and 249 cm^{-1} (HAOA) and at 442 and 255 cm^{-1} (Er(III) complex of HAOA) were assigned as $\Delta_{\text{as}}(\text{COO}^-)$ and $\Delta_{\text{s}}(\text{COO}^-)$ modes, respectively. The symmetrical COO⁻ stretching mode was observed in the IR spectra as medium and strong bands at 1405 and 1379



cm^{-1} for the ligand and its Er(III) complex, respectively, while in the Raman spectra this vibration appears as a strong peak at 1349 cm^{-1} only for the complex (Figs. 2 and 3).

In general, between the IR and Raman spectra of the ligand in comparison to the same spectra of the metal complex we can assert wavenumbers shifting, increases and/or decreases in relative intensities, and appearances and/or disappearings of bands. These changes can be caused by a decrease in the force constants of the bonds and polarization of the C-C, C-H bonds in the pyrimidine rings⁴⁶. The formation of complexes with lanthanides perturbs not only the aromatic systems of the rings, but also the quasiaromatic systems⁶³⁻⁶⁹. The metal affects the Er-O bonds and this effect is transferred to the C-O bonds. After that, the force constant of OCC_{ring} bond is changed, which reflects in the displacement of electronic charge around bonds between heterocyclic rings, and heterocyclic rings and protons⁶⁹. The pyrimidine ring bending vibration and the skeletal deformation bands of the free ligand, mainly in the $900\text{-}300 \text{ cm}^{-1}$ wavenumber region, show considerable changes on complex formation (Figs. 2 and 3; Table 1). These changes may be attributed to distortion of the pyrimidine rings upon complexation.

Furthermore, the spectra in the frequency region below 600 cm^{-1} are particularly interesting, since they provide information about metal-ligand vibrations. The new bands at 611 cm^{-1} and at 501 cm^{-1} present only in the IR spectrum of the complex, which can not be observed in its Raman spectrum, can be due to the Er-O interactions^{43,44,53}. In the low wavenumbers region of the Raman spectrum of the complex (Fig. 3), the band that can be due to the Er-O vibrations⁶⁴⁻⁶⁸, is the band at 394 cm^{-1} , which confirm the presence of the Er-O interaction. The metal affects the carboxylate anion as well as the ring structure. The ionic potential of the metal is the most important parameter responsible for the influence of the metal on the rest of the molecule⁶⁹⁻⁷¹. The carboxylic acids interact with the metals as symmetric^{72,73}, bidentate carboxylate anions and both oxygen atoms of the car-

boxylate are symmetrically bonded to the metal⁷⁴. In this sense, we can observe in the Raman spectrum of the Er(III) complex a weak shoulder at 207 cm^{-1} , which can be due to the O1-Er-O3 vibration modes (Table 1)^{68,75-77}.

Thus, on the basis of the experimental and theoretical results, we are able to suggest that in the Er(III) complex studied, the metal ion coordinated to the carboxylic oxygen atoms, as it is shown in Fig. 4.

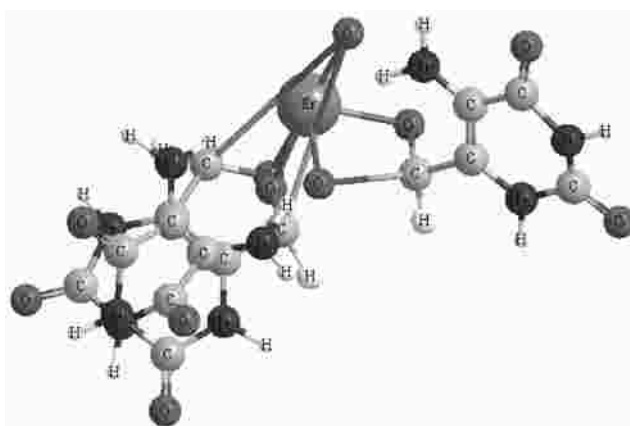


Fig. 4: Suggested metal-ligand coordination in the investigated Er(III) complex

Pharmacology

The lanthanide inhibiting ROS involves strong oxyphilicity inherent in lanthanides, because of the availability of oxygen sites on these free radicals, makes them excellent targets for Ln(III) coordination attack. This causes lanthanides to play the role of scavengers of reactive oxygen species, therefore presenting good potential for lanthanides as future drugs for a number of degenerative diseases due to ROS. The involvement of lanthanides in ROS removal is quite different from the inhibition of ROS by organic compounds. Most of the organic antioxidants scavenge free radicals by single electron exchange with radicals and thus transform themselves into radicals, hence acting as “pro-oxidants”. Lanthanides very easily interact with either free radicals or peroxides but are not transformed as radicals. However the mechanistic understanding about the role of Ln(III) as scavengers of antioxidant remains very meager^{28,29,34,35}.

Synthesis and Vibrational Characterization of New Er(III) Complex with Hepatoprotective and Antioxidant Activity

In the present study we performed comparative evaluation of the antioxidant effects and hepatotoxicity of the ligand and the newly synthesized erbium(III) complex. The tested compounds were investigated for possible hepatotoxicity on rat hepatocytes, isolated by two-stepped, collagenase perfusion, and for possible antioxidant activity in a model of non-enzyme-induced lipid peroxidation on isolated rat liver microsomes, model of lipid membrane.

Effects of HAOA and ErAOA on isolated rat liver microsomes

One of the most suitable sub-cellular *in vitro* systems for investigation of drug metabolism is isolated microsomes.

Administered alone, HAOA and ErAOA, did not reveal statistically significant toxic effects on isolated rat microsomes. The level of malondialdehyde (MDA), marker for lipid peroxidation, was not increased statistically significant from both HAOA and ErAOA, compared to the control (non-treated microsomes) (Fig. 5).

In conditions of non-enzyme-induced lipid peroxidation,

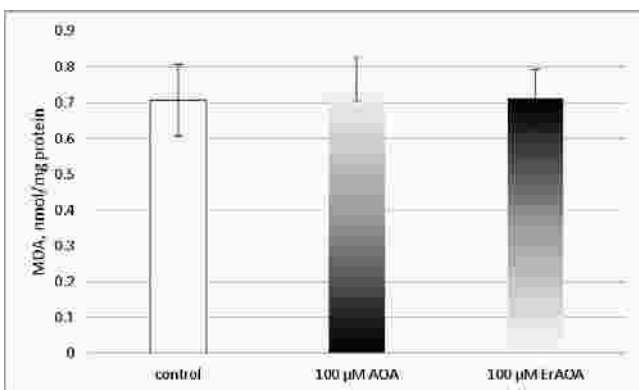


Fig. 5: Effects of 100 μM HAOA and ErAOA, administered alone, on isolated rat microsomes

the examined compounds HAOA and ErAOA, revealed statistically significant antioxidant activity, compared to toxic agent – Fe²⁺/AA (iron/ascorbate). The antioxidant effect was most prominent in complex ErAOA (Fig. 6). Microsomes incubation with Fe²⁺/AA, resulted in statis-

tically significant increase of the amount of MDA with 191 % vs control (non-treated microsomes). In non-enzyme-induced lipid peroxidation model, pre-treatment with HAOA and ErAOA at concentration 100 μM, significantly reduced lipid damage by 44 and by 67 %, respectively, as compared to the toxic agent (Fe²⁺/AA) (Fig. 6).

The antioxidant effect was most prominent in pre-treatment with the complex ErAOA.

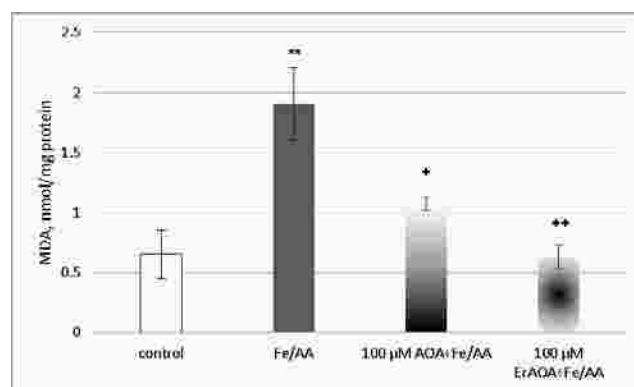


Fig. 6: Effects of 100 μM HAOA and ErAOA, in non-enzyme-induced lipid peroxidation, on isolated rat microsomes

** P < 0.01 vs control (non-treated microsomes)
+ P < 0.05; ++ P < 0.01 vs toxic agent (Fe²⁺/AA)

Effects of HAOA and ErAOA on isolated rat liver hepatocytes

In vitro studies are suitable for assessing new perspective compounds. The perspective new compounds, with proved pharmacological activity and predictable hepatic metabolism, must be examined for cyto- and hepatotoxicity. Convenient, well-controlled biological model systems with high drug-metabolizing capacities, which can be used in experimental toxicology, are isolated rat hepatocytes.

Administered alone, the compounds HAOA and ErAOA, revealed statistically significant cytotoxic effects on freshly isolated rat hepatocytes. The cytotoxicity of complex ErAOA was lower than those of HAOA (Table 2).



Table 2: Effects of 100 μ M HAOA and ErAOA, administered alone, on parameters, characterizing the functionally-metabolizing capacity of isolated rat hepatocytes

Group	Cell viability, %	LDH leakage, μ mol/min/ 10^6 cells	GSH level, nmol/ 10^6 cells	MDA level, nmol/ 10^6 cells
Control	89 \pm 3.5	0.115 \pm 0.01	20 \pm 3.1	0.055 \pm 0.01
100 μ M HAOA	66 \pm 4.1 **	0.253 \pm 0.01 **	15 \pm 2.2 *	0.110 \pm 0.01 **
100 μ M ErAOA	71 \pm 3.5 **	0.230 \pm 0.01 **	17 \pm 2.1 *	0.100 \pm 0.01 **

* P < 0.05; ** P < 0.01 vs control (non-treated hepatocytes)

The ligand HAOA decreased the cell viability (measured by Trypan blue exclusion) and level of reduced glutathione (GSH) with 26% and 25%, respectively; and increased lactate dehydrogenase (LDH) leakage and MDA production with 120% and 100%, compared to the control (non-treated hepatocytes) (Table 2).

The complex ErAOA decreased the cell viability and level of GSH with 20 % and 15 %, respectively; and increased LDH leakage and MDA production with 100 % and 82 %, compared to the control (non-treated hepatocytes) (Table 2).

The microsomal fraction, which is prepared by differential centrifugation, contains fragments from the endoplasmic reticulum and preserve the enzyme activity, mostly cytochrome P450 enzymes. Microsomes are used as a model of lipid membrane in experiments, related to the process of lipid peroxidation⁷⁸. Here, we show that HAOA and ErAOA revealed statistically significant antioxidant effect in non-enzyme-induced lipid peroxidation in isolated microsomes. The antioxidant effects were more prominent in the complex ErAOA compared to HAOA. These effects of ErAOA might be due to the presence of Er(III) ion in this complex.

In experimental toxicology, the *in vitro* systems are widely used for the investigation of the xenobiotics biotransformation, and for revealing the possible mechanisms of toxic stress and its prevention. Isolated liver cells are a convenient model system for evaluation of

the cytotoxic and cytoprotective effects of some promising biologically active compounds both newly synthesized and derived from plants. On isolated rat hepatocytes, both HAOA and ErAOA revealed statistically significant cytotoxic effects, but the complex ErAOA showed lower cytotoxicity than HAOA. This lower cytotoxicity might be due to the complexation process.

Conclusions

The complex of Er(III) with 5-aminooorotic acid has been synthesized and characterized by elemental and vibrational spectral analyses. IR and Raman spectra of 5-aminooorotic acid and its Er(III) complex were recorded and the marker bands of characteristic functional groups were identified, in order to use them as data bank for further application in trace analysis of rare-earth complexes.

The vibrational analysis performed for the studied species, 5-aminooorotic acid and its Er(III) complex, helped to explain the vibrational behavior of the ligand vibrational modes, sensitive to interaction with Er(III). The vibrational studies and the previous density functional calculations revealed that the mode of binding was bidentate through the carboxylic oxygen atoms. Theoretical and spectral studies gave evidence for the coordination mode of the ligand to Er(III) ion and hence they were in agreement with the other literature studies and theory predictions.

Synthesis and Vibrational Characterization of New Er(III) Complex with Hepatoprotective and Antioxidant Activity

According to our expectations the Er(III) complex as other investigated earlier by us lanthanide(III) complexes possesses antioxidant activity and its effects are clearly expressed. The antioxidant effects were more prominent in the complex ErAOA compared to the ligand HAOA and this observation might be due to the presence of Er(III) ions in the complex. The lower cytotoxicity of the complex ErAOA might be also due to the complexation process and to the influence of Er(III) ions. Taken together the results from the pharmacology screening give us reason to conclude that the Er(III) complex of 5-aminoorotic acid necessitates further more detailed pharmacological evaluation. These results confirmed our previous observations on the cytotoxicity of lanthanide(III) complexes with other biologically active ligands.

Acknowledgements

The authors gratefully acknowledge the financial support from the Medical University-Sofia Grant Commission (through the project No. 78/2018).

References

1. Van der Meersch H., 2006, *J. Pharm. Belg.*, **4**, 97-104.
2. Rosenfeldt F.L., 1998, *Cardiovasc. Drugs Ther.*, **12**, 147-152.
3. MacCann M.T., Thompson M.M., Gueron I.C., Tuchman M., 1995, *Clin. Chem.*, **41**, 739-743.
4. Michalska D., Hernik K., Wysokinski R., Morzyk-Ociepa B., Pietraszko A., 2007, *Polyhedron*, **26**, 4303-4313.
5. Ruasmadiedo P., Badagancedo J.C., Fernandez Garcia E., Dellano D.G., de los Reyes Gavilan C.G., 1996, *J. Food Protect*, **59**, 502-508.
6. Kostova I., Peica N., Kiefer W., 2007, *Vibr. Spectrosc.*, **44**, 209-219.
7. Kostova I., Balkansky S., Mojzic J., 2010, *Int. J. Curr. Chem.*, **1**, 271-280.
8. Person W.B., Szczepaniak K., In *Vibrational Spectra and Structure*; Durig, J. R., Ed.; Elsevier: Amsterdam, 1993, p 239-325.
9. Rostkowska H., Szczepaniak K., Nowak M.J., Leszczynski J., Kubulat K., Person W.B., 1990, *J. Am. Chem. Soc.*, **112**, 2147-2160.
10. Gould I.R., Hillier I.H., 1990, *J. Chem. Soc. Perkin Trans*, **2**, 329-330.
11. Thomas Jr. G.J., Tsuboi M., In *Advances in Biophysical Chemistry*; Bush, C. A., Ed.; JAI Press: Greenwich, CT, 1993, p 1-70.
12. Lagant P., Vergoten G., Efremov R., Peticolas W.L., 1994, *Spectrochim. Acta A*, **50**, 961-971.
13. Rush T., Peticolas W.L., 1995, *J. Phys. Chem.*, **99**, 14647-14658.
14. Aamouche A., Berthier G., Coulombeau C., Flament J.P., Ghomi M., Henriot C., Jobic H., Turpin P.Y., 1996, *Chem. Phys.*, **204**, 353-363.
15. Aamouche A., Ghomi M., Coulombeau C., Grajcar L., Baron M.H., Jobic H., Berthier G., 1997, *J. Phys. Chem. A*, **101**, 1808-1817.
16. Nepveu F., Gaultier N., Korber N., Jaud J., Castan P., 1995, *J. Chem. Soc. Dalton Trans.*, **24**, 4005-4014.
17. Helios K., Duczmal M., Pietraszko A., Michalska D., 2013, *Polyhedron*, **49**, 259-268.
18. Kostova I., Peica N., Kiefer W., 2006, *Chem. Phys.*, **327**, 494-505.
19. Kostova I., Peica N., Kiefer W., 2007, *J. Raman Spectrosc.*, **38**, 205-216.
20. Kostova I., Traykova M., Rastogi V.K., 2008, *Med.*



- Chem.*, **4**, 371-378.
21. Kostova I., Stefanova T., 2010, *J. Rare Earths*, **28**, 40-46.
22. Kostova I., Stefanova T., 2010, *J. Trace Elem. Med. Biol.*, **24**, 7-13.
23. Kostova I., Traykova M., 2006, *Med. Chem.*, **2**, 463-470.
24. Kostova I., Momekov G., 2008, *J. Coord. Chem.*, **61**, 3776-3792.
25. Kostova I., Stefanova T., 2009, *J. Coord. Chem.*, **62**, 3187-3197.
26. Kaur J., Tsvetkova Y., Arroub K., Sahnoun S., Kiessling F., Mathur S., 2017, *Chem. Biol. Drug Design*, **89**, 269-276.
27. Misra S.N., Ramchandriah G., Gagnani M.A., Indiradevi M., Shukla R.S., 2017, *Appl. Spectrosc. Rev.*, **38**, 433-493.
28. Ajlouni A.M., Taha Z.A., Al-Hassan K.A., Anzeh A.M., 2012, *J. Luminesc.*, **132**, 1357-1363.
29. Xi P.X., Xu Z.H., Liu X.H., Chen F.J., Huang L., Zeng Z.Z., 2008, *Chem. Pharmac. Bull.*, **56**, 541-549.
30. Peng Y., Hu J.X., Lu H., Wilson R.M., Motevalli M., Hernández I., Gillin W.P., Wyatt P.B., Ye H.Q., 2017, *RSC Advances*, **7**, 128-131.
31. Ahmed Z., Aderne R.E., Kai J., Resende J.A., Cremona M., 2016, *Polyhedron*, **119**, 412-419.
32. Karbowski M., Rudowicz C., Nakamura T., Murakami R., Ishida T., 2016, *Chem. Phys. Lett.*, **662**, 163-168.
33. Cherkasova E.V., Peresyphkina E.V., Virovets A.V., Cherkasova T.G., 2016, *Russ. J. Inorg. Chem.*, **61**, 174-179.
34. Gueye M.N., Dieng M., Thiam I.E., Lo D., Barry A.H., Gaye M., Retailleau P., 2016, *South Afr. J. Chem.*, **70**, 8-15.
35. Antonenko T.A., Shpakovsky D.B., Gracheva Y.A., Balashova T.V., Pushkarev A.P., Bochkarev M.N., Milaeva E.R., 2017, *Inorg. Chim. Acta*, **455**, 276-282.
36. A Hernanz A., Billes F., Bratu I., Navarro R., 2000, *Biopolymers Bioospectroscopy*, **57**, 187-198.
37. Wysokiński R., Morzyk-Ociepa B., G³owiak B.T., Michalska D., 2002, *J. Mol. Struct. Theochem*, **606**, 241-251.
38. Baran E.J., Mercader R.C., Hueso-Ureña F., Moreno-Carretero M.N., Quiros-Olozabal M., Salas-Peregrin J.M., 1996, *Polyhedron*, **15**, 1717-1721.
39. Darensbourg D.J., Draper J.D., Larkins D.L., Frost B.J., Reibenspies J.H., 1998, *Inorg. Chem.*, **37**, 2538-2546.
40. Lewandowski W., Kalinowska M., Lewandowska H., 2005, *J. Inorg. Biochem.*, **99**, 1407-1423.
41. Lalioti N., Raptopoulou C.P., Terzis A., Panagiotopoulos A., Perlepes S.P., Manessi-Zoupa E., 1998, *J. Chem. Soc. Dalton Trans.*, **8**, 1327-1334.
42. Horn K.H., Böres N., Lehnert N., Mersmann K., Näther C., Peters G., Tuczek F., 2005, *Inorg. Chem.*, **44**, 3016-3030.
43. Li X., Shi Q., Sun D., Bi W., Cao R., 2004, *Eur. J. Inorg. Chem.*, **2004**, 2747.
44. Icbudak H., Olmez H., Yesilel O.Z., Arslan F., Naumov P., Jovanovski G., Ibrahim A.R., Usman A., Fun H.K., Chantrapromma S., Ng S.W., 2003, *J. Mol. Struct.*, **657**, 255-270.
45. Papaefstathiou G.S., Manessi S., Raptopoulou C.P., Behrman E.J., Zafirooulos T.F., 2004, *Inorg. Chem.*

Synthesis and Vibrational Characterization of New Er(III) Complex with Hepatoprotective and Antioxidant Activity

- Comm.*, **7**, 69-72.
46. Lacher J.R., Bitner J.L., Emery D.J., Seffl M.E., Park J.D., 1955, *J. Phys. Chem.*, **59**, 610-614.
47. Lencioni S., Pellerito A., Fiore T., Giuliani A.M., Pellerito L., Cambria M.T., Mansueto C., 1999, *Appl. Organometal. Chem.*, **13**, 145-157.
48. Exner K., Fischer G., Bahr N., Beckmann E., Lukan M., Yang F., Rihs G., Keller M., Hunkler D., Knothe L., Prinzbach H., 2000, *Eur. J. Org. Chem.*, **5**, 763-785.
49. Castaneda J., Denisov G.S., Kucherov S.Y., Schreiber V.M., Shurukhina A.V., 2003, *J. Mol. Struct.*, **660**, 25-40.
50. Gonzalez-Sanchez F., 1958, *Spectrochim. Acta*, **12**, 17-33.
51. Hadzi D., Sheppard N., 1953, *Proc. Roy. Soc. Ser. A*, **216**, 247-251.
52. Ortiz S., Alcolea Palafox M., Rastogi V.K., Tomer R., 2012, *Spectrochim Acta A*, **97**, 948-962.
53. Lin-Vien D., Colthup N.B., Fateley W.G., Grasselli J.G., The Handbook of Infrared and Raman Characteristic Frequencies of Organic Molecules; Eds. H. B. Jovanovich; Academic Press Inc., San Diego, 1991, 140.
54. Dolish F.R., Fateley W.G., Bentley F.F., Characteristic Raman Frequencies of Organic Compounds, John Wiley & Sons Inc., 1974, 128.
55. Orza J.M., García M.V., Alkorta I., Elguero J., 2000, *Spectrochim Acta A*, **56**, 1469-1498.
56. Szabo A., Èešljèviæ V.I., Kovács A., 2001, *Chem. Phys.*, **270**, 67-78.
57. Lewandowski W., Barañska H., 1991, *Vib. Spectrosc.*, **2**, 211-220.
58. Sourisseau C., Fouassier M., Mauricot R., Boucher F., Evain M., 1997, *J. Raman Spectrosc.*, **28**, 973-978.
59. Lu Y., Deng G., Miao F., Li Z., 2003, *Carbohydrate Res.*, **338**, 2913-2919.
60. Sohn J.R., Chun E.W., Pae Y.I., 2003, *Bull. Korean Chem. Soc.*, **24**, 1785-1791.
61. Jayaraman A., Sharma S.K., Wang S.Y., Shieh S.R., Ming L.C., Cheong S.W., 1996, *J. Raman Spectrosc.*, **27**, 485-490.
62. Fielicke A., Meijer G., Von Helden G., 2003, *Eur. Phys. J.*, **D24**, 69-72.
63. Lewandowski W., Dasiewicz B., Koczon P., Skierski J., Dobrosz-Teperek K., Swislocka R., Fuks L., Priebe W., Mazurek A.P., 2002, *J. Mol. Struct.*, **604**, 189-193.
64. Koczon P., Lewandowski W., Mazurek A.P., 1999, *Vib. Spectrosc.*, **20**, 143-150.
65. Kakiuchi M., Abe T., Nakayama H., 2001, *Geochem. J.*, **35**, 285-293.
66. Wang K., Li Y.S., 1997, *Vib. Spectrosc.*, **14**, 183-188.
67. Boerio F.J., Hong P.P., Clark P.J., Okamoto Y., 1990, *Langmuir*, **6**, 721-727.
68. Kwon Y.J., Son D.H., Ahn S.J., Kim M.S., Kim K., 1994, *J. Phys. Chem.*, **98**, 8481-8487.
69. Galdecka E., Galdecki Z., Huskowska E., Amirkhanov V., Legendziewicz J., 1997, *J. Alloys Compounds*, **257**, 182-190.
70. de Andrés A., Taboada S., Martínez J.L., 1993, *Phys. Rev.*, **B47**, 14898-14904.
71. Cho B.O., Lao S.X., Chang J.P., 2003, *J. Appl. Phys.*, **93**, 9345-9351.



-
72. Zaidi S.I., Agarwal R., Eichler G., Rihter B.D., Kenney M.E., Mukhtar H., 1993, *Photochem. Photobiol.*, **58**, 204-210.
73. Deby C., Goutier R., 1990, *Biochem. Pharmacol.*, **39**, 399-405.
74. Lowry O.H., Rosebrough N.J., Farr A.L., Randal R.J., 1951, *J. Biol. Chem.*, **193**, 265-275.
75. Kim H.J., Chun Y.J., Park J.D., Kim S.I., Roh J.K., Jeong T.C., 1997, *Planta Med.*, **63**, 415-418.
76. Mitcheva M., Kondeva M., Vitcheva V., Nedialkov P., Kitanov G., 2006, *Redox Rep.*, **11**, 3-8.
77. Fau D., Berson A., Eugene D., Fromently B., Fisch C., Pessayre D., 1992, *J. Pharmacol. Exp. Ther.*, **263**, 69-77.
78. Oh K.Y., Roberts V.H., Schabel M.C., Grove K.L., Woods M., Frians A.E., 2015, *Radiology*, **276**, 110-118.



Ru(III) Catalysed Oxidation of Glucitol and Osmitrol with Chloramine T in Alkaline medium

Swarn Lata Bansal and Amrita Srivastava

Department of Chemistry, Lucknow University, Lucknow, U.P., India - 226007

Email: swtbansal28@gmail.com

Abstract

Kinetics of oxidation of Glucitol and Osmitrol by Chloramine T in alkaline medium in presence of Ru(III) homogeneous catalyst is reported. The empirical rate law in terms of disappearance of CAT is proposed as follows:

$$-\frac{d[\text{CAT}]}{dt} = k_1[\text{CAT}] + k_2[\text{Ru}]$$

where k_1 is the observed first order rate constant with respect to Chloramine T and k_2 is a constant depending upon the concentration of substrates and hydroxide ion.

Keywords: Kinetics, Mechanism, Oxidation, Chloramine T, Ruthenium (III) Catalyst

Introduction

Chloramine-T (CAT) is the most important member of organic haloamine family and behaves as an oxidizing agent in both acidic and alkaline media¹⁻⁵. It is a versatile oxidizing agent and shows a variety of kinetic results due to formation of its various oxidizing species depending upon the pH of the medium. Many reviews have reported the role of Ruthenium as a catalyst in redox reactions involving complexes⁶⁻⁸ but little attention has been paid to explore the catalytic role of Ru with N-halo compounds as oxidants⁹⁻¹⁰. The mechanism proposed for the oxidation of organic substrates involves the formation of a 1:1 complex of Ru and the anion of organic substrates as the first step followed by its decomposition to intermediate products and Ru(VI).

A lot of literature is available on the kinetics of oxidation of sugar alcohols¹¹⁻¹³ using various oxidants. Some work has been done on catalytic oxidation, using transition metal catalysts¹⁴⁻²⁰. Therefore in the present communication, an attempt has been made to study the kinetics and mechanism of Ru(III) catalysed oxidation²¹ of Glucitol and Osmitrol by CAT in alkaline medium. The study of sugar alcohols have been carried out due to its biological importance.

Materials and Methods

All the reagents were of analytical grade, and double distilled water was used throughout the work. The samples of Glucitol and Osmitrol used in this investigation were of E. Merck (India) brand. G.R. samples of sodium hydroxide, sodium carbonate and sodium bicar-



bonate were used by dissolving in distilled water. A stock solution of CAT (Loba, AR) was prepared in double distilled water and standardized using iodometric method and preserved in brown bottles. A solution of Ruthenium chloride (E. Merck) was prepared by dissolving a known weight of RuCl_3 in NaOH of known strength and stored in a black coated bottle to prevent photochemical oxidation. The standard solution of $\text{Hg}(\text{OAc})_2$ of known strength was also used without further purification. All other reaction vessels were also coated black from outside to avoid any photochemical degradation.

Kinetics

A thermostatic water bath was used to maintain the desired temperature with $\pm 0.1^\circ\text{C}$ accuracy. Requisite volumes of reagents, including substrate, was taken in a reaction vessel and thermostated at $35 \pm 0.1^\circ\text{C}$ for attaining thermal equilibrium. A measured volume of oxidant solution, which was also maintained separately at the same temperature, was rapidly added to the reaction vessel. The kinetics was followed by examining aliquots of the reaction mixture at regular intervals for unreacted oxidant using the iodometric method with starch as an indicator.

Result and Discussion

The kinetic measurements for the rate of the oxidation of Glucitol and Osmitrol were carried out in a wide range of reactant concentrations. CAT oxidation of these substrates have also been studied by us in aqueous

alkaline medium in the absence of Ru catalyst and it was noticed that the uncatalysed reaction takes place at very low concentrations. The present kinetic study involves catalysed as well as uncatalysed reactions occurring simultaneously²².

The reaction shows a zero order plot for the rate of oxidation of Glucitol (Fig 1). In order to avoid the possible error involved due to interference of the reaction products on the reaction rate, the initial $(-dc/dt)$ has been calculated. The values of $(-dc/dt)$, obtained at varying concentrations of CAT are presented in Fig 2, where $(-dc/dt)$ is plotted against the corresponding concentration of CAT. This deviation from the straight line clearly demonstrates that deactivation of Ruthenium plays a role in the reaction. The straight line intercepting the rate axis indicates that a part of the reaction is independent of the CAT concentration while the other part is dependent on it. In the oxidation of Glucitol by CAT, the reaction obeys first order kinetics. This confirms that the order with respect to CAT is zero even up to wide range of concentrations. Similarly the kinetic data collected for Osmitrol (Fig 3) shows that the reaction is taking place in two parts, one in which Ru (VI) catalysed oxidation shows zero order dependence of the reaction rate and other in which uncatalysed oxidation indicates dependence of the reaction rate on $[\text{CAT}]$ in each case. Figure 4 demonstrates that the reaction rate, which follows nearly first order kinetics at low Glucitol concentration, tends to decrease at higher concentration.

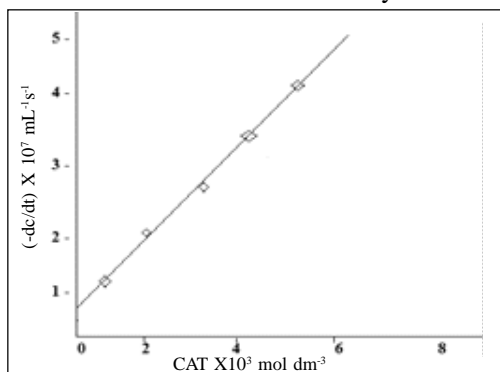


Fig.1 Rate of oxidation of Glucitol at different concentrations of CAT

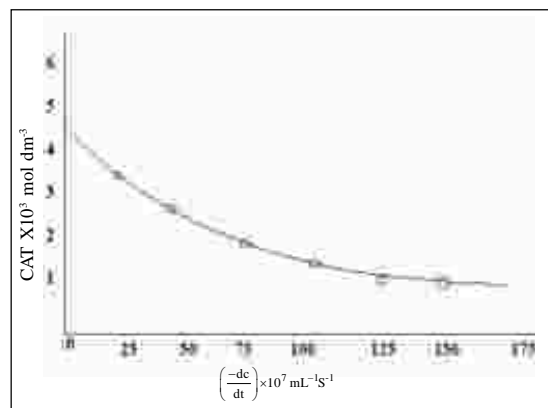


Fig. 2 Rate (dc/dt) obtained at different concentrations of CAT

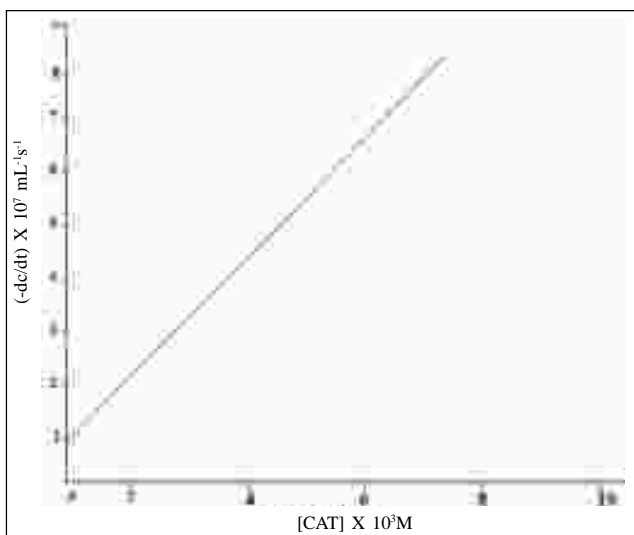


Fig. 3 Kinetic data for Osmitol

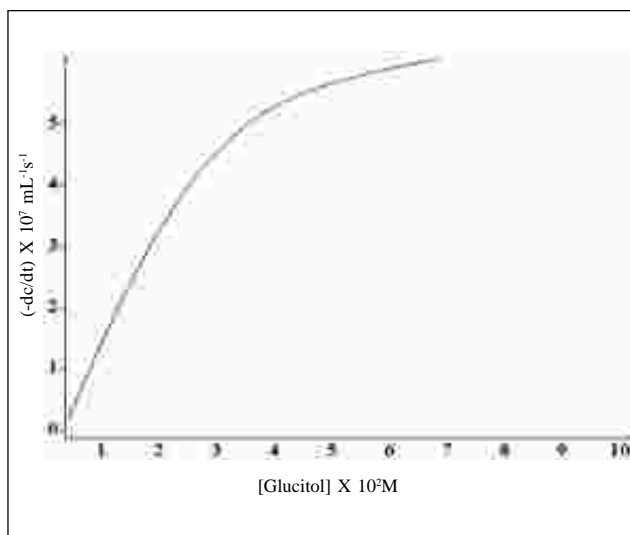


Fig. 4 Reaction rate data showing first order kinetics at low Glucitol concentrations

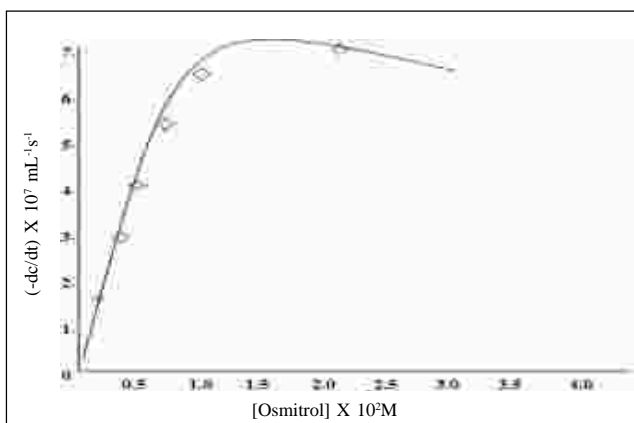


Fig. 5 Reaction rate data showing first order kinetics at low concentrations of Osmitol

The result presented in Fig 5 again indicates that the reaction rate follows nearly first order kinetics at low Osmitol concentrations. The kinetic study of glucitol carried out in alkaline buffer containing sodium carbonate and bi-carbonate, indicates that reaction rate follows nearly first order kinetics at low hydroxyl concentration and shows retarding effect at higher concentrations (Table 1). Similarly, hydroxyl ion variation in the case of kinetics of osmitol oxidation indicates the same trend as it observed in case of Glucitol (Fig 6).

Table 1: Kinetics of Glucitol

$[\text{Na}_2\text{CO}_3] = 10 \times 10^{-2} \text{ M}$
 $[\text{CAT}] = 2.5 \times 10^{-3} \text{ M}$

$[\text{Glucitol}] = 5 \times 10^{-2} \text{ M}$
 $[\text{RuO}_4] = 4.0 \times 10^{-4} \text{ M}$

$\mu = 1.30 \text{ M}$

pH	$(-dc/dt) \times 10^7$	$(-dc/dt) \times 10^2 / [\text{OH}^-]$
10.0	1.40	3.5
10.5	1.46	3.3
11.0	1.51	3.2
11.5	1.56	3.0
12.0	1.60	2.8
12.5	1.63	2.6



Fig 7 indicates the effect of Ru on the oxidation rates of Glucitol and Osmitol. The straight line indicates the direct proportionality of the reaction rate with respect to the catalyst concentration and the intercept is for the uncatalysed path of the reaction.

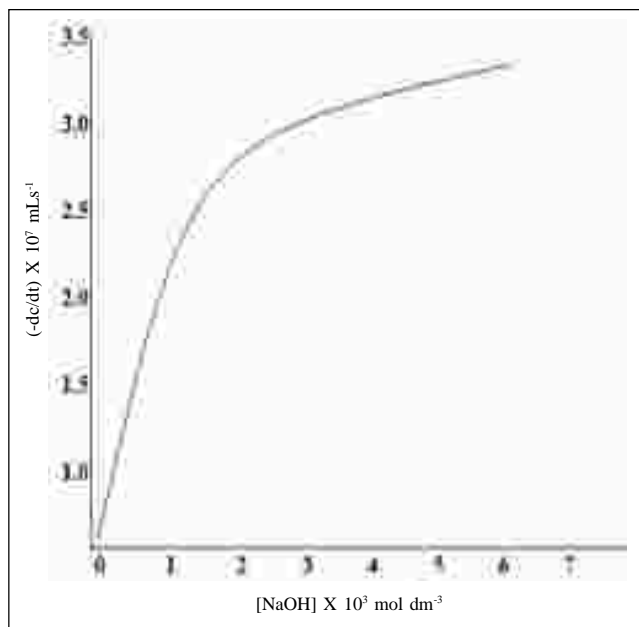


Fig.6 Effect of Hydroxyl ion on the oxidation of Osmitol

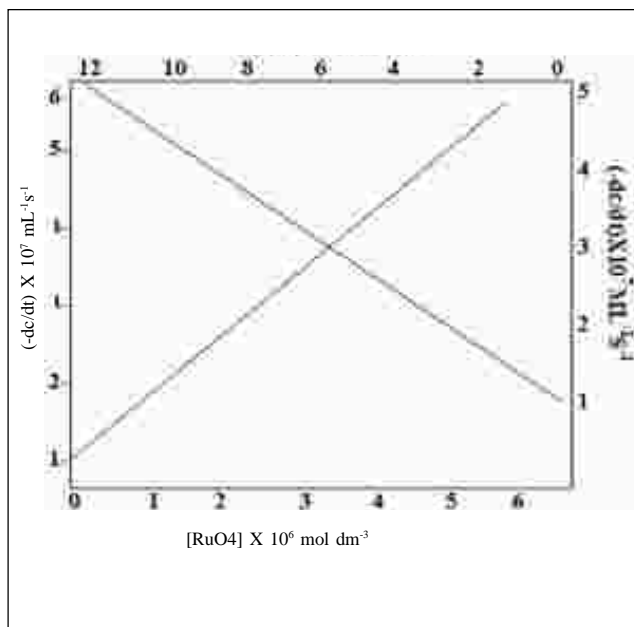
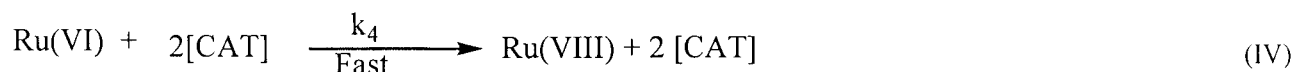
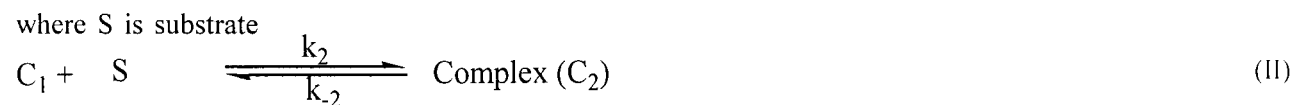
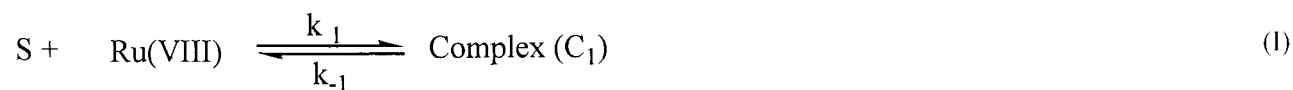


Fig. 7 Effect of Ruthenium Tetraoxide on the oxidation of Glucitol and Osmitol

On the basis of experimental results obtained, we can assume the first order dependence of the reaction rate on catalyst, alcohol and hydroxyl ion at lower concentrations and zero order on CAT. Thus, under these conditions, a probable rate law might be given as

$$\frac{-d[\text{CAT}]}{dt} = k_1[\text{CAT}] + k_2[\text{RuO}_4] \dots\dots\dots (1)$$

where [CAT] is Chloramine T concentration and k_1 is the observed first order rate constant with respect to CAT and k_2 is a constant depending upon the concentration of the substrates and hydroxyl ion. The first term on the right hand side of Equation 1 is due to the uncatalyzed oxidation and the second term is due to the oxidation taking place with catalyst Ruthenium tetra oxide.



where [S] represent the respective polyhydric alcohols.

Assuming the steady state conditions for the concentrations of Complexes C₁ and C₂ we get,

$$[C_1] = \frac{k_1[Ru(VIII)][S] + k_{-2}[C_2]}{k_{-1} + k_2[S] + k_2[OH^-]} \quad (2)$$

$$[C_2] = \frac{k_2[C_1][S]}{k_{-2}} = K[C_1][S] \quad (3)$$

where $K = \frac{k_2}{k_{-2}}$

Eliminating C₂ from Equation (2), the concentration of C₁ would be

$$C_1 = \frac{k_1[Ru(VIII)][S]}{k_{-1} + k_3[OH^-]} \quad (4)$$

The total Ru(VIII) concentration might be obtained from Eq. 5

$$[Ru(VIII)]_0 = [Ru(VIII)] + [C_1] + [C_2] \quad (5)$$

Substituting the value of Ru(VIII) in Eq. 3 and eliminating C₂, the value of C₁ comes out to be

$$[C_1] = \frac{k_1[S][Ru(VIII)]_0}{k_{-1} + k_3[OH^-] + k_1[S]\{1 + k(S)\}} \quad (6)$$

The rate law in terms of decreasing concentration of CAT would be

$$\frac{-d[CAT]}{dt} = \frac{2d[Ru(VI)]}{dt} = 2k_3[C_1][OH^-] \quad (7)$$

From Eqs. (6) and (7), the rate law comes out to be

$$\frac{-d[CAT]}{dt} = \frac{2k_1k_3[S][Ru(VIII)]_0[OH^-]}{k_{-1} + k_3[OH^-] + k_1[S]\{1 + k(S)\}} \quad (8)$$

Eq. 8 is valid only up to the first stage of oxidation of substrate. The actual rate law in terms of Chloramine T (CAT), should be multiplied by the equivalence of CAT as obtained for the respective organic substrates.



The validity of rate law as given by Eq. 8 can be verified under different conditions. When no complex C_2 is formed ($k = 0$) and Eq. 8 reduces to

$$-\frac{d[\text{CAT}]}{dt} = \frac{2k_1 k_3 [\text{S}] [\text{Ru(VIII)}]_0 [\text{OH}^-]}{k_{-1} + k_3 [\text{OH}^-] + k_1 [\text{S}]} \quad (9)$$

Similarly the retarding effect of Glucitol also shows under the conditions

$$-\frac{d[\text{CAT}]}{dt} = \frac{2k_1 k_3 [\text{S}] [\text{Ru(VIII)}]_0 [\text{OH}^-]}{k_{-1} + k_3 [\text{OH}^-]} \quad (10)$$

The retarding effect due to the variation of hydroxyl ion on the oxidation of Osmitrol is very well explained by Eq. 10. The oxidation products of Glucitol and Osmitrol could not be determined significantly. The formation of oxalic acid was confirmed by TLC and UV spectral analysis. UV spectra showed absorbance band at 256 nm. (Fig. 8) This indicates that the complex formation has taken place between Ru (VIII) and substrate.

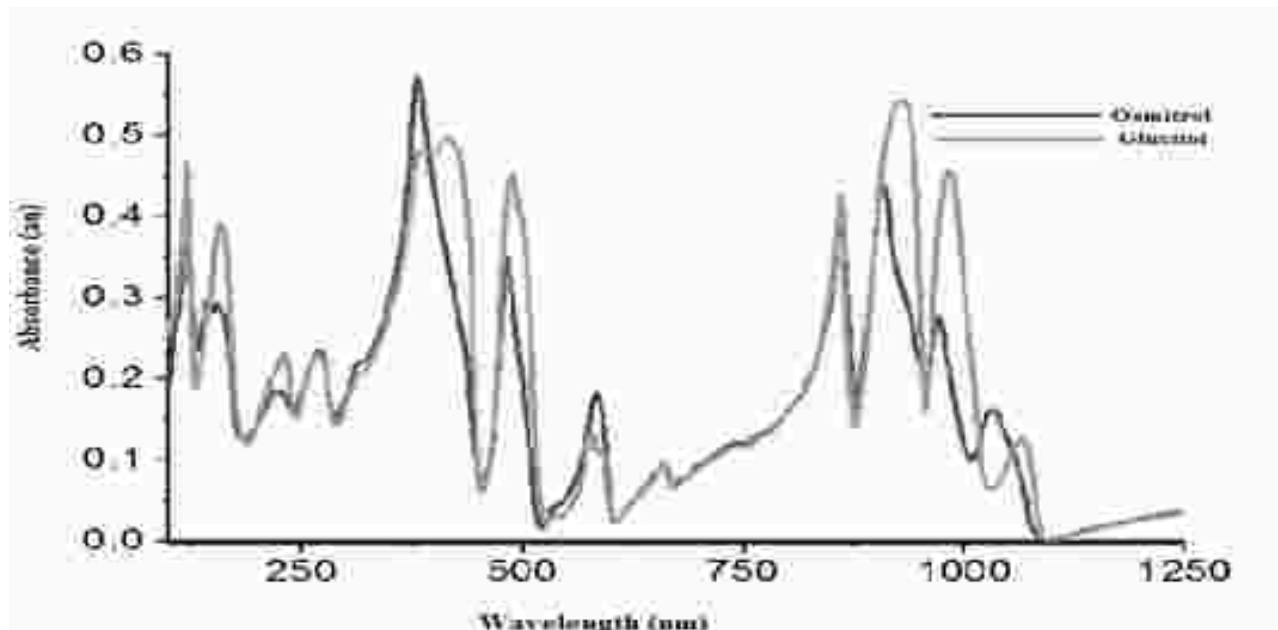


Fig. 8: UV spectra of Glucitol and Osmitrol

The rate law is in agreement with all kinetic observations and the proposed mechanistic steps are supported by negligible effect of ionic strength.

References

1. Rangappa K.S., 2004, *J. Ind. Chem. Soc.*, 81.
2. Neelu Kamboo and Santosh Kumar Uppadhya, 2000, *Transition Metal Chemistry*, **25**, 461-464.
3. Mishra S.P., Anju Singh, Jyoti Verma, Srivastava V.K. and Singh R.A., 2005, *Asian Journal of Chemistry*, **17(3)**, 1415-1422.

4. Srivastava S. and Pushpanjali, 2008, *Bulletin of the Catalysis Society of India*, **7**, 12-19.
5. Kumar P., Gupta and Vehari, C.K., 1985, *React. Kinet. Catal. Lett.*, **29**, 297-305.
6. Srivastava S., Ajaya Awasthi and Vartika Srivastava, 2003, *Oxidation communication*, **26(3)**, 426-431.
7. Srivastava S., Sarika Singh and Parul Srivasata, *Asian Journal of Chemistry*, 2008, **20(1)**, 317-328.
8. Singh, B. Aniruddh K. Singh, Chhaya, Ashish and Kumud Lata Singh, 2011, *Int. J. of Pure and Applied Chem.*, **6**, 23-29.
9. Ajaya Kumar Singh, Reena Negi, Bhawana Jain, Vokraj Katre, Surya P. Singh Virendra K. Singh, Singh, A.K., Negi, R., Jain, B. et al., 2009, *Catal Lett*, **132(1)**, 285-291.
10. Prashanth P.A., Mantelingu, K., Anandamurty A.S., Anitha N., Rangaswamy and Rangappa K.S., 2001, *Journal of Indian Chemical Society*, **78**.
11. Lakshman Kumar Y., Venkata Nadh R. and Radga Krishna Murti P.S., (Russian), 2016, *J. Physical Chem. A*, **90(2)**, 300-307.
12. Srivastava S., Sarika Srivastava and Parul Srivastava, 2008, *Asian J. of Chemistry*, **20(1)**, 317-323.
13. Srivastava S. and Singh S., 2006, *Oxidation Communication*, **29(3)**, 708-713.
14. Singh S.P. and Singh A.K., 2009, *J. Carbohydr. Chem.*, **28**, 278-292.
15. Chandra Kumar Singh, 2012, *Search and Research*, **3**, 39-44.
16. Singh J.V., Anupam Awasthi, Deepti, Ashish Tomar and Agarwal G.L., 2012, *Orient. J. Chem.*, **28(3)**.
17. Ashok Kumar Singh, Neena Gupta, Shala Rahmani, Vinod Kumar Singh and Singh B., 2003, *Journal of Chemistry*, **42**, 1871-1875.
18. Bharat Singh, Aniruddh Kumar Singh, Chaya Singh, Ashish and Kumud Lata Singh, 2011, *IJPAC*, **6(1)**, 23-29.
19. Singh B., Singh M., Bhatnagar P. and Kumar A., 1994, *Oxid. Commun.*, **17**, 48.
20. Neena Gupta, Shala Rahmani and Singh A.K., 1999, *Oxidation Communication*, **22(2)**, 237-243.
21. Badole M.K., Malviya L.N., Sariya K.S. and Siriah V.K. 2012, *Orient. J. Chem.*, **28(3)**.
22. Asghar B.H., Altass H.M., Fawzy A. and Saudi J., 2015, *Chem. Soc. in press*.
23. Sharanabasamma K., Angadi M.A., Salunke M.S. and Tuwar S.J., 2012, *Solution Chem.* **41**, 187-199.



Physicochemical properties of Kappa-Carrageenan Packed with Zinc Oxide Nanoparticles Biocomposite Films

Flyndon Mark S. Dagalea^{1*} and Karina Milagros R. Cui-Lim^{1,2}

¹Department of Physical Sciences, College of Science,

²University Research and Development Services,

University of Eastern Philippines, University Town, Northern Samar, Philippines 6400

Email: flydondagalea@gmail.com

Abstract

Kappa-Carrageenan, a natural polymer derived from seaweeds has been gaining attention because of its biodegradability and low cost production. This study discusses the physicochemical properties of the films with and without the incorporation of Zinc oxide nanoparticles (ZnONps) to Kappa-Carrageenan. Physicochemical properties, viz. moisture content, degradation time, wavelength spectra, structural composition, and surface morphology were determined for biocomposite films with and without ZnONps.

After several tests, Zinc oxide nanoparticles incorporated in Kappa-Carrageenan exhibited some changes to its physicochemical properties: lower moisture content and longer degradation time. ZnONps was seen on the surface of the biocomposite film. However, structural composition analysis showed no new formation of functional group. The biocomposite films could be a substitute for the existing drug capsule because of its longer time of decomposition, low water content and drug safety.

Keywords: Zinc Oxide Nanoparticles (ZnONps), Biocomposite Films, Kappa-Carrageenan (kC), Physicochemical Properties

Introduction

Kappa-Carrageenan is a natural polymer product derived from the extract of seaweeds. This paper discusses the changes in the physicochemical properties of the KC biocomposite films packed with ZnONps. Incorporation of metal oxide in polymer based substances modified some of the characteristics.

The biocomposite films with ZnONps created new products of use to the pharmaceutical and packaging industries like capsule and packaging plastics with higher

degradation time for preservation of medicine and foods. Pharmaceutically produced capsules and industry produced packaging films could be replaced with these biocomposite films of KC/ZnONps.

Seaweeds produce a carbohydrate known as Carrageenan. A natural polymer like polysaccharides, it has been receiving a great deal of attention because of its biodegradability and low cost. The innate properties and structure of Carrageenan may be used for non-food applications.

Physicochemical properties of Kappa-Carrageenan Packed with Zinc Oxide Nanoparticles Biocomposite Films

A wide range of applications is possible as ZnO has important advantages. It is bio-safe, biocompatible and can be used for biomedical applications without coating. With these unique characteristics, ZnO could be one of the most important nanomaterials in future research and applications¹.

The use of acidic electrolyzed water in the production of Carrageenan and gelatin hydrosols and hydrogels has not caused undesirable changes in their chemical and texture properties².

This study deals with the physicochemical properties of biocomposite film from Kappa-Carrageenan filled with Zinc oxide nanoparticles.

Materials and Methods

Preparation of Zinc oxide from Zinc nitrate

Zinc oxide was prepared by the method reported in literature³. Nanorod Zinc oxide was prepared by using Zinc nitrate and Sodium hydroxide precursors and starch as a stabilizing agent. 0.1g Kappa-Carrageenan was dissolved in 500 mL of lukewarm distilled water. Zinc nitrate, 14.874 grams (0.1 mol), was added to the above solution, followed by constant stirring for 1 hour using magnetic stirrer to completely dissolve Zinc nitrate. After complete dissolution of Zinc nitrate, 0.2 M of NaOH solution was added dropwise with constant stirring. The reaction was allowed to proceed for 2 hours. After the completion of reaction, the supernatant solution was kept overnight and discarded carefully. Rest of the solution was centrifuged for 10 min and the supernatant solution

was discarded. The nanoparticles obtained were washed thrice using distilled water. Washing was carried out to remove the by-products and the excessive starch bound to the nanoparticles. After washing, the nanoparticles were dried at 80°C overnight.

Preparation of Biocomposite Films

The films were reported as per method reported in literature⁴. Five grams of ZnONps was dispersed in 95mL water to get 0.92% ZnONps solution, stirred for 1 hour, and then sonicated in an ultrasonic bath for 30 minutes. The solution was used to prepare the aqueous dispersion with addition of 2 g of Kappa-Carrageenan. A mixture of sorbitol and glycerol (3:2) was added as plasticizer. The biocomposite solution was heated to 85±5°C and allowed to stay for 45 minutes to allow gelatinization. Upon completion of starch gelatinization, the solution was cooled to room temperature. A portion of the solution was dispersed in a petri dish. Films were dried under controlled conditions in a humidity chamber. Control films were prepared similarly and stored at 23 ± 2°C and 50 ± 5°C.

Determination of the Physicochemical Properties of Kappa-Carrageenan packed with Zinc Oxide Nanoparticles (KC/ZnONps)

Test for Moisture Content of the Biocomposite Films:

Films were conditioned at 58% RH and 25°C for 7 days. The weight difference was determined after drying of the equilibrated films in an oven at 105°C for 24h. Moisture content (%) was calculated using the formula:

$$\text{Moisture content (\%)} = \frac{\text{Initial dried weight of film} - \text{final dried weight of film}}{\text{Initial dried weight of film}} \times 100$$

Test for Degradation Time of the Biocomposite Films

Thermogravimetric analysis was done in the temperature range of 95-600°C to determine the degradation time of the sample. The temperature range used was based on the degradation of KC and ZnONps.

Test for Wavelength Spectra of the Biocomposite Film Solution

The UV-visible transmission spectra of the biocomposite film solution were recorded from 350 to 550nm using a UV-vis spectrophotometer. The appropriate wavelength was used to know if ZnONps was incorporated into



KC. Wavelength of 370 nm was used for ZnO.⁵ Distilled water was used as the blank solution.

Test for Structural Formation of the Biocomposite Films

FTIR spectra was recorded using an attenuated total reflection (ATR) method in Smart Itr. The thin films were applied directly onto the ZnSe ATR cell. For each spectrum, 64 consecutive scans of 500 to 4000 cm^{-1} resolution were recorded.

Test for Surface Morphology of the Biocomposite Films:

The conditioned bionanocomposite samples were placed in a Scanning Electron Microscope (SEM) and the surface microstructure of films was investigated. Magnification from 500 to 4000 μm was used.

Results and Discussion

Zinc oxide was successfully synthesized from Zinc nitrate. The biocomposite films exhibited changes in its wavelength spectra, moisture content, degradation time, surface morphology. No new formation of functional group was observed.

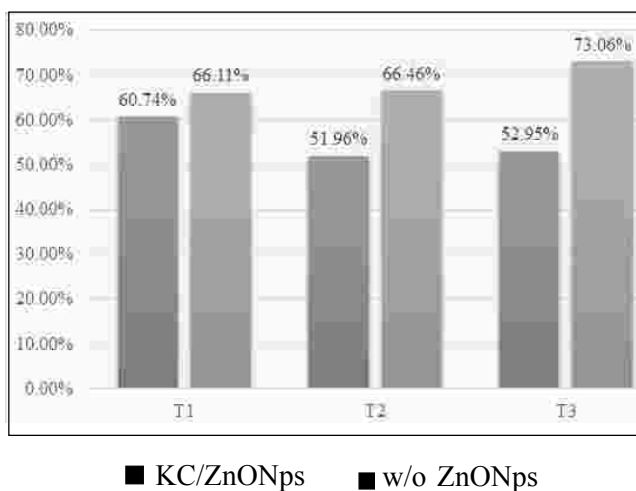


Fig 1. Comparative Chart of Moisture Content

Moisture content plays an important role in this film, greater moisture content indicates that the degradation is rapid. Increasing the nanoparticle (ZnO) content of films results in the formation of more hydrogen bonds⁴ and free water molecules do not interact as strongly with nanocomposite films as compared to the composite alone. Hence, increase in ZnONps levels leads to decreased moisture content and with high degradation time and consequently products will be preserved for a longer period of time.

Using the t-test, results showed that there was significant difference between the biocomposite film with and without the ZnONps. Thus, the KC/ZnONps films can replace the commercially available drug capsules or the plastic films in the packaging industry.

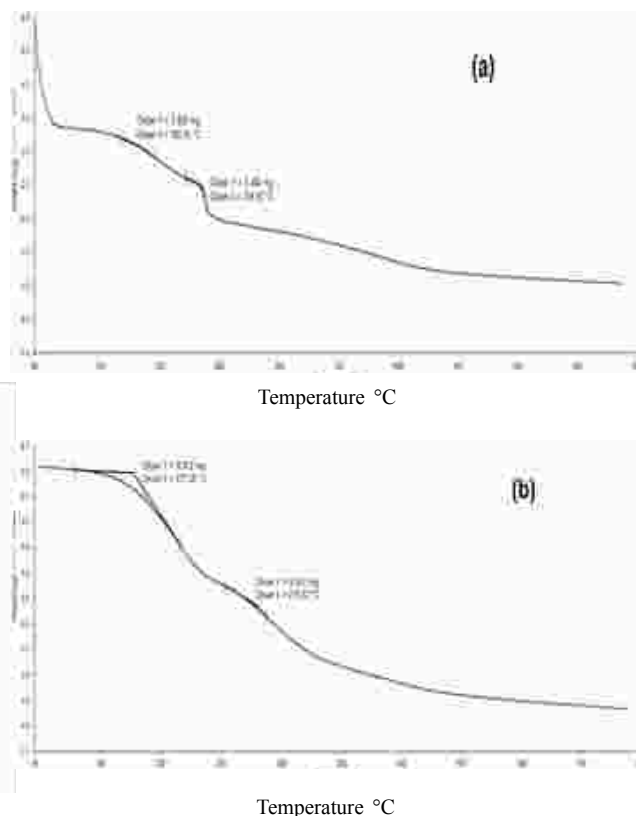


Fig 2. Degradation Time of the Biocomposite Films from a) KC and b) KC/ZnONps

Physiochemical properties of Kappa-Carrageenan Packed with Zinc Oxide Nanoparticles Biocomposite Films

KC/ZnONps exhibited different degradation times than ZnONps. Between 95-150°C, the biocomposite film from KC started to degrade rapidly and lost approximately 1.5mg of mass and continued as the temperature increased (a). The KC/ZnONps started to degrade at 150-200°C. This only implies that the incorporated ZnONps

into KC extends the degradation time of the biocomposite film (b). Thus, biocomposite material incorporated with metal oxide takes longer time to degrade. Thus, KC/ZnONps has been upgraded to have a longer shelf life but products that use biocomposite films with metal oxide will take a longer time to decompose.

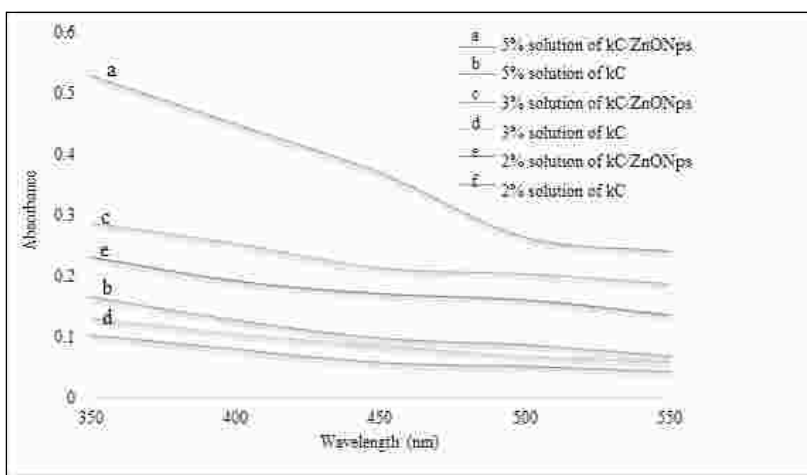


Fig 3. Spectra Analysis

Different concentration (5%, 3% and 2%) of the KC filled with ZnONps film and KC film solutions were analyzed. Figure 3 reveals that the biocomposite films incorporated with metal oxides changed their visible spectra. Nafchi⁴ suggested that biocomposite films incorporated with ZnONps could be used as UV-shield-

ing films and heat insulators in the packing industry because of its capacity to absorb UV light. This property is important especially in the case of pharmaceutical capsules since the drug inside the capsules could be protected from unwanted rays that might change its properties or cause damage⁶.

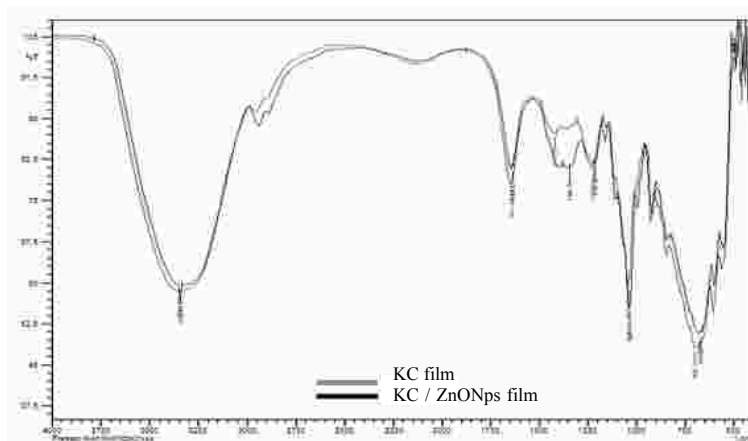


Fig 4. FTIR spectra



The structural formation analysis by FTIR showed that there were no changes in the peaks of the films. The Alkyne ($\equiv\text{C-H}$) group was present in both film samples.

It is postulated that ZnONps will only coat KC due to the van der Waals interaction and that the biocomposite material, Kappa-Carrageenan, will take longer time to decompose because of the incorporation of Zinc oxide.

Scanning electron microscopy (SEM) revealed that films without ZnONps had holes in it at a magnification of 4000 with 20 μm diameter (a). Furthermore, SEM results for the film with ZnONps revealed that the metal oxide was attached to the surface of the films. Also, it is seen that Zinc Oxide nanoparticles covered some of the holes present in the untreated film (b). This implies that the metal oxide incorporated is only on the surface of the biocomposite film. The presence of a metal oxide enhances its physicochemical properties. Nano-sized ZnO suspension clearly has much higher activity than the micron-sized ZnO⁷.

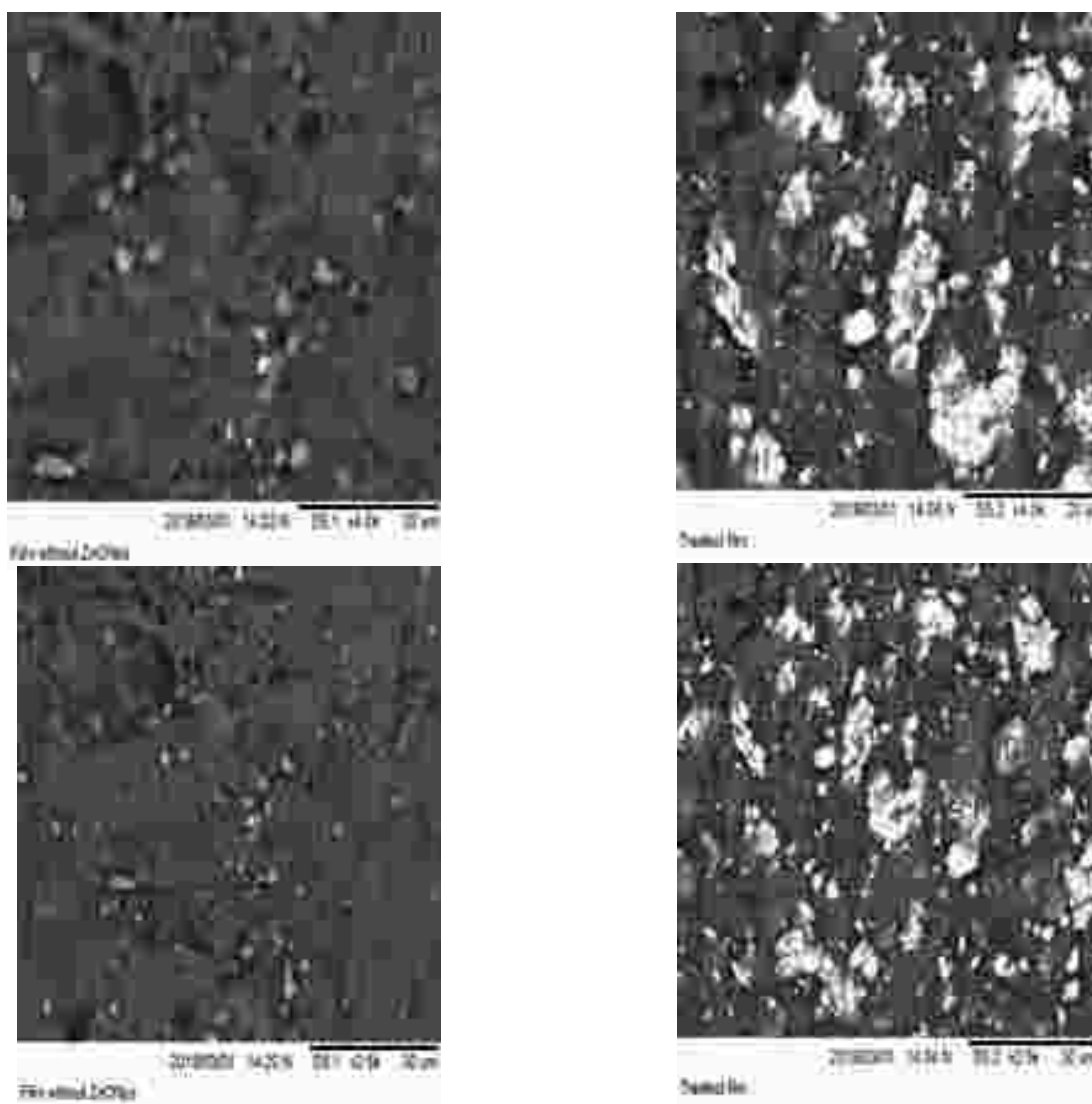


Fig 5. SEM Micrographs of the KC film without ZnONps (a) magnification =4,000, (c) magnification =2,500. The films with ZnONps (b) magnification = 4,000 and (d) Magnification = 2,500

Comparative analysis of KC/ZnONps and KC films

Table 1. Comparative Data of the Sample films

Parameters	KC films	KC/ZnONps film
Moisture Content	68.54% (high water content)	55.22% (low water content)
Degradation Time	Started between 95-150°C, rapidly	Started between 150-200°C, slowly
Wavelength spectra	Low absorbance	High absorbance
Structural composition	No formation of new groups	No formation of new groups
Surface morphology	Holes are seen in the surface of the film	ZnO was present in the surface

The physicochemical properties of the untreated and treated films are seen in Table 1. Moisture content was higher in KC film than the KC/ZnONps film which indicates that KC has more water content than the KC/ZnONps. The degradation time proves that KC film degraded and lost weight faster than the KC/ZnONps film. Wavelength spectra and structural composition revealed that the film has no new functional group. Surface morphology indicates the presence of ZnONps in the KC film.

Conclusions

Biocomposite film from KC/ZnONps has more chances of being substituted in the market as new drug capsule and packaging plastic materials due to its longer time of decomposition, lesser moisture content, better drug protection and resistance to bacterial contamination.

References

1. Kathirvelu S., D'Souza Louis and Dhurai Bhaarathi, 2009, *Indian Journal of Fibre and textile Research*, **34**, 267-273.
2. Brychcy Ewa, Magdalena Malik, Piotri Drozdowski, Zaneta Krol and Andrzej Jarmoluk, 2015, *Polymers*, **7**, 2638-2649.
3. Rao N., Srinivasa Rao and Mandara V.B., 2015, *American Journal of Material Science*.
4. Nafchi, Abdorreza Mohammadi, Alias, Abd Karim, Mahmud, Shahrom, and Robal, Marju, 2012, *Journal of Food Engineering*, **113**, 511-519.
5. Paul, Subhankar and Ban, Deependra Kumar, 2014, *International Journal of Advance in Chemical Engineering*, **1**, 1.
6. Rahman M. Aizuddin Abdul, Mahmud, Shahrom, Alias, and Nor, Abdul Fauzi Mohd, 2013, *Journal of Physical Science*, **24** (1), 17-28.
7. Zhang L., Jiang Y., Daskalakis N., Jenken L., Povey M., O'Neil A.J. and York D.W., 2009, *Journal of Nanoparticle Research*.



Synthesis and Diagnosis of Heterogeneous Compounds, Pyrimidine and Oxazepine from Alcofenac Drug and Evaluation of their Biological Activity

Fatimah Ali Hussein^{1*}, Hala Shkyiar Lihimes², Luma Ahmed Mohammed Ali³ and Sana Hitur Awad⁴

^{1,2,3} Department of Chemistry, College of Science, University of Babylon, 00964, Babylon, Iraq

⁴Department of Chemistry, College of Science for Women University of Baghdad, 00964, Baghdad, Iraq

*E-mail : afatema770@gmail.com

Abstract

This paper deals with the preparation of the derivative of pyrimidine using three steps followed by Biginelli reaction in the last step. Compound(A3) was prepared in three successive steps. The first step was the formation of compounds (A1a), (A1b) and (B) using coupling reagent, N,N'-dicyclohexylcarbodiimide (DCC) and 1-hydroxy benzotriazole (HOBt). In the second step, compounds (A2a, A2b) were prepared by oxidation of the -CH₃ group in the compounds (A1a) and (A1b) and converting it into aldehyde group using oxidizing agent SiO₂. In the third step, compounds (A3a,A3b) were prepared by the classical Biginelli method which involves cyclo condensation of compound (A2a), ethylacetoacetate and urea. The derivatives of N-Arylhydrazine and oxazepine were then prepared to form compounds (A3a,A3b) which were then reacted with hydrazine hydrate in 99% ethanol to yield hydrazide derivative compounds (A4a,A4b). The Schiff bases (A5a, A5b) were prepared from the corresponding aryl aldehydes. Oxazepine derivatives (A6a,A6b) were synthesized by reaction of compounds (A5a,b) with appropriate anhydrides. The compounds were characterized by spectroscopic methods, H¹NMR and FTIR and C.H.N analysis. The compounds prepared were tested for biological activity.

Keywords: Pyrimidine, Oxazepine, Hydrazide, Biginelli Reaction, Alcofenac, Oxidation

Introduction

In 1966, Alclofenac, 4-allyloxy-3-chlorophenylacetic acid was synthesized as one of a series of substituted aryl acetic acids¹. Clofenac was found to be similar to traditional aspirin, naproxen and fenoprofen², and has a wide range of medicinal applications- antihypertensive and antifungal¹²-antihistamines, nonsteroidal and anti-rheumatoidal.

It has the following characteristics³-reduced body heat action, anti-inflammatory action and reduced time for platelet work. The side effect of using this medication is rashes⁴.

Pyrimidine is a diazine containing nitrogen atoms in positions 1 and 3 and is classified as a heterogeneous aromatic compound⁵. Oxazepine denotes any seven-

membered ring containing an oxygen and nitrogen atom. 1,3-Oxazepine is a class of heterocyclic oxazepines⁶ which are prepared by the addition of maleic anhydride to Schiff bases⁷. The heterogeneous solid drugs contain nitrogen and play an important part in living cell metabolism. Among these, the six and seven heterocyclic derivatives are used in medicine as anti-cancer, antimicrobial and antiviral agents and pain relievers.^{8,9}

Material and Methods

All chemicals were obtained from Merck and BDH and used without any further purification. The melting points were determined on melting point apparatus SMP30, England in Babylon University. FTIR spectra of compounds were recorded using KBr disk on Shimadzu FT-IR-8300. ¹H-NMR spectra in solvent DMSO-d₆ were recorded by Bruker (500MHz) in Iran (Tehran University) using TMS as internal standard.

General Procedure for Preparation of Compounds

1-Synthesis amide compounds (A1)¹⁰: 1mmole of compound (S) in MeCN (10mL) was mixed with 1 mmol of (DCC), 1 mmol of (HOBt) and 1 mmol of substituted aniline or aliphatic amine. The mixture reaction was stirred at -5C° for 1h and at 23 C° for 48h. The precipitate was filtered, washed with saturated NaCl solution, 5% NaHCO₃ solution, 1M HCl and water and recrystallized using MeCN.

2-Synthesis of 2-(4-(allyloxy)-3-chlorophenyl)-N-(2-chloro-4 formylphenyl) acetamide (A2)¹¹

1mmole(11.5mg) of selenium dioxide (SeO₂) was mixed with 5mL 1,4-dioxane and 4drops of water and the mixture was heated at 50C° with stirring. 1mmole of compound (A1) was added sequentially in 12mL 1,4-dioxane and the mixture refluxed for 48 h. with stirring. SeO₂ was precipitated and the mixture was cooled to room temperature and the compound(A2) was recrystallized with dioxane.

3-Synthesis of ethyl 4-(4-(2-(4-(allyloxy)-3-chlorophenyl)acetamido)-3-chlorophenyl)-6-methyl-2-

oxo-1,2,3,4-tetrahydropyrimidine-5-carboxylate (A3)

A mixture of 0.6mmole of compound (A2), 0.6m mole ethyl acetoacetate and 0.9mmole urea in 25mL absolute ethanol was refluxed for 18 h. at 80C° in presence of a few drops of catalyst HCl. The mixture was poured into crushed ice and stirred. The compound was extracted with chloroform, washed with water and the precipitate was dried over MgSO₄.

4-Synthesis of 2-(4-(allyloxy)-3-chlorophenyl)-N-(2-chloro-4-(5-(hydrazinecarbonyl)-6-methyl-2-oxo-1,2,3,4-tetrahydropyrimidin-4-yl)phenyl)acetamide (A4)

2mmole of compound (A3) in ethanol was refluxed with 4mmole 99%hydrazine hydrate for 4 hrs and cooled in an ice bath . The precipitate was filtered and recrystallized with diethyl ether.

5-Synthesis compounds (A5a,b) of N-arylhydrazone derivatives of 4-allyloxy-3-chlorophenylacetic acid

1.9 mmol of hydrazide(A4) was mixed with 1.9 mmol p-nitrobenzaldehydes in 15 mL of ethanol and stirred at room temperature for 1to 2h. in the presence of two drops of conc. HCl catalyst. The hydrazones (A5a,b) were isolated by concentrating the reaction mixture under reduced pressure, followed by neutralization with 10% sodium bicarbonate solution. The resulting precipitate was filtered, washed with 5 mL water and dried.

6-Synthesis of 4-(4-(2-(4-(allyloxy)-3-chlorophenyl)acetamido)-3-chlorophenyl)-6-methyl-N-(2-(4-nitrophenyl)-4,7-dioxo-1,3-oxazepan-3-yl)-2-oxo-1,2,3,4-tetrahydropyrimidine-5-carboxamide (A6a,A7a)

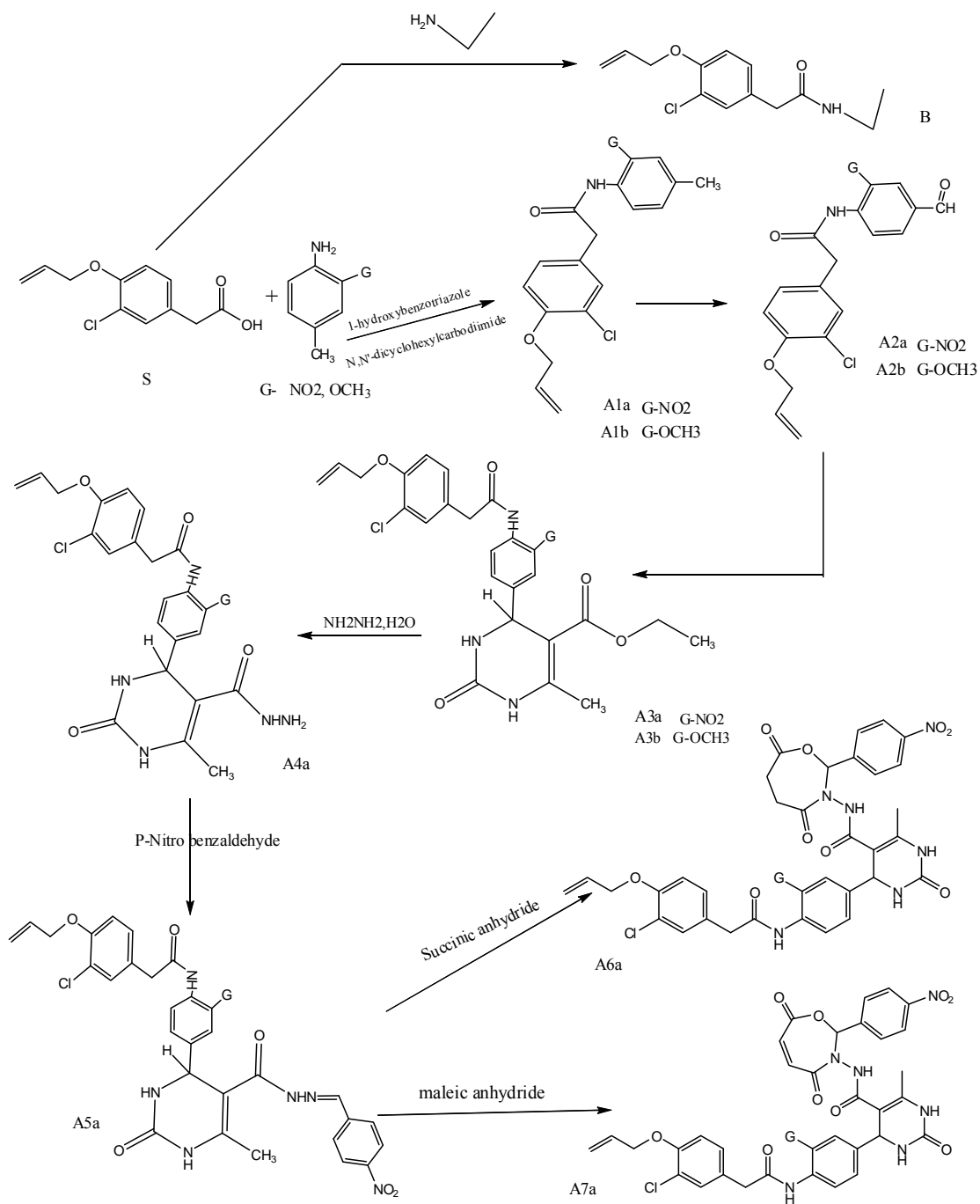
1.8 mmol of compound (A5) was refluxed with 1.8mmol of the corresponding anhydride in 20 mL absolute ethanol for 3 hrs. in a water bath at 78°C. After removal of the solvent, the product was recrystallized from ethanol.

Results and Discussion

Alclofenac (S) was the starting material for the formation of amide bond by coupling reaction using DCC



and HOBt. Compounds A1a, A1b, B were synthesized by the reaction of carboxylic acid (S) with 4-methyl-2-nitroaniline, 4-methyl-2-methoxyaniline and ethyl amine respectively as shown in Scheme 1.



Scheme 1

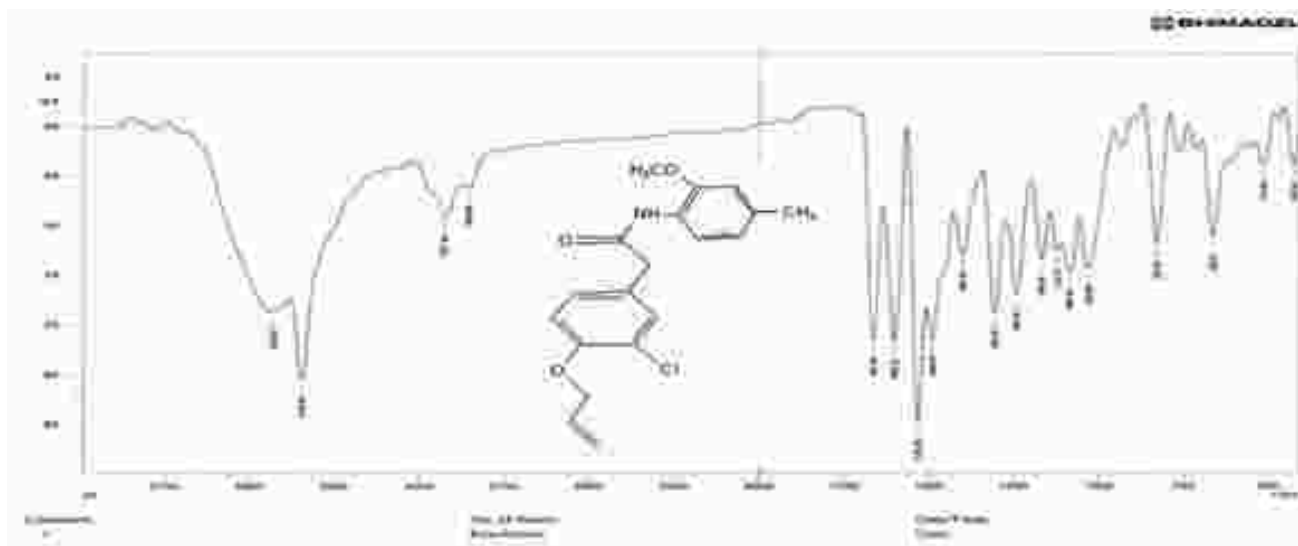


Fig.1:IR Spectrum of compound A_{1b}

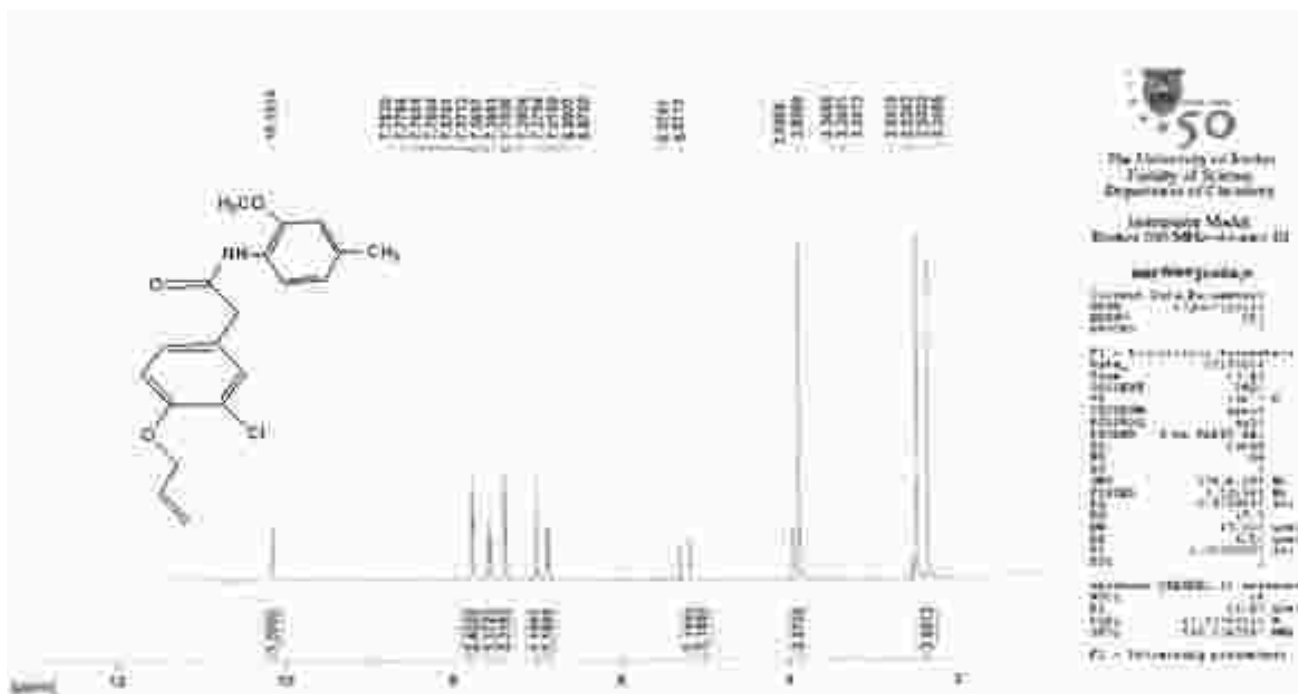


Fig.2: ¹H_{NMR} of compound A_{1b}

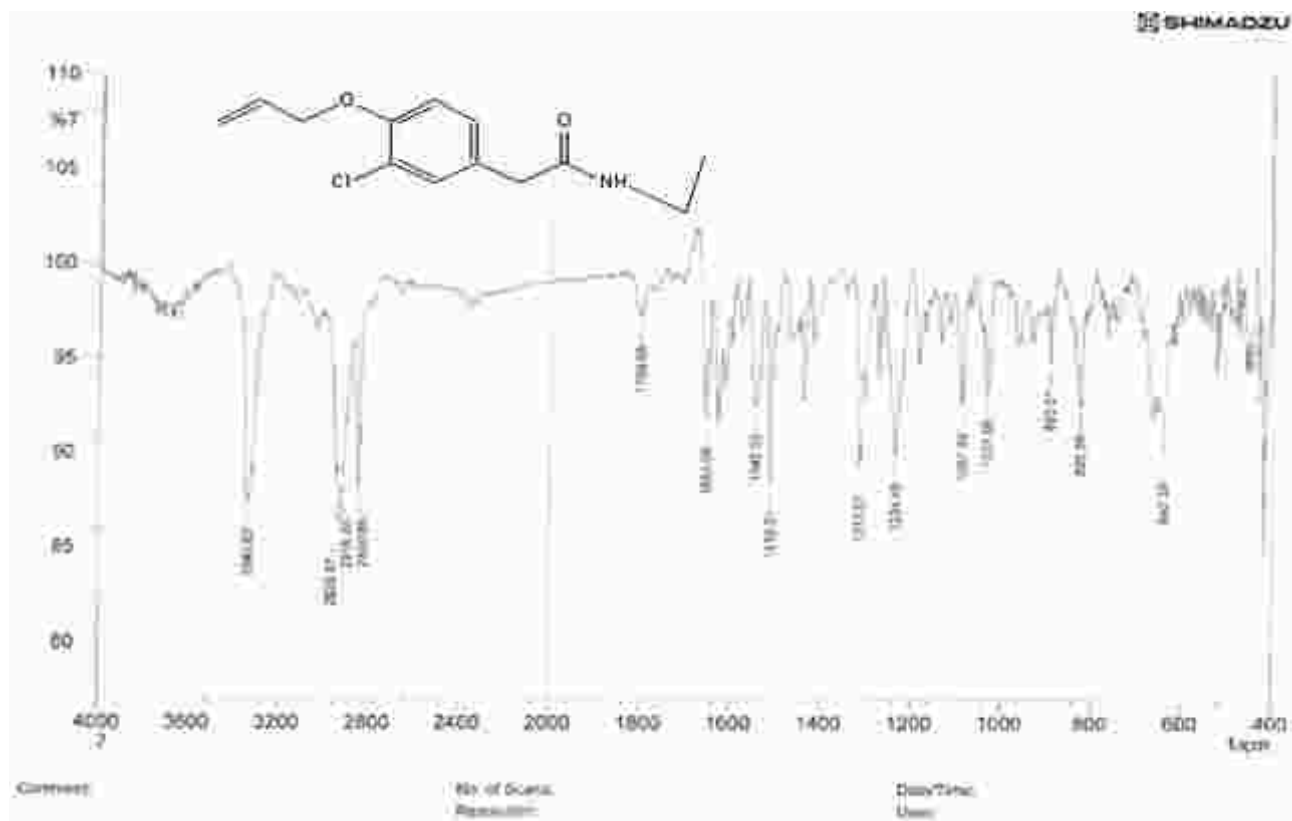


Fig.3: IR spectrum of compound (B)

Compounds (A1a) and (A1b) were identified by FT-IR, ¹H-NMR and elemental analysis, while compound (B) was examined by FT- IR and elemental analysis. In FT-IR spectra, the peaks appear at 3340 cm⁻¹ and 1665cm⁻¹. These peaks belong to N-H amide and C=O amide of compound (A1a). Also the peaks appearing at 3342 cm⁻¹ and 1653 cm⁻¹ are due to N-H amide and C=O amide of compound (A1b) (Figure 1)

In ¹H-NMR spectra of compound (A1a), the observed singlet peak appeared at 10.19 ppm which belongs to N-H amide, doublet peak (6.87-7.78 ppm) for seven protons of aromatic system, peak at (3.89,3.93 ppm) for two protons of (=CH₂) group, a singlet peak at 2.5 ppm for three protons of methyl group, (5.23,5.33) ppm for three protons of (=C-H). For compound (A1b), the appearance of singlet peak at 9.98 ppm is for N-H amide,

doublet peak at (6.81-7.63 ppm) for aromatic system protons, singlet peak at 3.85 ppm for three protons of (-OCH₃), 3.73,3.82 ppm for two protons of (=CH₂), (5.34,5.25) ppm for three protons of (=C-H) and 2.4 ppm for (3H,CH₃) as illustrated in Figure 2. For compound (B), the new peaks in FT-IR spectra 3341, 2916 and 1651cm⁻¹ belong to N-H amide, CH aliphatic and C=O amide respectively in Figure 3.

For all the compounds prepared, the calculated values of C, H and N percentages as obtained by elemental analysis are listed in Table 1.

The IR and NMR spectra of other compounds prepared are not included due to their routine nature. The IR frequencies and ¹H-NMR signals of all compounds prepared are listed in Table 3.

Oxidation of methyl group by SeO_2

Compounds (A2a,A2b) were prepared by refluxing SeO_2 (in excess) with the compounds (A1a- A1b) and solvent (1,4-dioxane) for 48 hours as shown in Scheme 1. The synthesis of compounds (A2a) and (A2b) has been confirmed by FT-IR and ^1H NMR (Table 2)

Compound (A3a) (target compound) was prepared by the classical Biginelli method which involves cyclocondensation of the compound (A2a), ethylacetoacetate and urea in acidic conditions as shown in Scheme 1. The reaction was performed by heating mixture of three components dissolved in ethanol with a few drops of HCl and refluxed for 18h. In FT-IR spectra, the new peak at 1721cm^{-1} belongs to C=O ester and peaks which disappear are due to C=O (1734cm^{-1}) and C-H aldehyde (2854cm^{-1}) (Table 2)

Compound (A4) was prepared by treating compound (A3) with hydrazine hydrate in ethanol. The IR spectra showed $3248\text{-}3325\text{cm}^{-1}$ frequency for N-H amide stretching, $1661\text{-}1670\text{cm}^{-1}$ for C=O amide stretching, which was indicated by the disappearance of the broad band for -OH stretching of COOH group in Alclofenac.

Compound (A5) (N-arylhydrazone derivatives) have been obtained by reaction of compound (A4) with aromatic aldehydes, catalyzed by few drops of 68-77% concentrated hydrochloric acid (Scheme 1). The compound (A5a) was characterized by FTIR spectral data which showed bands due to C=O at $1662\text{-}1683\text{cm}^{-1}$ and a sharp band at 1515cm^{-1} indicating the presence of C=N group and disappearance of -NH_2 band at 3325cm^{-1} . The FTIR spectral data showed the presence of -OCH_3 group in compound (A5b) as indicated by a sharp peak at 1193cm^{-1} . The ^1H NMR signal at 8.12 ppm indicated proton singlet of -NH groups.

Compound (A5) was converted to the oxazepane derivatives (A6a,b) by reaction with the corresponding anhydrides.

The IR frequency 3300cm^{-1} was due to -NH bands

and $1655\text{-}1669\text{cm}^{-1}$ due to C=O groups. The IR spectra shows the disappearance of the absorption bands of -NH_2 (Table 2)

The ^1H -NMR spectra of compound (A5) showed signals at : 3.81, 3.82 (s,d, 4H, =CH₂), 2.30 (s, 3H, -CH₃), 8.3 (s, 1H, -CONH), 6.83-7.6 (m, Ar-H).

The oxazepane derivative compound (A6) was characterized by FTIR and showed a combination of both lactone and lactam in 7-membered heterocyclic ring, (C=O)(lactone/lactam) absorption band at $1660\text{-}1680\text{cm}^{-1}$, (cis-CH=CH) double bond of maleic anhydride as indicated by the absorption band at $(1600\text{-}1610)\text{cm}^{-1}$, bands due to -NH at 3115cm^{-1} and disappearance of the NH_2 absorption bands (Table 2).

Biological Activity

Biologic activity was studied using two types of bacteria (Gr+) and (Gr-) i.e. *Escherichia coli* and *Staphylococcus aureus*.

As shown in Tables 3 and 4, some of these compounds are active and some are inactive. All compounds were inactive at concentration $1 \times 10^{-5}\text{M}$, but active in the concentration range $1 \times 10^{-4}\text{M}$ - $1 \times 10^{-3}\text{M}$. (Tables 3 and 4).



Table1: Physical Properties of Compounds (A1-A7)

Compound No.	Mol. Formula	Mol.Wt.	M.P. (°C)	Yield (%)	Color	C.H.N		
						C	H	N
A1a	C ₁₈ H ₁₇ ClN ₂ O ₄	350.2	133-135	73	Colorless	Fou.61.73 Cal. 61.52	4.89 4.09	4.00 3.80
A1b	C ₁₉ H ₂₀ ClNO ₃	345.8	131-134	77	Colorless	56.99 56.09	5.83 5.75	4.05 3.93
B	C ₁₃ H ₁₆ ClNO ₂	381.7	181-183	65	Colorless	63.94 63.04	7.15 7.00	4.97 4.17
A2a	C ₁₈ H ₁₅ ClN ₂ O ₅	364.2	170-172	68	Yellow	59.36 59.20	4.15 4.11	3.85 3.80
A2b	C ₁₉ H ₁₈ ClNO ₄	359.8	115-118	76	Yellow	63.42 63.32	5.04 5.00	3.89 3.84
A3a	C ₂₅ H ₂₅ ClN ₄ O ₇	518.3	239-241	78	Red	57.92 57.78	4.86 4.84	8.11 8.09
A3b	C ₂₆ H ₂₈ ClN ₃ O ₆	513.6	245-247	80	White	60.76 60.66	5.49 5.42	8.18 8.15
A4a	C ₂₃ H ₂₃ ClN ₆ O ₆	504.3	268-270	69	White	54.77 54.07	4.60 4.58	13.89 13.85
A4b	C ₂₄ H ₂₆ ClN ₅ O ₅	499.9	270-272	70	White	57.66 57.46	5.24 5.20	14.01 13.99
A5a	C ₃₀ H ₂₆ ClN ₇ O ₈	637.47	278-280	78	brown	56.52 56.41	4.11 4.08	13.18 13.16
A5b	C ₃₁ H ₂₉ ClN ₆ O ₇	633.05	285-287	81	Darkbrown	58.82 58.79	4.62 4.60	13.28 13.22
A6a	C ₃₄ H ₃₀ ClN ₇ O ₁₁	737.5	237-239	85	Gray	55.37 55.27	4.10 4.08	11.39 11.29
A7a	C ₃₄ H ₂₈ ClN ₇ O ₁₁	735.5	242-244	87	Sliver	55.52 55.45	3.84 3.80	11.43 11.34

Table 2: Spectral Data of Compounds (A1-A7)

A1a	IR (cm-1): 3340 (NH) _{amide} , 1665 (C=O) _{amide} , (CH _{ar.}) 3039, (CH _{alph.}) 2936 1HNMR (δ ppm) : 6.87-7.78 (m, 6 H, Ar), 10.19 (s, 1H, NH), 3.81(s, 2H, CH ₂), 3.93(d, 2H, CH ₂), 2.5(s, 3H, CH ₃), 5.31, 5.42(s, d, 3H, CH)
A1b	IR (cm-1): 3342 (NH), 1653 (C=O) _{amide} , (CH _{ar.}) 3072, (CH _{alph.}) 2986 1HNMR (δ ppm) : 6.86-7.63 (m, 6 H, Ar), 9.89 (s, 1H, NH), 5.31, 5.42(s, d, 3H, CH), 3.71(s, 2H, CH ₂), 3.83(d, 2H, CH ₂), 2.4(s, 3H, CH ₃), 3.85(s, 3H, oCH ₃)
B	IR (cm-1): 3340 (NH), 1653 (C=O) _{amide} , (Al.-CH) 2918 1HNMR (δ ppm) : 6.84-7.33 (m, 3 H, Ar), 8.89 (s, 1H, NH), 5.31, 5.42(s, d, 3H, CH), 3.91, 3.83, 3.03, 1.41, 1.52(10H, CH ₂). 0.99(s, 3H, CH ₃)
A2a	IR (cm-1): 3343 (NH), 1660 (C=O) _{amide} , 1734 (C=O) _{ald.} , 2854(CH) _{ald.} 1HNMR (δ ppm) : 6.83-7.38 (m, 3 H, Ar), 10.1 (s, 1H, NH), 10.62 (s, 1H, CH _{ald.}), 3.81(s, 2H, CH ₂), 3.93(d, 2H, CH ₂), 5.31, 5.42 (s, d, 3H, CH)

A2b	IR (cm-1): 3346 (NH), 1665 (C=O)amide, 1722 (C=O)ald. , 2852 (CH) ald. 1HNMR (δ ppm) : 6.63-7.26 (m, 3 H, Ar), 10.2 (s, 1H, NH), 10.52 (s, 1H, CH ald.), 3.83(s, 2H, CH2),3.92(d, 2H, CH2), 5.31 ,5.42 (s,d, 3H, CH) ,3.83(s, 3H, OCH3)
A3a	IR (cm-1): 1721 (C=O)ester, 3359 (NH), 3037 (Ar-CH) 1HNMR (δ ppm) :9.82 (s, 1H, NH), 4.89 (s, 2H, NH), 5.31 ,5.42 (s,d, 3H, CH), 3.83,3.84(s, q, 4H, CH2), 1.72(t, 3H, CH3), 6.90-7.27 (m,4H, Ar)
A3b	IR (cm-1): 1724 (C=O)ester, 3357 (NH), 3032 (Ar-CH) 1HNMR (δ ppm) :8.82 (s, 1H, NH), 4.99 (s, 2H, NH), 5.21 ,5.32 (s,d, 3H, CH), 3.81,3.82(s, q, 4H, CH2), 1.72(t, 3H, CH3), 6.90-7.27 (m,4H, Ar) 3.82(s, 3H, OCH3)
A4a	IR (cm-1): 3351 (NH),3325 (NH ₂), 1661 (C=O)amide HNMR (δ ppm) : 6.83-7.76 (m, 4 H, Ar), 8.2 ,9.3 (s, 2H,CO NH), 4.12 (s, 1H, NH ₂), 3.83(s, 2H, CH2),3.92(d, 2H, CH2), 5.31 ,5.42 (s,d, 3H, CH) 2.32(s, 3H, CH3)
A5a	IR (cm-1): 3353 (NH), 1662 (C=O)amide ,1515(C=N) HNMR (δ ppm) : 6.83-7.6 (m, 8 H, Ar), 8.1 ,9.4(s, 2H,CO NH), 4.12 (s, 1H, NH ₂),3.81(s, 2H, CH2),3.82(d, 2H, CH2), 5.31 ,5.42 (s,d, 3H, CH) 2.30(s, 3H, CH3)
A6a	IR (cm-1): 3300 (NH), 1655 (C=O)amide HNMR (δ ppm) : 6.23-8.16 (m, 13 H, Ar), 8.1 ,9.4(s, 2H,CO NH), 3.81,3.82,2.51,2.54(8H, CH2), 5.31 ,5.42 (s,d, 3H, CH) 2.20(s, 3H, CH3)
A7a	IR (cm-1): 3310 (NH),(1658-1969) (C=O) HNMR (δ ppm) : 6.23-8.16 (m, 13 H, Ar), 8.3 ,9.6(s, 2H,CO NH), ,3.81,3.82, (4H, CH2), 5.31 ,5.42,6.2,6.8 (s,d,d 5H, CH) 2.23(s, 3H, CH3)

Table 3: Effect of Compounds on the Growth of Tested Bacteria (concentration $1 \times 10^{-3}M$)

Compound.	Gram positive		Gram negative	
	<i>S.aureus</i>	<i>E.coli</i>	<i>K.pneumonia</i>	<i>P.aeruginous</i>
A1a				
A1b	-	6mm	-	6mm
A2a	-	8mm	-	10mm
A3b	-	10mm	-	6mm
A4a	10mm	10mm	10mm	-
A4b	10mm	8mm	10mm	-
A5a	10mm	10mm	-	-
A5b	10mm	8mm	-	8mm
A6a	10mm	10mm	10mm	10mm



Table 4: Effect of Compounds on the Growth of Tested Bacteria (concentration 1×10⁻⁴M)

Comp.	Gram positive		Gram negative	
	<i>S.aureus</i>	<i>E.coli</i>	<i>K.pneumonia</i>	<i>P.aeruginous</i>
A1a				
A1b	-	-	-	4mm
A2a	-	8mm	-	8mm
A3b	-	8mm	-	4mm
A4a	-	6mm	8mm	-
A4b	-	8mm	8mm	-
A5a	-	10mm	-	-
A5b	10mm	-	-	-
A6a	10mm	8mm	8mm	6mm

Conclusions

We have synthesized and characterized a new series of Alclofenac- 4-allyloxy-3-chlorophenyl acetic acid derivatives (13) and evaluated their antibacterial activity.

References

1. Lan Hasloch, 1976, *Rheumatology*, **15(3)**, 228-229.
2. Brogden R.N., Heel, R.C., Speight T. M. and Avery G. S., 2012, *Evaluations of new drugs* **1,3**, 241.
3. *Journal of Pharmacology and Therapeutics*, 1982, **16(2)**, 167.
4. John O. Miners and Peter I Mackenzie, 1991, *Journal of Pharmacology and Therapeutics*, **51(4)**, 347.
5. Padarthi P., Sridhar S., Jagatheesh K. and Namasivayam E., 2013, *J. Res. Ayurveda Pharm.*, **4(3)**, 355-362.
6. Shiradkar M.R. and Nikalje A.G., 2010, *Org. Commun.*, **3(3)**, 57-69.
7. Tang Y., Fettinger J.C. and Shaw J.T, 2009, *Organic Letters*, **11(17)**, 3802–3805.
8. Tomma J., Khazaal M. and Al-Dujaili A., 2014, *Arabian Journal of Chemistry*, **7**, 157-163.
9. Liu X., Jia Y., Song B., Pang Z. and Yang S., 2013, *Bioorganic & Medicinal Chemistry Letters*, **23**, 720.
10. Al-Masoudi N.A., Hamed N.S. and Pannecouque C., 2010., *Arkivoc.*, 242-253.
11. Joi baria M.H., Marandi R. Rezaei G. and Mehrabiana R.Z., 2012, *Iranian J. Org. Chem.*, **4**, 775-777.
12. Article in Bausch & Lomb Incorporated, Senju Pharmaceuticals Co., Ltd. Osaka, Japan, 2013, 541-0046.



Effects of Salinity and Temperature on the Rate of Biodegradation of Domestic Waste Released into the Marine Waters around Mumbai City, India

Shivani S Dhage^{1*}, D V Prabhu² and Prakash S Kelkar³

¹ Aquara Labs, Mumbai 400104, India

² Department of Chemistry, Wilson College (Aff. University of Mumbai)
Mumbai 400007, India

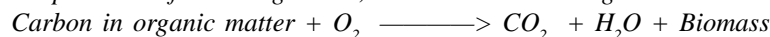
³ Rajiv Gandhi Science and Technology Commission, Government of Maharashtra,
Nagpur 440011, India.

Email: dvprabhu48@gmail.com

Abstract

Marine pollution around cities is largely due to the discharge of untreated industrial and domestic wastes. Mumbai City generates a large amount of domestic waste water which is released largely untreated into the coastal waters. As a result, the marine environment is adversely affected and marine life gets depleted.

The health of a water body is defined by physicochemical parameters like BOD, COD, DO, salinity and pH. Domestic waste water is rich in microorganisms which help in its biodegradation by a process of wet oxidation. In the presence of microorganisms, the carbonaceous organic matter in domestic waste gets oxidized:



The first order kinetics of biodegradation of domestic waste by wet oxidation has been studied with particular reference to the effects of 1) salinity in the range $[\text{Cl}^-] = 0$ to 20000 mg L^{-1} and 2) temperature (20C, 27C) on the rate of biodegradation. An inverse relationship was observed between the rate of biodegradation and salinity.

The relatively high temperatures in tropical regions significantly affect biodegradation rates. The chemical reactions occurring in the oceans during the degradation of organic wastes are governed by thermodynamic considerations hence the wet oxidation was studied at different temperatures and the thermodynamic activation parameters of the reaction were evaluated and interpreted.

The BOD values have been calculated at different salinities from the DO values determined at regular time intervals during the degradation process and correlated with the rate of biodegradation of domestic waste water. Dissolved Oxygen was determined by Alsteberg azide modification of the Winkler method.

Similarly, the kinetics of degradation of a synthetic sample, Glucose- Glutamic acid was studied. The slow degradation of organic matter in environmental effluents like domestic waste should be critically considered while planning the disposal options for organic wastes into the marine ecosystem. Recommendations have been made to local municipal authorities to treat domestic waste before discharge into the coastal waters.

Keywords: Domestic Waste Water, Wet Oxidation, Biodegradation, Dissolved Oxygen, Salinity, Temperature, Arrhenius Equation, Thermodynamic Activation Parameters, Glucose-Glutamic Acid



Introduction

Marine pollution is largely due to the unregulated discharge of industrial, agricultural and domestic wastes into the coastal waters due to which the marine environment experiences ecological stress. Mumbai City generates a large amount of domestic waste, a part of which is directly discharged into the coastal waters at different locations. It is estimated that 2671 MLD (million litres per day) of domestic waste is produced in the city out of which 655 MLD is directly discharged into the sea without treatment.¹

Domestic waste is rich in microorganisms which help in its biodegradation by a process of wet oxidation. In the presence of micro organisms, the carbonaceous matter in domestic waste gets oxidized:

Carbon in organic matter + O₂ → CO₂ + H₂O + biomass.

The negative impact of salinity on the rate of biodegradation of domestic waste has been studied in detail and reported.^{2,3} This paper reports the kinetics of biodegradation of domestic waste and a synthetic sample, Glucose-Glutamic acid with reference to the effect of temperature (20°C and 27°C) on the rate of biodegradation.

Materials and Methods

Domestic waste samples were collected using standard sampling methods from the waste water facility of Mumbai City.⁴ All other chemicals and reagents used in the study were of Analytical Grade (AR). "BOROSIL" brand glassware was used for all experiments.

The samples were suitably diluted using specially prepared dilution water.⁵ The diluted samples were seeded with a mixed bacterial culture which had been previously acclimatized to the oxidizable organic matter present in the samples. The micro organisms used were *Bacillus subtilis*, *Bacillus polymyxa* and *Pseudomonas*

sp. The dilution media were buffered to provide sufficient nutrients.

The amount of Dissolved Oxygen (DO) required for the biodegradation of organic matter in the waste effluent samples under study was determined in the beginning and at regular time intervals during the oxidation reaction by the Alsteberg azide modification of the Winkler method.

The experimental conditions of DO estimation in the samples under study are summarized below:

Test samples : Environmental sample-Domestic waste water

Synthetic sample – Glucose-Glutamic acid solution, 250 mg dm⁻³

Dilution media: Buffered distilled water with [Cl⁻¹] = 0 to 20000 mg dm⁻³

Incubation period (duration of test) : 5 days

Temperatures : 20°C and 27°C

Test frequency : Every day

Kinetic Measurements

The biodegradation of domestic waste was studied at different salinities ([Cl⁻¹]) = 0 to 20000 mg dm⁻³ at 20°C and 27°C. The biodegradation follows first order kinetics.⁶ The first order rate constants (k) were determined from the linear plots of log(DO) versus time in days. From the variation of rate of oxidation with temperature, the energy of activation (E) and other thermodynamic activation parameters were determined using a modified form of the Arrhenius equation

$$\log \frac{k_2}{k_1} = \frac{E}{2.303 R} \left[\frac{T_2 - T_1}{T_1 - T_2} \right]$$

Results and Discussion

The variation of the average values of 5 days of the rate of biodegradation of domestic waste and Glucose-Glutamic acid with salinity and temperature and related thermodynamic activation parameters are given in Tables

Effects of Salinity and Temperature on the Rate of Biodegradation of Domestic Waste Released into the Marine Waters around Mumbai City, India

1 and 2 respectively. The rates of biodegradation of both samples decrease with salinity ($[Cl^{-1}]$) but increase with temperature. The biodegradability of the synthetic sample, Glucose-Glutamic acid was found to be good. However, the rate of biodegradation of domestic waste water is affected due to multiple factors which make its wet oxidation complex. Subsequently, the prediction and evaluation of the assimilative capacity of the marine ecosystem to waste water discharge becomes difficult.

For both samples under study, there is a slight increase in free energy of activation (ΔG^*) with increase in temperature. Negative values of entropy of activation (ΔS^*) indicate a decrease in the degrees of freedom of the reacting system due to the formation of a rigid activated complex during the course of the reaction followed by reorientation of the solvent molecules around the activated complex resulting in decrease in disorder.⁷ For both samples, the entropy of activation remains constant at both temperatures. The variations in thermody-

Table 1

a) Variation of rate of biodegradation of domestic waste water with salinity and temperature
b) Thermodynamic activation parameters of biodegradation of domestic waste water

$[Cl^{-1}]$ mg dm ⁻³	Temp. K	k day ⁻¹	k x 10 ⁶ s ⁻¹	E kJ mol ⁻¹	K* x 10 ¹⁹	ΔH^* kJ mol ⁻¹	ΔG^* kJ mol ⁻¹	ΔS^* kJ K ⁻¹ mol ⁻¹
0	293	0.20	2.22	31.69	3.79	29.29	103.24	-0.3230
0	300	0.28	3.24	31.69	5.19	29.20	105.03	-0.3231
5000	293	0.12	1.39	38.20	2.28	35.76	104.59	-0.1778
5000	300	0.18	2.08	38.20	3.33	35.71	106.14	-0.1775
10000	293	0.13	1.51	30.69	2.46	28.25	104.39	-0.2529
10000	300	0.18	2.08	30.69	3.33	28.20	106.14	-0.2520
15000	293	0.13	1.51	19.57	2.46	17.13	104.39	-0.2350
15000	300	0.16	1.85	19.57	2.96	17.08	105.39	-0.2348
20000	293	0.13	1.51	30.69	2.46	28.25	106.14	-0.2600
20000	300	0.18	2.08	30.69	3.33	28.20	107.39	-0.2598

dynamic activation parameters indicate that the biodegradation of domestic waste is a non spontaneous reaction (Table 1).

Conclusions

- Salinity has negative effect on the biodegradation of domestic waste water.
- The rate of biodegradation of domestic waste water increases with temperature.

The slow degradation of effluents in marine waters should be critically considered while planning the disposal of organic wastes into the marine environment.

Acknowledgement

Authors wish to thank Dr Rakesh Kumar, Director CSIR-National Environmental Engineering Research Institute (NEERI), Mumbai and Dr V J Sirwaiya, Principal Wilson College, Mumbai for experimental facilities provided and support and encouragement throughout the study.



Table 2

a)Variation of rate of biodegradation of Glucose-Glutamic acid with salinity and temperature

b)Thermodynamic activation parameters of biodegradation of Glucose-Glutamic acid

[Cl ⁻¹] mg dm ⁻³	Temp. K	k day ⁻¹	k x10 ⁶ s ⁻¹	E kJ mol ⁻¹	K*x 10 ¹⁹	ΔH* kJ mol ⁻¹	ΔG* kJ mol ⁻¹	ΔS* kJ K ⁻¹ mol ⁻¹
0	293	0.24	2.78	67.86	4.55	65.42	102.90	-0.1279
0	300	0.46	5.33	67.86	8.52	65.37	103.79	-0.1281
5000	293	0.25	2.89	46.62	4.74	43.98	102.80	-0.2007
5000	300	0.39	4.51	46.62	7.22	43.93	104.20	-0.2009
10000	293	0.18	2.08	63.27	3.41	60.83	103.60	-0.1460
10000	300	0.33	3.82	63.27	6.11	60.78	104.62	-0.1462
15000	293	0.11	1.27	62.45	2.09	60.01	104.80	-0.1529
15000	300	0.20	2.31	62.45	3.20	59.96	105.87	-0.1531
20000	293	0.11	1.27	57.02	2.09	54.58	104.80	-0.1714
20000	300	0.19	2.20	57.02	3.52	54.53	106.00	-0.1716

References

1. Maharashtra Pollution Control Board Report published in "Hindusthan Times" Newspaper Mumbai issue, dated December 23, 2018.
2. Prabhu D.V., Dhage S.S. and Kelkar P.S., 2012, *Environmental Monitoring and Assessment*, **184 (9)**, 5301-5310. DOI 10.007/s10661-011-2341-y.
3. Prabhu D.V., Dhage S.S. and Kelkar P.S., 2018, *Research Journal of Chemistry and Environment* **23(9)**, 47-51.
- 4) APHA, WPCF, AWWA, 2005, Standard methods for the examination of water and waste water 21st Ed., NW, DC.
- 5) Loganathan B., Ramadhas V. and Venogopalan V.K., 1985, *Indian Journal of Marine Sciences* **14**, 186-189.
- 6) Clair N Sawyer, Perry L MacCarthy and Gene F Perkin, 2010, Chemistry for Environmental Engineering 5th Ed., McGraw Hill Inc., Columbus, USA.
- 7) Eichhorn G.L. and Trachenberg I.M., 1954, *Journal of American Chemical Society* **76**, 5184.



Physicochemical and Phytochemical Analysis of some Selected Herbal Medicinal Products Consumed in Wukari, Taraba State, Nigeria

Odoh Raphael and Ajiboye O. Emmanuel

Department of Chemical Sciences, Federal University Wukari, P.M.B 1020, Katsina-Ala Road, Taraba State, Nigeria

Email: odohraf@gmail.com; lekan.a.emma@gmail.com

Abstract

The increased proliferation of the use of herbal medicines in society today has generated curiosity regarding its efficacy. According to the World Health Organization (WHO), about 70% of the world population depends on herbal medicine as their basic therapy. This study aims at evaluating the physicochemical and phytochemical properties of some selected herbal medicines sold in Wukari, Taraba State, Nigeria. The samples were purchased from various herbal shops scattered around the metropolis and were evaluated for their physicochemical parameters and presence of some phytochemicals. The study revealed highly acidic and alkaline pH conditions in the herbal medicines and also the presence of some secondary metabolites like Alkaloids, Tannins, Terpenoids, Flavonoids, Reducing Sugars, Cardiac glycosides and Saponins in at least one of the eight herbal medicinal products analysed.

Keywords: Herbal Medicinal Products, Phytochemical, Physicochemical, Phytotherapy, Phyto-toxicity, Consumption

Introduction

Herbal medicines and their preparations have been widely used for thousands of years in developed and developing countries owing to their natural origin and lesser side effects and dissatisfaction with the after effects of synthetic drugs. Herbal medicine, also called botanical medicine, phytomedicine or plant medicine, uses active ingredients found in the aerial or underground parts of plants. Although herbal medicines have been used to treat many conditions, such as asthma, eczema, premenstrual syndrome, rheumatoid, arthritis, migraine, menopausal symptoms, chronic fatigue, and irritable bowel syndrome, among others²; the quality of these prepared herbal medicines still calls for concern among health authorities, pharmaceutical industries and

the public at large because the sale and consumption of these herbal medicinal products are not properly regulated in Nigeria. Phyto-toxicity in herbal medicines has been reported due to the adverse effects of plant extracts used in herbal medicines preparations due to errors in botanical identification, accidental ingestion of cardiotoxic plants, inappropriate combinations in phytotherapy and/or interference of medicinal plants with conventional pharmacological therapy^{3,4}. In a bid to determine the quality and efficacy of local herbal medicinal products, this current study evaluates physicochemical parameters (temperature and pH) and content OF some phytochemicals (Alkaloids, Tannins, Terpenoid, Flavonoids, Reducing Sugars, Cardiac glycosides and Saponins) in some selected herbal medicines consumed in Wukari, Taraba State, Nigeria.



Materials and Methods

The samples of herbal medicine products used were obtained from herbal medicine stores in Wukari metropolis. The herbal medicines named Med-Bunch herbal mixture and Super-7 herbal mixture were obtained from a local herbal medicine store at Takum junction area of Wukari town. Also, some herbal medicines named Gbogbonise Epajebu and Gbogbonise Ajurawalo herbal

medicines were obtained from an herbal medicine sales point at Ibi near Wukari town. Other herbal medicines named Koko Fresh herbal medicine, Al Mufeed herbal medicine and Zee herbal medicine were obtained from an herbal medicine shop located in the old market area of Wukari town and finally, an herbal medicine named Lamjib traditional medicine was obtained from a retail hawker along Puje road, Wukari town. The herbal medicines were labelled samples A – H (Table 1) and kept in the refrigerator prior to analysis.

Table 1: Details of the herbal medicinal products

SAMPLE	Herbal Medicinal Product	NAFDAC Reg. No. ^a	Other information
A	Lamjib Traditional Medicine	A1-5578	Mfg. Date: 01/01/2018 Exp. Date: 01/01/2019
B	Gbogbonise (Epajebu) Herbal Medicine	NA	-
C	Med-Bunch Herbal Mixture	A7-2124L	Mfg. Date: 08-2016 Exp. Date: 08-2020 Batch no.: 003
D	Super 7 Herbal Mixture	A7-2061L	Mfg. Date: 10-02-2017 Exp. Date: 10-02-2020
E	Gbogbonise (Ajurawalo) Herbal Medicine	NA	-
F	Koko fresh Herbal Medicine	NA	Mfg. Date: 15/03/2017 Exp. Date: 15/03/2020
G	Zee Herbal Medicine	NA	Mfg. Date: 15/03/2018 Exp. Date: 15/03/2021
H	Al- Mufeed Herbal Medicine	NA	Mfg. Date: 15/03/2018 Exp. Date: 15/03/2021

NA – not available; ^aNational Agency for Food Drugs Administration and Control, Nigeria

Chemicals, Reagents and Glassware

The reagents used in analysis of the herbal medicines were of analytical grade. They were manufactured by BDH Limited Poole England. Distilled water was used throughout the course of analysis. Glassware used were soaked in diluted Nitric acid for 24 hours and washed with distilled water.

Determination of Physicochemical Parameters of the Herbal Medicines

Determination of Temperature

The temperature of the herbal medicine samples was determined using a mercury-in-glass thermometer (GH ZEAL Ltd. London) and readings were taken twice.

Determination of pH

The pH of the herbal medicine samples was determined in their aqueous form; the pH was measured using a

Physicochemical and Phytochemical Analysis of some Selected Herbal Medicinal Products Consumed in Wukari, Taraba State, Nigeria

digital pH meter (WJEUIP, model PHS-25). Calibration of the pH meter was done twice using buffers of pH=4 and pH=7 before recording the pH reading of the samples.

Determination of Phytochemicals in Herbal Medicine

Methodology for qualitative analysis of phytochemicals in herbal medicines was carried out as earlier reported^{5,6,7}.

Flavonoids

Two drops of 1% NH_3 solution was added to 5 mL aqueous solution of the herbal medicine in a test tube followed by the addition of concentrated H_2SO_4 . A yellow colouration was observed which indicated the presence of flavonoid.

Terpenoid

5 mL of aqueous solution of herbal medicine sample was mixed with 2 mL of CHCl_3 in a test tube. 3 mL of concentrated H_2SO_4 was then carefully added to the mixture to form a layer. An interface with a reddish brown colouration was formed which shows the presence of Terpenoid.

Cardiac Glycosides

5 mL of aqueous herbal mixture was treated with 2 mL of glacial acetic acid containing one drop of ferric chloride solution and 1 mL of concentrated H_2SO_4 . A brown ring at the interface indicates the presence of a deoxysugar, characteristic of cardenolides.

Tannins

2 drops of FeCl_3 (0.1%) was added to 5 mL of the herbal medicines samples. A brownish-green or a blue black colouration was formed, which showed the presence of tannins.

Saponins

20 mL of 20% aqueous solution of the sample was shaken in a graduated cylinder for 15 min. A 2 cm layer of foam was formed which indicates the presence of saponins.

Reducing Sugars

5 mL of the sample was taken in a test tube and 1 mL of ethanol was then added to the sample. Thereafter, 1 mL of Fehling solution A and 1 mL of Fehling solution B were taken in another test tube and boiled after which

the mixture was poured into the aqueous solution of the sample and boiled in a water bath for 10 minutes. A colour change to yellow and then brick red precipitate indicates positive result.

Alkaloids

To 5 mL of the sample, two drops of Mayer's reagent was added along the side of a test tube. A white creamy precipitate indicates the presence of alkaloids. Wagner's test 5 mL of the sample, two drops of Wagner's reagent was added along the side of a test tube. A brown precipitate was formed which confirms the presence of Alkaloids.

Dragendroff's test 5 mL of the sample was warmed with 2 % H_2SO_4 for about 2 min, then filtered after which three drops of Dragendroff's reagent is added; a brick red precipitate indicated the presence of alkaloids.

Result and Discussion

The result of physicochemical and phytochemical analysis of the herbal medicine consumed in Wukari Local Government area of Taraba State are presented in the tables below.

Table 2: Mean Temperature of Herbal Medicinal Products Consumed in Wukari, Taraba State, Nigeria

Sample	Temperature (°C)
A	28.00 ± 0.01
B	28.00 ± 0.01
C	28.00 ± 0.01
D	28.00 ± 0.01
E	28.00 ± 0.01
F	28.00 ± 0.01
G	28.00 ± 0.01
H	28.00 ± 0.01



Table 3: Mean pH Value of Herbal Medicinal Products Consumed in Wukari, Taraba State, Nigeria

Sample	pH Value
A	1.05 ± 0.01
B	1.51 ± 0.01
C	2.75 ± 0.01
D	3.30 ± 0.01
E	12.30 ± 0.01
F	3.55 ± 0.01
G	3.40 ± 0.01
H	3.15 ± 0.01

Table 4: Phytochemical Parameter of the Herbal Medicine Samples

Sample	Phytochemicals						
	Tannins	Alkaloids	Saponins	Flavonoids	Terpenoid	Cardiac Glycoside	Reducing sugars
A	–	+	+	–	+	–	+
B	–	+	–	–	–	+	–
C	+	+	+	–	–	+	+
D	+	+	+	+	–	+	+
E	–	+	+	–	–	+	–
F	+	+	+	+	+	+	+
G	+	+	+	+	+	+	+
H	+	+	+	+	–	+	+

+ represents a positive result and – represents a negative result

The mean temperature of the herbal medicines is presented in Table 2. All the analysed herbal medicines had almost constant temperature of 28.00°C which is normal for aqueous solutions at room temperature.

The results of the mean pH value of the herbal medicinal products are presented in Table 3. The herbal medicines had pH values between the ranges of 1.05 – 12.30 with a total mean value of 3.88 ± 1.25 . The herbal medicines analysed were acidic with the exception of sample E (Gbogbonise Ajurawalo) which was highly basic. The herbal medicines were all liquid samples⁸. The acceptable pH range for fruits, vegetables, grasses, flowers, trees, shrubs and annual is 4.0 – 7.5, while that of food is pH 2.0 – 9.0⁹. None of the herbal medicines

analysed fell within this range. The effect of body pH imbalance has been documented. High acidity level can have a negative effect on all body systems, particularly the digestive, intestinal, circulatory, and respiratory and immune system¹⁰. All cells, organs and bodily fluid need a specific pH to function at their best. Enzymes are very sensitive to acidity levels, they take on specific shapes according to the pH of the medium they are in and consequently, they function below normal unless they are in a medium with the specific pH¹⁰. The direct effect of the oral ingestion of these highly acidic herbal medicines is that it increases acidity of the stomach fluids above the level needed for metabolism thereby inhibiting the action of enzymes. Also, when acids accumulate in the body, the body neutralises them using buffer

Physicochemical and Phytochemical Analysis of some Selected Herbal Medicinal Products Consumed in Wukari, Taraba State, Nigeria

systems, but when these systems are overloaded, the body utilises alkaline minerals from vital organs and bones to help neutralise the acidic compounds and eliminate them. This process, over time, can weaken vital organs and bones, and in the latter case, causes osteoporosis. Other effects, as shown from scientific studies includes dark urine with strong odour, poor digestion, fatigue, muscle and joint pain, excessive perspiration, migraine and bad breath¹⁰.

The results of the qualitative phytochemical screening indicate presence of various phytochemicals considered as active medicinal chemical constituents. Phytochemicals of medicinal importance such as terpenoids, reducing sugar, flavonoids, alkaloids, saponins, tannins and cardiac glycosides were present in the samples (Table 4). The result of the phytochemical analysis shows that the eight herbal medicines are rich in at least one of these phytochemicals. All the herbal medicines had alkaloids present in them. Tannins and reducing sugars were found to be present in 62.5% and 75% of the herbal medicines respectively. Flavonoids were present in 50% of the herbal medicines. Saponins and cardiac glycosides were both present in 87.5% of the herbal medicines while Terpenoids was found to be absent in 62.5% of the herbal medicines. The presence of secondary metabolites in the herbal medicines screened may be attributed to their use in treating various ailments and diseases as indicated on the product label. The presence of Alkaloids in the herbal medicines complements the results of Agbo *et al.*,¹² in the ten herbal medicines screened for alkaloids, including the ethanol extract while Adenike *et al.*,¹³ had contradicting results as only eight out of the twenty-one herbal medicines screened had alkaloids present. Alkaloids are used in medicines for reducing headache and fever; these are attributed to antibacterial and analgesic properties¹⁵. Alkaloids were also found in some herbal teas with antimalarial, antihypertensive, antidiabetic and antiobesity¹⁴. Also, Cardiac glycosides and saponins were found present in all samples except in sample A (Lamgib traditional medicine) and sample B (Gbogbonise Epajebu) respectively. Similar research carried out on *Cleistopharis*

patens, one of the components of the herbal mixtures had Cardiac Glycosides and Saponins in both the leaf and stem bark^{11,13,14} and saponins were found to be present in 71% and 40% respectively of the herbal medicines screened while Agbo *et al.*,¹² found cardiac glycosides and saponins to be present in 90% and 20% respectively in the herbal medicines analysed. One of the common health functions of saponins and cardiac glycosides is cholesterol reduction and cure of some heart related diseases respectively. Furthermore, reducing sugars were absent in two herbal medicines out of eight herbal medicine samples, i.e. sample B and sample E. Sample F (Koko Fresh) and sample G (Zee Herbs) had all the phytochemicals present while sample D and sample H (Super 7 and Al-Mufeed) contained all phytochemicals except Terpenoid. Terpenoid has been reported to have anti-inflammatory, anti-viral, anti-malarial, inhibition of cholesterol synthesis and anti-bacterial¹⁶. The herbal medicine with the least amount of phytochemicals present was sample B which gave positive result for Alkaloids and cardiac glycosides.

Conclusions

From this study of the eight herbal medicinal products consumed in Wukari area of Taraba State, it was revealed that the pH levels of the herbal medicinal products were acidic beyond the specified limits, some of which were highly acidic while one was highly basic and therefore are not recommended for ingestion. The study also revealed the presence of some phytochemicals (Alkaloids, Tannins, Terpenoids, Flavonoids, Reducing Sugars, Cardiac glycosides and Saponins) and hence confirms the acclaimed therapeutic functions claimed by the manufacturers. The analgesic, antimalarial, antibacterial, antifungal, antidiuretic, etc. activities prescribed on these herbal products are due to these phytochemicals.

References

1. WHO, 2007, Guidelines for assessing quality of herbal medicines with reference to contaminants and residues, Geneva, p. 1–89.



2. Falodun A., Adeyanju U.A, Erharuyi O., Imieje V., Ehizogie F., Okhwarobo A. and Hamann M., 2013. *Journal of Pharmaceutical and Allied Sciences.*, **10**, 1955-1964.
3. Goldman P., 2001. *Annals of Internal Medicine*, **135(8)-Part I**, 594–600.
4. Wojcikowski K., Johnson D.W. and Gobé G., 2004, *Nephrol.*, **9**, 313–318.
5. Harborne J.B., 1973, Phytochemical screening methods: A guide to modern techniques in plants analysis. Chapman and Hall. London, p. 47–74.
6. Trease G.E. & Evans W.C., 1983, Pharmacognosy, 12th ed. Tindall and Co., London, p. 343- 383.
7. Sofowora A.O., 1993, Medicinal Plants and Traditional Medicine in Africa. University of Ife Press, 2nd Ed., p. 320.
8. Chionyedua T.O., Ngozi A. and Isiaka A.O., 2015, **5(2)**, 148–156.
9. Edebi N.V., and Gideon O.A., 2011. *J. Chem. Pharm. Res.*, **3(2)**, 88-97.
10. Alfred Vogel, 2017, Body pH-effect of a high acidity level and what you can do., www.avogel.ca.
11. Osuntokun O.T., 2015, *Journal of Advances in Medical and Pharmaceutical Sciences*, **4(2)**, 1-14
12. Agbo B.E. and Mbotto C.I., 2012, *Scholars Research Library Archives of Applied Science Research*, **4(5)**, 1974-1990.
13. Adenike O., Babatunde A. Adewoyin and Oluwatoyin A.O., 2007, *Tropical Journal of Pharmaceutical Research*, **6(1)**, 661-670.
14. Omogbai B.A. and Ikenebomeh M., 2013, *European Scientific Journal*, **9(18)**, 149–160.
15. Pietta P.G., 2000, *J. Nat. Prod.*, **63**, 1035-1042.
16. Mahato S.B. and Sen S., 1997, *Phytochemistry*, **44**, 1185-1236.



Detection of Organochlorine Pesticides in *Typhadomingensis* in Euphrates River, Iraq

Amerah Imran. H. AL-Janabi

Department of Biology, College of Biotechnology, University of Al-Qassim Green, Iraq

Email: amirah.imran77@gmail.com

Abstract

This study deals with the detection of Organochlorine pesticides in *Typhadomingensis* at five different sites in the Euphrates river in the middle of Iraq. The highest percentage of the organochlorine compound was detected at site 5 for Endrin Ketone (25.058%) as compared with lowest percentage for TCMX Compound (0.385%) at the same site.

Keywords: Organochlorine Compounds, Pesticides, Euphrates River.

Introduction

Organochlorine pesticides are persistent environmental contaminants in the ecosystem because of their ability to accumulate in the tissue of living organisms¹. Pesticides are major pollutants when they reach water bodies by drifting along with rain water from the adjacent agricultural lands. Pesticides alter the physiological and biochemical processes of harmful organisms^{2,3} and thus increase agricultural productivity.

Studies were conducted on the estimation of chlorinated organic pesticides in living organisms. Detection of pesticide residues, their distribution and their spread in some aquatic organisms has been reported⁴. These included three types of fish: *Liza abu*, *Carassius auratus*, and *Alburnus mossulensis*, one species of *Macrobrachium nipponense* and two species of *Potomogon crispus* and *Ceratophyllum demersum*

Aquatic plants have been used as vital indicator to detect the accumulation of pollutants in the aquatic ecosystem because of their ability to accumulate pollutants

in their tissues. They are good biomarkers to detect pollutants in water bodies⁵. The present study deals with the use of the aquatic plants found in Euphrates River as a vital indicator for pesticide pollution.

Materials and Methods

Description of the study area

The study area on the Euphrates River included five sites from Al-Musayyib site to Al-Kufa site (Fig.1)

Site 1- located on the Euphrates River in Al- Musayyib, near the bridge of Al-musayib characterized by a high level of water in the river and some types of plants.

Site-2- located on the Euphrates River before branching at Al-Hindiyadum at about 2 km adjacent to the cement plant Al-Suda, and is characterized by high water level and the presence of some plant species.

Site 3- located on the Euphrates River after passing through the city of Al-Suda and 15 km away from the first site. The river water is adversely affected by the



human activity of the city of Sadda. The site has aquatic plants

Site 4- located on the Euphrates River about 15 km to the north of the city of Hindi characterized by intensive agricultural activity.

Site 5- located on the Euphrates river in the city of Al-Hindi before branching to the rivers oAl-Kufa and Al-

Abbasiyah. The site is characterized by carrot crops and presence of aquatic plants.

Sample Collection

The samples of *Typhadomingensis* were collected from the sites under study using standard methods. They were placed in sterile bags and stored in a box until they reached the laboratory and then were stored in the frozen state till the time of analysis.

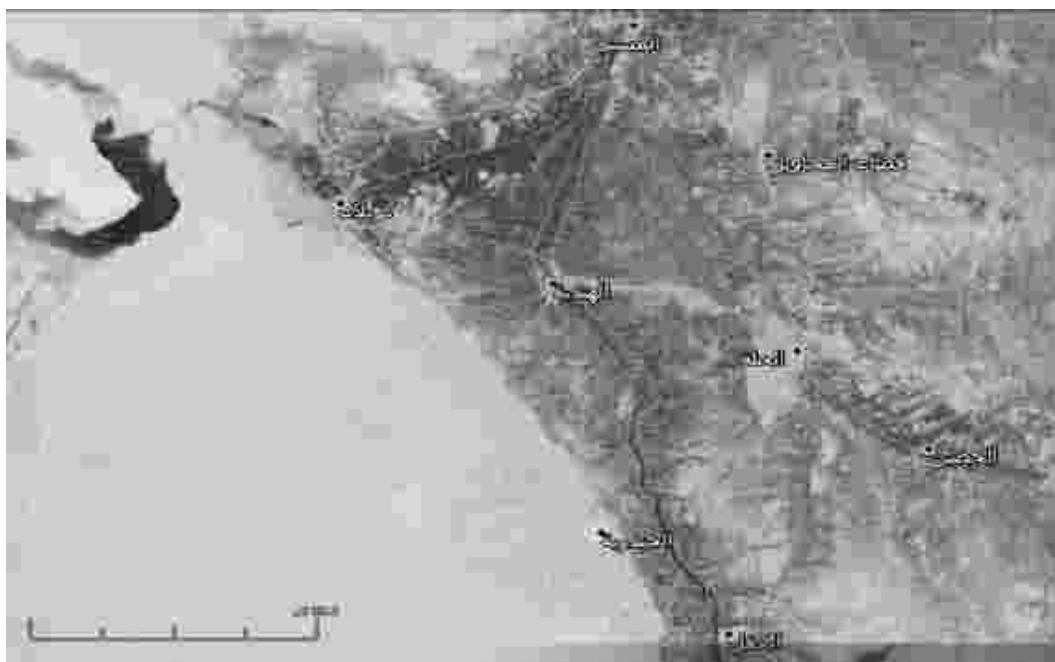


Fig. 1: Study sites on the Euphrates River (<http://maps.google>)

Extraction and Estimation of Pesticides

Pesticides were extracted from *Typhadomingensis* by taking 5 g of the *Typhadomingensis* to be extracted, mixed with 5 g NaOSO₄ and then extracted with 1:1 ether:acetone solvent in cold condition⁶. A shaker was used to stop bubbles in the funnel and the mixture was put aside for 30 minutes. The mixture was then filtered and stored in glass containers⁷.

Pre-concentration of extract: The dissolved sample was concentrated to 1 mL using rotary evaporator.

Clean-up of extract⁸: A 30 cm long glass separation column was filled with 20 mL silica gel (90%, < 45 micrometers) and the column was washed with n-hexane to remove contaminants

The mixture of the extract and 1 g of anhydrous sodium sulphate Na₂SO₄ was loaded on the column and eluted with a mixed solvent of dichloromethane and hexane (20: 80) to obtain the first separation of liquids (30 mL) and in the second separation, a mixed solvent containing dichloromethane, hexane, and acetonitrile (50: 49.5: 0.5) was used to obtain 30 mL of separated liquids.

Subsequently the separated phase was concentrated in the rotary evaporator device to 1 mL.

Preparation of standards: The standards were prepared using ethyl acetate as solvent. The standards were prepared daily and diluted using ethyl acetate. The calibration curve was prepared using four concentrations of the compounds under study. The solutions of the compounds and the standards were stored at -4°C and in the dark.

Characterisation using GC-MS: A GC-MS device was used along with Varian 3800 electron microscope and ion-trap mass spectrometer (Varian Instruments, Sunnyvale, CA, USA). The samples were injected into the apparatus directly using a 10 µL syringe. The GC device was equipped with an automatic injector and temperature programming device. The quality and quantity of the peaks of compounds were determined by using computer programs and GC-MS library, which was specially created to calibrate new compounds using standards.

The separation column used was a fused-silica capillary column (30 m length × 0.2 mm I.D. × 0.25 µm film thickness) and helium gas with a gas flow rate of 1 mL/min and was maintained at 300°C. The concentration of samples was calculated using the following equation:

$$\text{concentration } (\mu\text{g/L}) = \frac{(A) - (Vt)}{(Vi)(Vs)}$$

where

A = Amount of material injected (ng). Vi = Volume of extract injected (µL)

Vt = Volume of total extract (µL). Vs = Volume of water extracted (µL).

Statistical analysis

The results obtained were analyzed statistically by using variance analysis in two directions (Anova: Two-Factor) and conducted by Microsoft Excel 2010. The mean of the coefficients were compared when the differences were significant by using the Least Difference

Significant difference (LSD) at a probability level ($P < 0.05$)⁹.

Results and Discussion

Organic chlorinated pesticides in *Typhadomingensis*

Figures 2-6 show the percentage of organochlorine compounds in *Typha domingensis* at sites 1-5. Tables 1-5 show the concentration of chlorinated organic pesticides in aquatic *Typha domingensis* at sites 1-5. Among all the pesticides investigated, the percentage of Endrine ketone and Endrine aldehyde was found to be highest at all sites.

Conclusions

The following chlorinated organic pesticides were detected in aquatic *T. domingensis* at different sites in Euphrates River: TCMX (Tetrachlorometaxylene), alpha-benzene hexachloride, Gamma-BHC (Gamma-benzene hexachloride) and Beta-BHC (Beta-benzene hexachloride), Delta-benzene hexachloride, Heptachlor, Aldrin, Heptachlor-epoxide, Trans-Chordane, Cis-Chordane, P-DDE (P, Dichlorodiphenyldichloroethylene), Endosulfan I and Dieldrin, Endrin and P, P'-DDD (P, P'-Dichlorodiphenyldichloroethane), Endosulfan II and P, P'-DDT (P, P'-Dichlorodiphenyltrichloroethane), Endrin aldehyde, Methoxychlor, Endosulfansulfate, Endrin ketone and Decachlorobiphenyl.

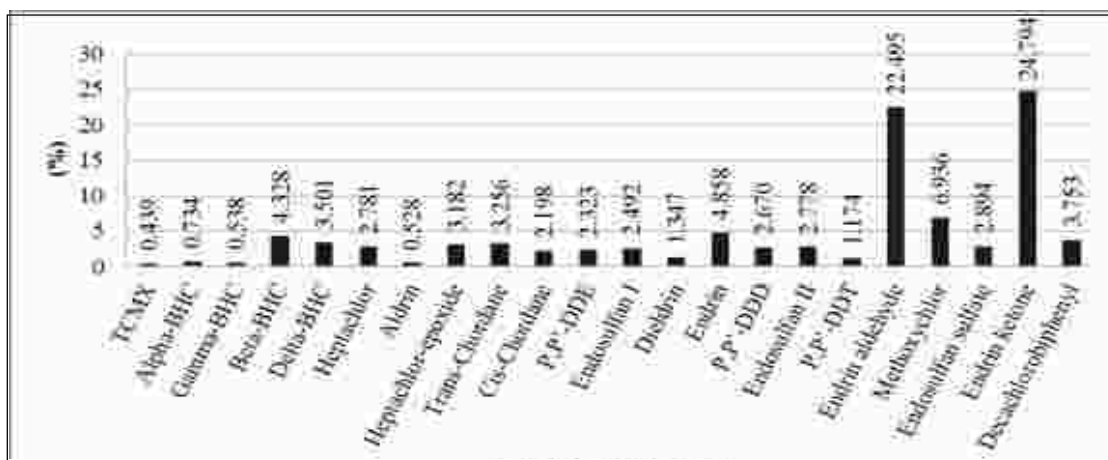


Fig.2: Percentage of organochlorine pesticides in *T. domingensis* at site 1

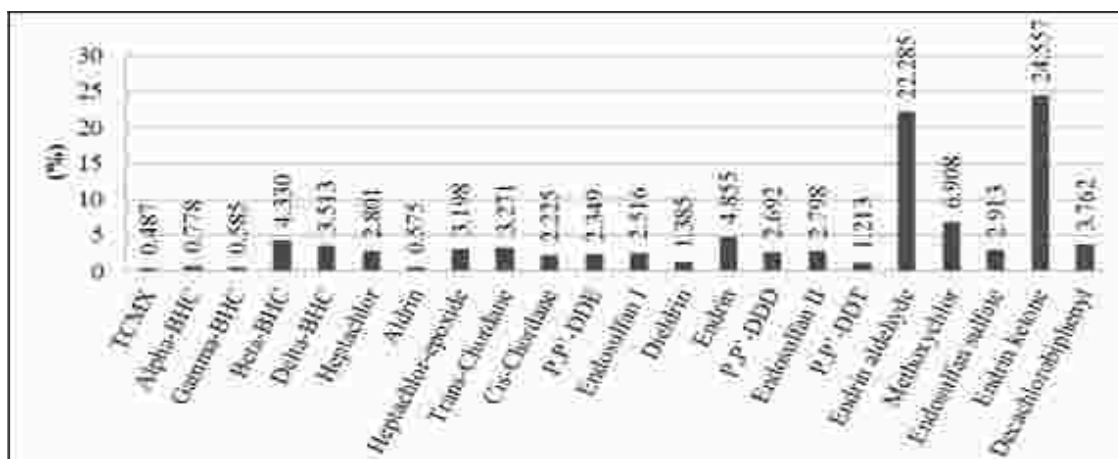


Fig.3: Percentage of organochlorine pesticides in *T. domingensis* at site 2

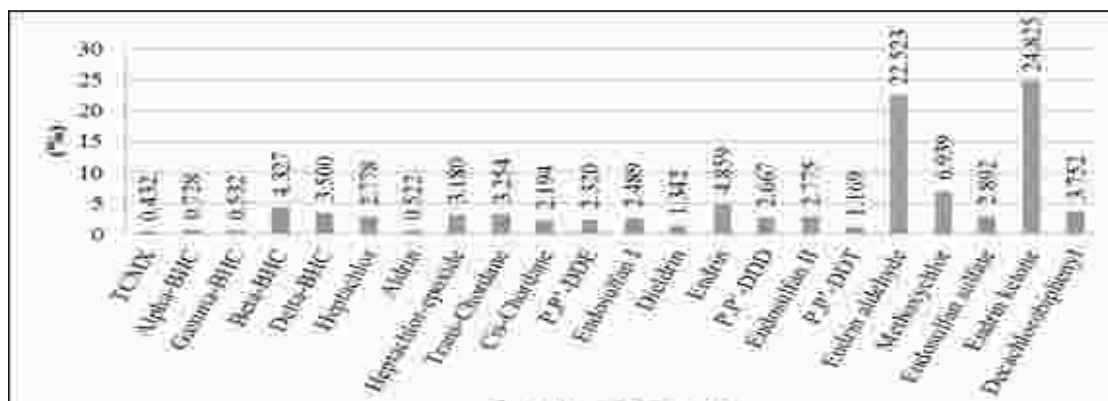


Fig.4: Percentage of organochlorine pesticides in *T. domingensis* at site 3

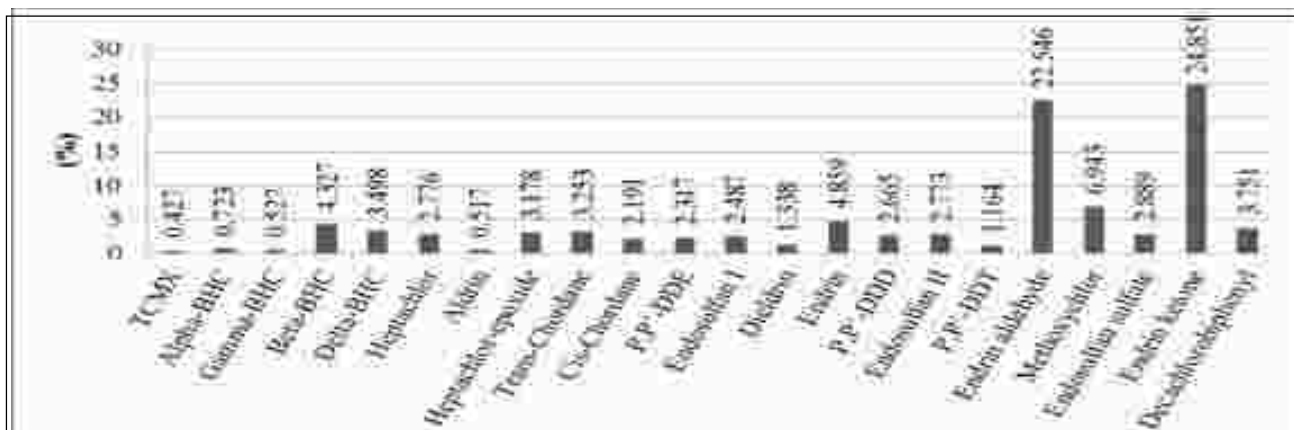


Fig.5: Percentage of organochlorine pesticides in *T. domingensis* at site 4

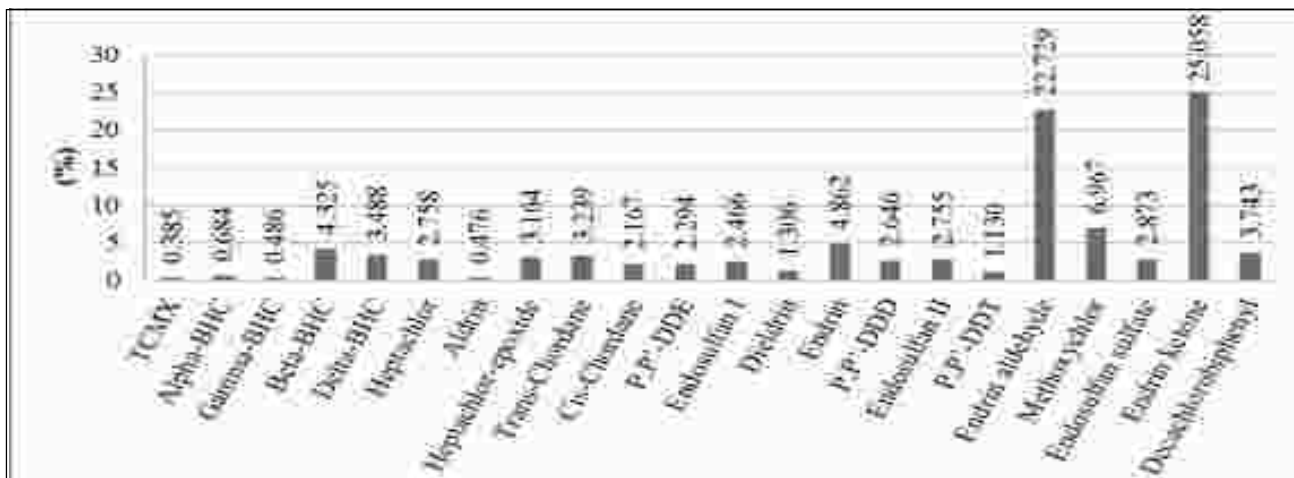


Fig.6: Percentage of organochlorine pesticides in *T. domingensis* at site 5

Table 1: Concentration of chlorinated organic pesticides in aquatic *T. domingensis* ($\mu\text{g} / \text{kg}$) at site 1 during the seasons of 2013-2014

SD \pm Seasonal mean	Spring 2013	Winter 2013	Autumn 2013	Summer 2013	Compounds
2.893 \pm 8.234	9.747	11.991	6.865	4.334	TCMX
4.500 \pm 13.768	16.122	19.611	11.639	7.703	Alpha-BHC
3.434 \pm 10.097	11.894	14.556	8.472	5.469	Gamma-BHC
24.074 \pm 81.210	93.798	112.466	69.817	48.759	Beta-BHC
19.572 \pm 65.699	75.934	91.111	56.437	39.317	Delta-BHC
15.648 \pm 52.179	60.361	72.496	44.774	31.086	Heptachlor
3.381 \pm 9.915	11.683	14.305	8.315	5.357	Aldrin
17.832 \pm 59.706	69.030	82.858	51.267	35.669	Heptachlor-epoxide
18.238 \pm 61.102	70.639	84.781	52.471	36.519	Trans-Chlordane
12.473 \pm 41.241	47.764	57.436	35.339	24.428	Cis-Chlordane
13.155 \pm 43.589	50.468	60.670	37.364	25.857	P,P'-DDE
14.078 \pm 46.770	54.132	65.049	40.108	27.794	Endosulfan I



7.842 ± 25.283	29.383	35.464	21.572	14.713	Dieldrin
26.963 ± 91.163	105.261	126.171	78.403	54.818	Endrin
15.046 ± 50.105	57.973	69.641	42.985	29.824	P,P'-DDD
15.633 ± 52.125	60.299	72.422	44.727	31.053	Endosulfan II
6.898 ± 22.031	25.638	30.988	18.767	12.733	P,P'-DDT
123.018 ± 422.112	486.434	581.831	363.895	256.290	Endrin aldehyde
38.278 ± 130.147	150.162	179.845	112.033	78.551	Methoxychlor
16.266 ± 54.309	62.814	75.428	46.611	32.383	Endosulfan sulfate
135.536 ± 465.243	536.111	641.215	401.102	282.547	Endrin ketone
20.944 ± 70.427	81.378	97.620	60.515	42.195	Decachlorobiphenyl
	98.501	118.088	73.339	51.245	SD ± Mean
	131.818 ±	157.577 ±	98.729 ±	69.673 ±	
65.551 = interferences	32.776 = Compounds		13.976 = Seasons		LSD_{0.05}

Table 2: Concentration of chlorinated organic pesticides in aquatic *T. domingensis* (µg / kg) at site 2 during the seasons of 2013-2014

SD ± Seasonal mean	Spring 2014	Winter 2013	Autumn 2013	Summer 2013	Compounds
4.460 ± 14.244	16.576	20.035	12.134	8.233	TCMX
6.936 ± 22.775	26.402	31.780	19.492	13.426	Alpha-BHC
5.293 ± 17.116	19.885	23.988	14.612	9.982	Gamma-BHC
37.105 ± 126.720	146.122	174.895	109.161	76.705	Beta-BHC
30.167 ± 102.815	118.589	141.982	88.539	62.153	Delta-BHC
24.118 ± 81.976	94.587	113.290	70.563	49.466	Heptachlor
5.211 ± 16.835	19.560	23.601	14.369	9.810	Aldrin
27.485 ± 93.577	107.948	129.261	80.570	56.529	Heptachlor-epoxide
28.110 ± 95.729	110.427	132.225	82.426	57.839	Trans-Chordane
19.225 ± 65.118	75.171	90.079	56.021	39.204	Cis-Chordane
20.276 ± 68.737	79.339	95.063	59.142	41.406	P,P'-DDE
21.698 ± 73.640	84.986	101.812	63.372	44.392	Endosulfan I
12.087 ± 40.521	46.841	56.214	34.802	24.229	Dieldrin
41.558 ± 142.062	163.791	196.018	122.395	86.044	Endrin
23.190 ± 78.780	90.905	108.890	67.806	47.521	P,P'-DDD
24.094 ± 81.893	94.491	113.176	70.491	49.415	Endosulfan II
10.632 ± 35.510	41.069	49.314	30.479	21.179	P,P'-DDT
189.606 ± 652.148	751.287	898.320	562.419	396.569	Endrin aldehyde
58.997 ± 202.147	232.995	278.745	174.227	122.622	Methoxychlor
25.071 ± 85.258	98.368	117.809	73.394	51.464	Endosulfan sulfate
208.900 ± 718.626	827.853	989.848	619.766	437.039	Endrin ketone
32.282 ± 110.101	126.980	152.014	94.825	66.587	Decachlorobiphenyl
	153.371	183.561	114.591	80.537	SD ± Mean
	203.169 ±	242.871 ±	152.170 ±	107.386 ±	
101.033 = Interferences	50.516 = Compounds		21.540 = Seasons		LSD_{0.05}

Detection of Organochlorine Pesticides in *Typhadomingensis* in Euphrates River, Iraq

Table 3: Concentration of chlorinated organic pesticides in aquatic *T. domingensis* ($\mu\text{g} / \text{kg}$) at site 3 during the seasons of 2013-2014

SD \pm Seasonal mean	2014 Spring	Winter 2013	Autumn 2013	Summer 2013	Compounds
3.255 \pm 9.116	10.818	13.343	7.576	4.728	TCMX
5.063 \pm 15.342	17.989	21.916	12.947	8.518	Alpha-BHC
3.864 \pm 11.212	13.232	16.229	9.384	6.004	Gamma-BHC
27.084 \pm 91.217	105.379	126.382	78.400	54.709	Beta-BHC
22.020 \pm 73.767	85.281	102.357	63.347	44.086	Delta-BHC
17.605 \pm 58.556	67.762	81.413	50.225	34.826	Heptachlor
3.804 \pm 11.006	12.995	15.945	9.206	5.879	Aldrin
20.063 \pm 67.024	77.514	93.072	57.530	39.980	Heptachlor-epoxide
20.519 \pm 68.595	79.324	95.235	58.885	40.937	Trans-Chordane
14.033 \pm 46.250	53.588	64.471	39.609	27.335	Cis-Chordane
14.800 \pm 48.893	56.632	68.109	41.889	28.943	P,P'-DDE
15.839 \pm 52.471	60.753	73.036	44.976	31.121	Endosulfan I
8.822 \pm 28.297	32.910	39.751	24.122	16.405	Dieldrin
30.334 \pm 102.415	118.276	141.800	88.060	61.526	Endrin
16.928 \pm 56.223	65.074	78.202	48.212	33.405	P,P'-DDD
17.587 \pm 58.495	67.691	81.330	50.172	34.789	Endosulfan II
7.761 \pm 24.638	28.696	34.715	20.966	14.177	P,P'-DDT
138.402 \pm 474.751	547.117	654.443	409.254	288.192	Endrin aldehyde
43.064 \pm 146.274	168.792	202.186	125.894	88.226	Methoxychlor
18.300 \pm 60.952	70.521	84.712	52.292	36.284	Endosulfan sulfate
152.485 \pm 523.276	603.006	721.253	451.113	317.733	Endrin ketone
23.563 \pm 79.086	91.407	109.679	67.935	47.324	Decachlorobiphenyl
	110.670 148.302 \pm	132.708 177.283 \pm	82.363 111.076 \pm	57.505 78.386 \pm	SD \pm Mean
73.748 =interferences	36.874 =Compounds		15.723 =Seasons		LSD_{0.05}

Table 4: Concentration of chlorinated organic pesticides in aquatic *T. domingensis* ($\mu\text{g} / \text{kg}$) at site 4 during the seasons of 2013-2014

SD \pm Seasonal mean	Spring 2013	Winter 2013	Autumn 2013	Summer 2013	Compounds
2.321 \pm 6.410	7.623	9.423	5.312	3.282	TCMX
3.609 \pm 10.849	12.737	15.535	9.141	5.984	Alpha-BHC
2.754 \pm 7.904	9.345	11.481	6.601	4.192	Gamma-BHC
19.310 \pm 64.943	75.040	90.014	55.805	38.915	Beta-BHC
15.699 \pm 52.503	60.712	72.885	45.073	31.342	Delta-BHC
12.551 \pm 41.658	48.221	57.954	35.719	24.740	Heptachlor
2.712 \pm 7.758	9.176	11.279	6.475	4.102	Aldrin
14.303 \pm 47.695	55.174	66.265	40.926	28.415	Heptachlor-epoxide
14.628 \pm 48.815	56.464	67.808	41.892	29.097	Trans-Chordane
10.005 \pm 32.885	38.116	45.875	28.151	19.399	Cis-Chordane
10.552 \pm 34.768	40.286	48.469	29.775	20.545	P,P'-DDE
11.292 \pm 37.320	43.224	51.981	31.976	22.099	Endosulfan I
6.290 \pm 20.084	23.373	28.251	17.108	11.606	Dieldrin



21.627 ± 72.927	84.235	101.006	62.692	43.775	Endrin
12.069 ± 39.995	46.305	55.664	34.284	23.727	P,P'-DDD
12.539 ± 41.615	48.171	57.895	35.681	24.713	Endosulfan II
5.533 ± 17.476	20.370	24.660	14.858	10.019	P,P'-DDT
98.672 ± 338.380	389.973	466.490	291.684	205.375	Endrin aldehyde
30.702 ± 104.196	120.250	144.058	89.666	62.811	Methoxychlor
13.047 ± 43.366	50.188	60.306	37.192	25.779	Endosulfan sulfate
108.713 ± 372.976	429.819	514.122	321.528	226.435	Endrin ketone
16.800 ± 56.294	65.079	78.106	48.344	33.650	Decachlorobiphenyl
	78.812	94.542	58.631	40.909	SD ± Mean
	105.731 ±	126.392 ±	79.190 ±	55.885 ±	
52.578 = Interferences	26.289 = Compounds		11.210 = Seasonal		LSD_{0.05}

Table 5: Concentration of chlorinated organic pesticides in aquatic *T. domingensis* ($\mu\text{g} / \text{kg}$) at site 5 during the seasons of 2013-2014

SD ±Seasonal Mean	Spring2014	Winter 2013	Autumn2014	Sumer2013	Copounds
1.930 ± 4.760	5.770	7.267	3.847	2.159	TCMX
3.002 ± 8.453	10.023	12.350	7.032	4.407	Alpha-BHC
2.291 ± 6.004	7.202	8.978	4.920	2.916	Gamma-BHC
16.060 ± 53.443	61.841	74.294	45.843	31.795	Beta-BHC
13.057 ± 43.096	49.924	60.049	36.917	25.497	Delta-BHC
10.439 ± 34.077	39.535	47.630	29.137	20.006	Heptachlor
2.256 ± 5.882	7.061	8.811	4.815	2.841	Aldrin
11.896 ± 39.097	45.318	54.543	33.468	23.062	Heptachlor-epoxide
12.166 ± 40.029	46.391	55.825	34.272	23.630	Trans-Chordane
8.321 ± 26.780	31.131	37.584	22.842	15.564	Cis-Chordane
8.776 ± 28.346	32.935	39.741	24.194	16.517	P,P'-DDE
9.391 ± 30.468	35.379	42.662	26.024	17.810	Endosulfan I
5.231 ± 16.134	18.869	22.926	13.659	9.083	Dieldrin
17.987 ± 60.083	69.488	83.437	51.571	35.837	Endrin
10.037 ± 32.693	37.941	45.725	27.944	19.164	P,P'-DDD
10.429 ± 34.041	39.494	47.581	29.106	19.983	Endosulfan II
4.602 ± 13.965	16.371	19.940	11.788	7.762	P,P'-DDT
82.066 ± 280.860	323.770	387.409	242.023	170.240	Endrin aldehyde
25.535 ± 86.089	99.441	119.243	74.005	51.669	Methoxychlor
10.851 ± 35.497	41.171	49.586	30.362	20.870	Endosulfan sulfate
90.417 ± 309.633	356.910	427.025	266.844	187.756	Endrin ketone
13.972 ± 46.250	53.556	64.390	39.638	27.416	Decachlorobiphenyl
	64.978	78.045	48.193	33.453	SD ±Mean
	87.936 ±	105.120 ±	65.862 ±	46.479 ±	
43.729=Interferences	21.865 = Compounds		9.323 = Seasons		LSD_{0.05}

References

1. World Health Organisation (WHO), 2004, Guideline values for chemicals of health significance and Guidelines for drinking water quality.
2. Mullick A., Jaha A. and Sharma O.P., 2014, *International Journal of Pharmacology and Biological Sciences*, **5(3)**, 543
3. Rani Manju, Gupta R.K., Jyoti Yadav and Sandeep Kumar, 2017, *Journal of Entomology and Zoology studies*, **5(2)**,1369-1371
4. Ali B.S.A., 2012, Residues of some insecticides in water, sediments and neighbourhoods from eastern Hor al-Hammar, Iraq. PhD thesis, Faculty of Agriculture, University of Basra, Iraq.
5. Kaur M., Sharma J.K., Gill J.P., Aulakh R.S., Bedi J.S. and Joia B.S., 2008, *Bull. Environ. Contam. Toxicol.*, **80(2)**, 154-157
6. Steinwandter H., 1992, Development of micro extraction methods in residue analysis, Cairns, T. and Sherma, J., eds. Emerging strategies for pesticide analysis, p. 3-50, CRC, Boca Raton, F.L., U.S.A.
7. US Environmental Protection Agency (US EPA), 2002, Method 3570, Revision C, Microsclar Extraction (MSE), Washington D C, USA.
8. US Environmental Protection Agency (US EPA), 1996, Method 3630, Revision B, Silica gel cleanup, SW-846 Manual, Washington DC, USA.
9. Steel R.G.D., and Torrie J.H., 1980, Principles and procedures of Statistics –a biometrical approach, USA, p.633



Antimicrobial Property of Kappa-Carrageenan Filled with Zinc Oxide Nanoparticles (ZNONPS) in Textile Fabrics

Judy Ann H. Bremsis¹ and Karina Milagros R. Cui-Lim^{1,2*}

¹Department of Physical Sciences, College of Science,

²University Research and Development Services,

University of Eastern Philippines, University Town, Northern Samar, Philippines 6400

Email: karina_cui@yahoo.com

Abstract

Nanotechnology is an emerging interdisciplinary technology that has been booming in recent decades. The application of nanoscale materials and structures, usually ranging from 1 to 100 nanometers (nm), is an emerging area of nanoscience and nanotechnology. Kappa-Carrageenan, a natural polymer is a product derived from seaweeds and has been gaining attention due to its biodegradability and low cost production. Zinc oxide nanoparticles were prepared by wet chemical method using zinc nitrate and sodium hydroxide as precursors and Kappa Carrageenan as stabilizing agent and were found to be effective against *Staphylococcus aureus* and *Escherichia coli* bacteria. It has clear zones of inhibition 7 mm against *S. aureus* and 2.33 against *E. coli* which were within the standard radius i.e. 2 mm.

Keywords: Nanotechnology, Zinc Oxide Nanoparticles, Kappa Carrageenan, Antibacterial Activity.

Introduction

All the leading textile industries are focusing on value added applications such as microbe resistant, electromagnetic protected and thermoregulatory fabrics. Nanotechnology is an umbrella term covering a wide range of technologies concerned with structures and processes on the nanometer scale. Nanotechnology is regarded as a key technology which will not only influence technological development in the near future, but will also have economic, social and ecological implications.

Zinc oxide (ZnO) is described as a functional, strategic and versatile inorganic material with a broad range of

applications. It is known as II–VI semiconductor, since zinc and oxygen are classified into groups two and six, respectively, in the periodic table. ZnO holds unique optical, chemical sensing, semi-conducting, electric conductivity, and piezoelectric properties.

With the growing public health awareness of the pathogenic effects, malodors and stain formations caused by microorganisms, there is an increasing need for antibacterial materials in many areas like medical devices, health care, hygienic application, water purification systems, hospital, dental surgery equipment, textiles, food packaging, and storage¹.

Antibacterial activity of Zinc oxide nanoparticles

Antimicrobial Property of Kappa-Carrageenan Filled with Zinc Oxide Nanoparticles (ZNONPS) in Textile Fabrics

(ZnONps) has received significant interest worldwide due to the availability of technology to synthesize particles in the nanometer range. Many microorganisms exist in the range from hundreds of nanometers to tens of micrometers. ZnONps exhibit attractive antibacterial properties due to increased specific surface area as the reduced particle size leads to enhanced particle surface reactivity. ZnO is a bio-safe material that has photo-oxidizing and photocatalysis impact on chemical and biological species.

Materials and Methods

Synthesis of Zinc Oxide Nanoparticles

The synthesis was done as per method available in literature². Zinc oxide nanoparticles (ZnONps) were prepared by using zinc nitrate and sodium hydroxides precursors and Kappa Carrageenan as stabilizing agent. About 0.1 g of Kappa Carrageenan was dissolved in 500 mL of lukewarm distilled water. About 14.84 g (0.1mol) of zinc nitrate was added to the above solution, followed by constant stirring for 1 hour, using a magnetic stirrer. After complete dissolution of zinc nitrate, 0.2 mol of sodium hydroxide solution was added dropwise with constant stirring. The reaction was allowed to proceed for 2 hr. After the completion of the reaction, the solution was kept overnight, and the supernatant solution was carefully discarded. Rest of the solution was centrifuged at 10 rpm for 10 min and the supernatant was discarded. The nanoparticles obtained were washed thrice with distilled water. Washing was carried out to remove the by-products and the excessive starch bound to the nanoparticles. After washing, the nanoparticles were dried at 80°C overnight.

Coating of Textile with ZnONps

Zinc oxide nanoparticle was applied to a textile "Katrina" by a pad-dry-cure method. The textile was cut to a size of 30 by 30 cm, and was immersed in a solution of 2% ZnONps for 5 minutes. After soaking, the textile was air dried and then cured for 3 minutes in a drying oven at 140°C. The coated fabric was soaked for 5 minutes in 2.0 g/L sodium lauryl sulphate to remove any un-

bound nanoparticles. Then, the fabric was rinsed 10 times to completely remove any traces of soap. The fabric was finally dried.

Microbial Screening

a. Preparation of Bacterial Subculture in Nutrient Agar

About 28.0 g of Mueller Hinton Agar was suspended in 1000 mL sterilized distilled water. The mixture was boiled with frequent agitation to completely dissolve the medium and it was then sterilized in an autoclave at about 121°C for 15 minutes. The medium was allowed to cool at about 50°C then aseptically poured into each petri dish and allowed to solidify.

b. Preparation of the Filter Paper Disc for the Sample and for the Positive and Negative Control

A treated textile fabric of dimensions 6 mm diameter and 1mm thickness was prepared with the use of sterilized brand new paper puncher. Sterile textile discs were labeled as+ (treated textile with synthesized zinc oxide), C(Chloramphenicol) as positive control and – (plain textile) for the negative control. Sterile discs labeled + were soaked in zinc oxide nanoparticles. Then the sterilized disc labeled C was soaked in reconstituted powder of chloramphenicol for 12 hours prior to use.

Antimicrobial Sensitivity Test

A modified antimicrobial sensitivity test³ was used to determine the antimicrobial activity of synthesized zinc oxide from Kappa Carrageenan against *E.coli* and *S. aureus*. The pure isolates of subcultures *E.coli* and *S. aureus* were aseptically harvested onto the surface of nutrient agar plates with the use of sterilized cotton swab. The labeled textile disc was aseptically and carefully soaked into the surface of Nutrient Agar using a sterilized pick up forceps. The inoculated plates were incubated at 37°C for 48 hours. After the inoculation, the plates were inspected for the presence of any clear zone of inhibition around sample discs. Presence of more than 2 mm clear zone around the sample disc indicated that the organism was susceptible to the chemical agent present



in the discs and hence, inhibiting the growth. Apart from that, absence of any clear zone suggested that the organisms were resistant to the chemical agent present in the disc.

Results and Discussion

Results of the antimicrobial test for synthesized ZnONps against the bacteria *Staphylococcus aureus* and *Escherichia coli*. are shown in Figures 1 and 2.

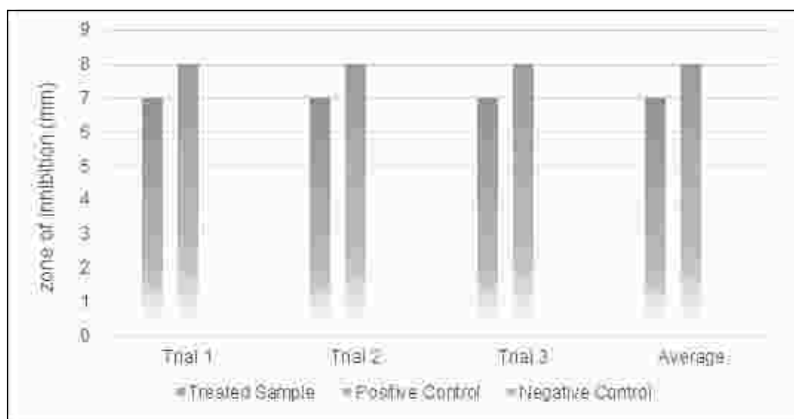


Fig 1. Comparative Chart of the Zone of inhibition for *S. aureus*

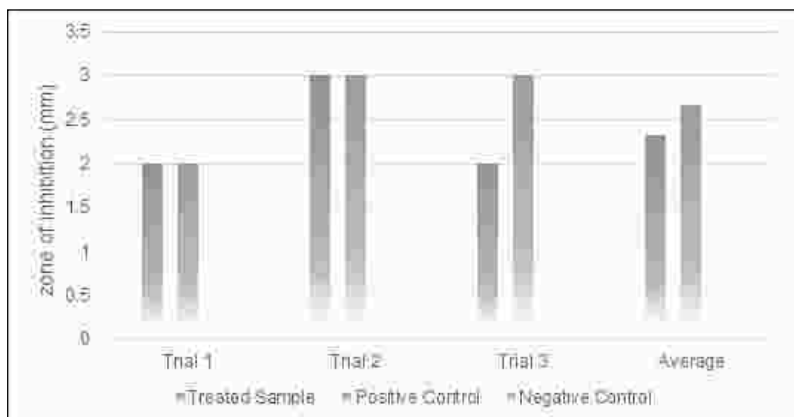


Fig 2. Comparative Chart of the Zone of inhibition for *E. coli*

As shown in Figures 1 and 2 above, after three trials, ZnONps showed antimicrobial activity against both *S. aureus* showing a clear zone of inhibition of 3.67 mm mean in all treatments and *E. coli* showing a zone of inhibition of 2.33 mm mean in all treatments. This implied that the sample had the potential in inhibiting the growth of *E. coli* and *S. aureus* bacteria, indicated

by the presence of clear zone of inhibition. Absence of any clear zone suggested that the organisms were resistant to the chemical agent present in the disc. On the other hand, results of the positive control i.e. reconstituted powder of chloramphenicol indicated a clear zone of inhibition. (Figure 3)

Antimicrobial Property of Kappa-Carrageenan Filled with Zinc Oxide Nanoparticles (ZNONPS) in Textile Fabrics



Fig 3. Microbial Test Plates

Conclusions

The antimicrobial property of Textile Kappa Carrageenan filled with ZnONps against *Staphylococcus aureus* and *E. coli* inhibits the bacterial growth in textile fabrics.

References

- 1a. Shahidi Sheila and Jakub Wiener., 2007, "Antibacterial Agents in Textile Industry". Department of Textiles, Faculty of Engineering, Islamic Azad University, Arak Branch, Arak Iran and Department of Textile Chemistry, Faculty of Textile, Technical University of Liberec, Liberec, Czech Republic.
- b. Sirelkhatim Amna, Shahrom Mahmud, Azman Seeni, Noor Haida, Mohamad Kaus, Ling Chuo Ann, SitiKhadijah, Mohd Bakhori, Habsah Hasan, and Dasmawati Mohamad., 2015, "Review on Zinc Oxide Nanoparticles: Antibacterial Activity and Toxicity Mechanism".
2. Rao N., Srinivasa Rao and Mandava V.B., 2015, *American Journal of Material Science*.
3. Bauer A.W., Kirby M.M., Sherris J.C. and Turck M., 1996, *The American Journal of Clinical Pathology*, **45**, 4.



Historical Landmarks in the Development of the Periodic Table

S. Vasudevan

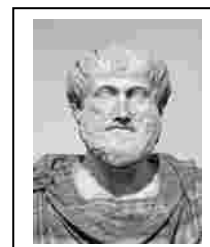
Electromorganics Divison,
CSIR-Central Electrochemical Research Institute, Karaikudi-630003, India

Email: vasudevan65@gamil.com

The development of the periodic table of the elements is one of the most significant achievements in science with broad implications in chemistry, physics, astronomy and other natural sciences. So the United Nations (UN) General Assembly (72nd session) declared 2019 as the International Year of the Periodic Table of chemical elements (IYPT 2019). Accidentally, the IYPT will coincide with the 150th anniversary of the discovery of the periodic system by Dmitry Mendeleev, a Russian chemist who, in 1869 wrote out the known elements (of which there were 63 elements at the time) on cards and then arranged them according to their chemical and physical properties in columns and rows. As a result of the development, the periodic table stares from the wall of just about every chemistry laboratory in schools and colleges. The periodic table was not actually started with Dmitry Mendeleev. Many scientists/chemists had attempted with arranging the elements.

1. Aristotle's Periodic Table

Going back to ancient times (400 BC), we can see the roots of our understanding of the elements that make up the periodic table. In ancient Greece, Aristotle and Plato thought that everything on the planet came from four root sources. They were fire, water, air and earth (Figure 1). In ancient times, elements like gold and silver were readily accessible; however, the elements that Aristotle chose were Earth, Water, Fire, and Air. Therefore, we can say that the ancient Greeks did understand the nature of elements and what they were in a basic way. But they didn't do much to advance our understanding of matter; that is something that would come later.



E 1 Earth	W 2 Water	A 3 Air	F 4 Fire	
<table border="1"> <tbody> <tr> <td>Et 5 Ether</td> </tr> </tbody> </table>				Et 5 Ether
Et 5 Ether				

Fig. 1: Aristotle's Periodic Table

2. Antoine Lavoisier Periodic Table (1770 - 1789)

Antoine Lavoisier (1789) wrote the first list of 33 elements. He classified them as metals and nonmetals, though we now know that some were compounds or mixtures.

192 DES SUBSTANCES SIMPLES.
TABLEAU DES SUBSTANCES SIMPLES.

	Noms nouveaux.	Noms anciens correspondans.
<i>Substances simples qui appartiennent aux trois régnes & qu'on peut regarder comme les élémens des corps.</i>	Lumière.....	Lumière. Chaleur, Principe de la chaleur.
	Calorique.....	Fluide igné. Feu. Matière du feu & de la chaleur.
	Oxygène.....	Air déphlogistiqué. Air empiréal. Air vital. Base de l'air vital.
	Azote.....	Gaz phlogistiqué. Mofete. Base de la mofete.
	Hydrogène.....	Gaz inflammable. Base du gaz inflammable.
<i>Substances simples non métalliques oxidables & acidifiables.</i>	Soufre.....	Soufre.
	Phosphore.....	Phosphore.
	Carbone.....	Charbon pur.
	Radical muriatique.	Inconnu.
	Radical fluorique.	Inconnu.
	Radical boracique.	Inconnu.
	Antimoine.....	Antimoine.
	Argent.....	Argent.
	Arsenic.....	Arsenic.
	Bismuth.....	Bismuth.
<i>Substances simples métalliques oxidables & acidifiables.</i>	Cobalt.....	Cobalt.
	Cuivre.....	Cuivre.
	Etain.....	Etain.
	Fer.....	Fer.
	Manganèse.....	Manganèse.
	Mercure.....	Mercure.
	Molybdène.....	Molybdène.
	Nickel.....	Nickel.
	Or.....	Or.
	Platine.....	Platine.
<i>Substances simples sulfifiables terreuses.</i>	Plomb.....	Plomb.
	Tungstène.....	Tungstène.
	Zinc.....	Zinc.
	Chaux.....	Terre calcaire, chaux.
	Magnésie.....	Magnésie, base du sel d'Épsum.
Baryte.....	Barôte, terre pesante.	
Alumine.....	Argile, terre de l'alun, base de l'alun.	
Silice.....	Terre siliceuse, terre vitrifiable.	

Fig 2: Traité Élémentaire de Chimie, Cuchet, Paris, 1789, p. 192



3. John Dalton's Periodic Table (1808 - 36)

In 1803, the English school teacher and part-time scientist, John Dalton published his first list of elements when he printed his atomic theory and his early gas law work. His original list showed only five elements: hydrogen, oxygen, azote (nitrogen), carbon and sulphur along with their atomic weight (Figure 3).

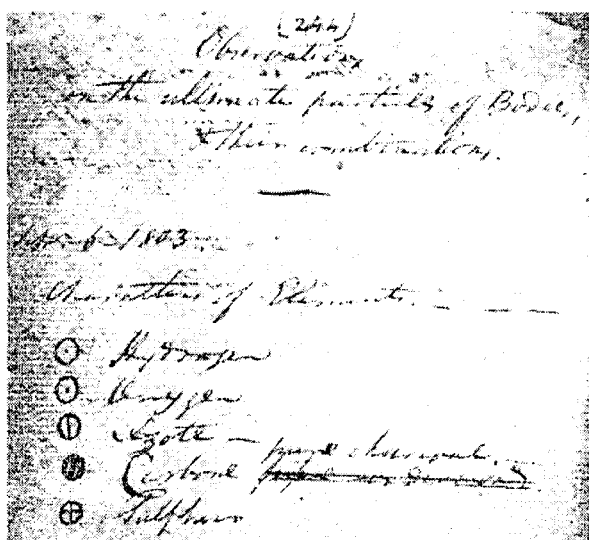
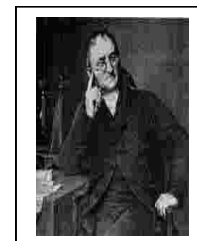


Fig. 3: Dalton's first list of elements published in 1803 contained only five elements.

Latter Dalton attempted to create a system to symbolize the elements, making them easier to write them down quickly. So Dalton's first volume of his second major work was published in 1808, his newest work included more elements and even compounds. (Figure 4)

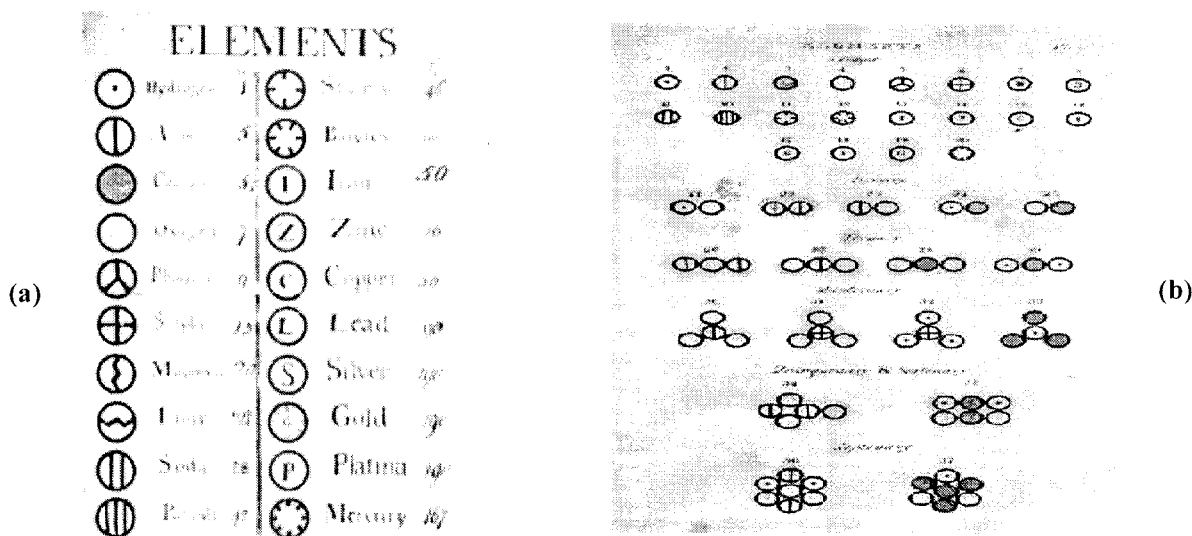


Fig. 4: Dalton's second list of elements (a) with their atomic masses and (b) some combinations of elements

Historical Landmarks in the Development of the Periodic Table

When the second volume of his work came out in 1827, the list of elements had grown to 36 (Figure 5). His symbols may look strange since they were not easy to remember and have not been used since the work was published.





































 Oxygen	 Hydrogen	 Nitrogen (Azote)	 Carbon	 Sulphur	 Phosphorus	 Gold	 Platinum (Platina)	 Silver
 Mercury	 Copper	 Iron	 Nickel	 Tin	 Lead	 Zinc	 Bismuth	 Antimony
 Arsenic	 Calcium (Lime)	 Manganese	 Uranium	 Tungsten	 Titanium	 Cerium	 Potassium (Potash)	 Sodium (Soda)
 Calcium	 Magnesium (Magnesia)	 Barium (Barytes)	 Strontium	 Aluminium	 Silicon	 Yttrium	 Beryllium	 Zirconium

Fig. 5: Second volume of Dalton's work with the list of 36 elements.

However, Dalton's symbols did have some benefits: each symbol represented one atom and the formula of a compound was made up of the symbols of its elements, it showed how many of these atoms were present in the molecule.

4. Jöns Berzelius Periodic Table (1779–1848)

A few years later Dalton's system was superseded with the chemical symbols and formulae by Jöns Berzelius, which are still used today. Berzelius was a Swedish chemist. In 1828 he compiled a table of relative atomic weights, where oxygen was set to 100, and which included all of the elements known at the time. Of significance for the periodic table is that he invented the modern system of chemical notation and established the basic symbols for the elements as used today. In this system elements are given symbols, and compounds represented by combining element symbols and numbers representing proportions. Students working in Berzelius laboratory are credited with discovering lithium, and vanadium. Other elements attributed to Berzelius are silicon, selenium, thorium, and cerium. Together with John Dalton and Antoine Lavoisier he is considered a father of modern chemistry.





Element	Berz. present	Element	Berz. present	Element	Berz. present
Aluminium	Al	Glucinum	Gl Be	Potassium	Po K
Argentum (Silver)	Ag	Hydrargyrum (Mercury)	Hg (Hy) Hg	Rhodium	Rh (R) Rh
Arsenic	As	Hydrogenium	H	Silicium	Si
Aurum (Gold)	Au	Iridium	I Ir	Sodium	So Na
Barium	Ba	Magnesium	Ms Mg	Stibium (Antimony)*	Sb (St) Sb
Bismuth	Bi	Manganese	Ma (Mn) Mn	Strontium	Sr
Boron	B	Molybdenum	Mo	Sulphur	S
Calcium	Ca	Muriatic Radicle	M Cl	Tellurium	Te
Carbon	C	(Chlorine)		Tin	Sn (St) Sn
Cerium	Ce	Nickel	Ni	Titanium	Ti
Chromium	Ch Cr	Nitric Radicle	N	Tungsten	Tn (W) W
Cobalt	Co	Osmium	Os	Uranium	U
Columbium (Cb)	Cl Nb	Oxygenium	O	Yttrium	Y
Cuprum (Copper)	Cu	Palladium	Pa Pd	Zinc	Zn
Ferrum (Iron)	Fe	Phosphorus	P	Zirconium	Zr
Fluoric Radicle	F	Platinum	Pt		
		Plumbum (Lead)	Pb (P) Pb		

5. Johann Döbereiner's Periodic Table (1780–1849)

Döbereiner was a German chemist whose examinations of the correspondence of certain elements prompted the development of the Periodic Table. Because he was a coachman's son, he had a small opportunity, for formal schooling. However, he was apprenticed to an apothecary, read widely, and attended science lectures. Eventually, he was able to attend the University of Jena, where he became assistant professor and later become the supervisor of science institutions. Although he had numerous scientific achievements, he is best known for his contributions to the creation of the Periodic Table. Between 1817 and 1829, he began to group elements with similar properties into groups of three, or triads. This accomplishment initiated when he realized that the atomic weight of Strontium was halfway between the weight of calcium and barium. He also noted that the elements possessed similar chemical properties. Thus, by 1829 he had discovered the halogen triad composed



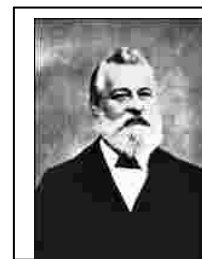
Historical Landmarks in the Development of the Periodic Table

of chlorine, bromine and iodine, and the alkali metal triad of lithium, sodium and potassium. Furthermore, he suggested that nature encompassed triads of elements whereby the middle element has properties that were an average of the other two elements. However, the poor accuracy of measurements, such as atomic weight, hindered the classification of more elements.

Alkali formers		Salt formers	
Li	7	Cl	35.5
Na	23	Br	80
K	39	I	127

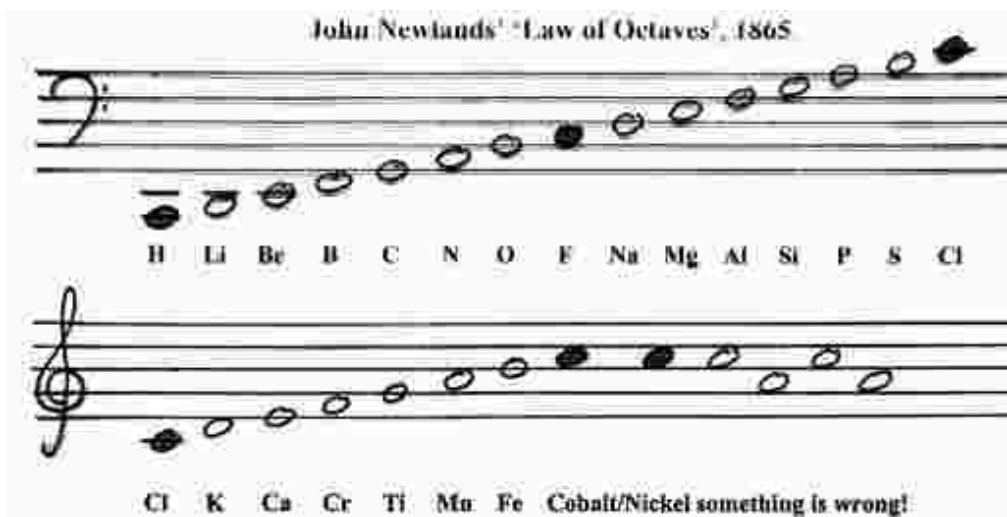
6. Newlands Periodic Table (1837–1898)

Newlands continuing the work of Döbereiner with triads and the work of Jean-Baptiste Dumas families of similar elements, published in 1865 his 'Law of Octaves', an innovative concept proposing the periodicity of the chemical elements arranged in order of atomic weight. He pointed out that every eighth element in this grouping shared a resemblance and suggested an analogy with the intervals of the musical scale. John Newlands put forward his law of octaves in 1864 in which he arranged all the elements known at the time into a table in order of relative atomic mass. When he did this, he found that each element was similar to the element eight places further on. However, this law had some setbacks. For example, he placed iron, a metal, in the same group as oxygen and sulfur, two nonmetals. Additionally, this musical analogy was ridiculed. However, it was found to be profound after the work of Mendeleev and Meyer were published. Newlands was also the first chemist to assign atomic numbers to the element.



Newlands' Octaves (his 'Periodic Table' of 1866)						
H	Li	Ga	B	C	N	O
F	Na	Mg	Al	Si	P	S
Cl	K	Ca	Cr	Ti	Mn	Fe
Co, Ni	Cu	Zn	Y	In	As	Se
Br	Rb	Sr	Ce, La	Zr	Di, Mo	Ro, Ru
Pd	Ag	Cd	U	Sn	Sb	Te
I	Cs	Ba, V	Ta	W	Nb	Au
Pt, Ir	Tl	Pb	Th	Hg	Bi	Th

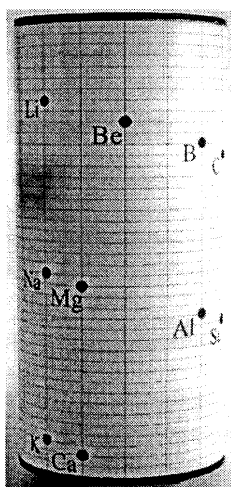
Newlands' Version of the Periodic Table



Newlands' "Law of Octaves"

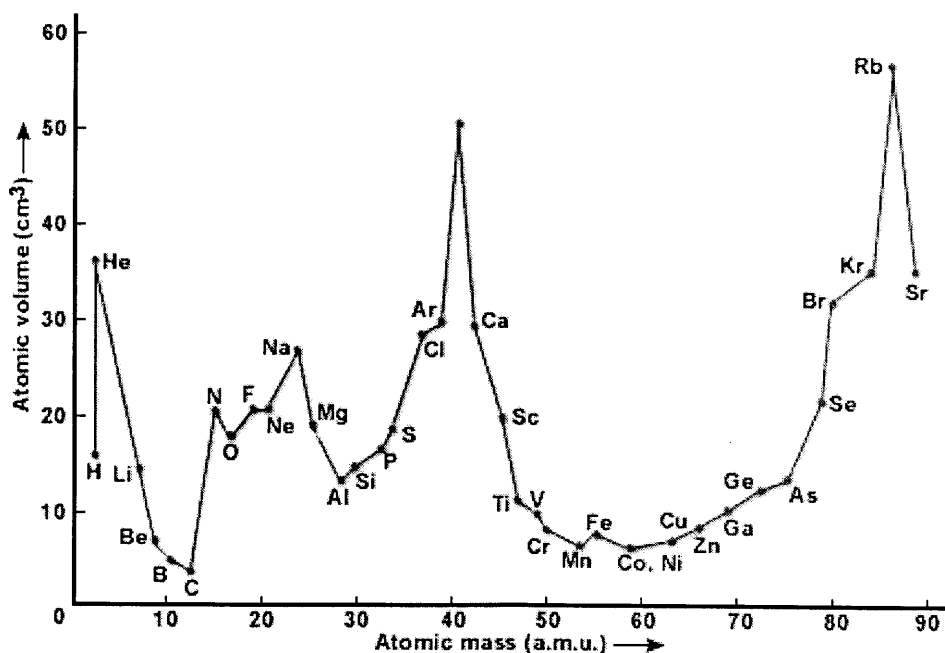
7. de Chancourtois Periodic Table

In 1862, before Newlands announced his Law of Octaves and Mendeleev described his Periodic System, de Chancourtois presented his idea on periodic table before the French Academy of Sciences. de Chancourtois called his idea "vis tellurique" or telluric spiral because the element tellurium came in the middle. It was also somewhat appropriate coming from a geologist as the element tellurium is named after the Earth. He plotted the atomic weights on the outside of a cylinder such that one complete turn corresponded to an atomic weight increase of 16. However, the concept was poorly presented and difficult to understand.



8. Lulius Lothar Meyer Periodic Table (1830-1895)

Meyer was a contemporary of Mendeleev. He qualified in medicine at Zürich, Switzerland, and then studied and taught at various German universities. Though his first interest was physiology, he was primarily interested in Chemistry. Meyer was examining the physical properties of the elements and noticed a periodicity in their molar volume. He independently developed a periodic table based on atomic masses. He found that if the atomic volumes of the elements were plotted against their atomic weight, a series of peaks were produced. The peaks were formed by the alkali metals Sodium, Potassium, Rubidium, and Cesium. Each fall and rise to a peak, corresponded to a period like the waves. In each period a number of physical properties other than atomic volume also fell and rose, such as valence and melting point. Meyer was the first scientist to introduce the concept of valence as a periodic property.



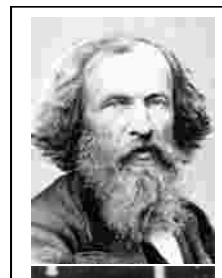
In 1864, Meyer published a preliminary list of 28 elements classified into 6 families by their valence. Then in 1868 he prepared an expanded version, and in 1870 published his list as a table that in many ways was similar to Mendeleev's.

9.0 Mendeleev's Periodic Table (1834-1907)

Dmitri Mendeleev, was a Siberian-born Russian chemist. Mendeleev was investigating the variation



in the chemical properties of the elements and noticed their periodic variation. When his family's glass factory was destroyed by fire, Mendeleev moved to St. Petersburg, Russia, to study science. He became ill and was not expected to recover, but he finished his PhD with the help of his professors and fellow students. He is the best known for his development of the first version of the Periodic Table and utilized it to anticipate the elements yet to be discovered. Legend says that on the night of 17, February 1869, Mendeleev went to bed frustrated because he could not decipher the greatest puzzle of all the Periodic Table. That night, he dreamed of a table where all the elements fell into the correct place. His first Periodic Table arranged the elements in order of increasing atomic mass and grouped them by similarity of properties. When a gap existed in the table, Mendeleev predicted that a new element would one day be discovered and assumed its properties. He arranged the 63 known elements into a Periodic Table and recorded it in his book, Principles of Chemistry, in 1869. Furthermore, Mendeleev revealed that the properties of certain elements were inaccurate. Because the noble gases had not yet been discovered, they were not included in this table.



			Ti = 50	Zr = 90	? = 180
			V = 51	Nb = 94	Ta = 182
			Cr = 52	Mo = 96	W = 186
			Mn = 55	Rb = 104,4	Pt = 197,4
			Fe = 56	Ru = 104,4	Ir = 198
		Ni = 59	Co = 59	Pd = 106,6	Os = 199
			Cu = 63,4	Ag = 108	Hg = 200
H = 1			Zn = 65,2	Cd = 112	
Be = 9,4	Mg = 24		? = 68	Ur = 116	Au = 197?
B = 11	Al = 27,4		? = 70	Sn = 118	
C = 12	Si = 28		As = 75	Sb = 122	Bi = 210?
N = 14	P = 31		Se = 79,4	Te = 128?	
O = 16	S = 32		Br = 80	J = 127	
F = 19	Cl = 35,5		Rb = 85,4	Cs = 133	Tl = 204
Li = 7	Na = 23		K = 39	Ba = 137	Pb = 207
			Ca = 40		
			? = 45		
			Ce = 92		
		?Er = 56	La = 94		
		?Yt = 60	Di = 95		
		?In = 73,6	Th = 118?		

10. Henry Moseley's Periodic Table (1887 - 1915)

Henry Moseley was an English chemist who discovered the application of the X-ray spectra to study atomic structure. He found that the wavelength of an X-ray depended on the nuclear charge of an atom. In 1913, he photographed the X-ray spectrum of 10 elements that held successive places in the Periodic Table. Moseley's discoveries produced a more accurate positioning of the elements in the Periodic



Historical Landmarks in the Development of the Periodic Table

Table – the use of atomic number as the organizing principal for the periods. Argon, for example, although having an atomic mass greater than that of potassium, was placed *before* potassium in the periodic table. While analyzing the frequencies of the emitted x-rays, Moseley noticed that the atomic number of argon is 18, whereas that of potassium is 19, which indicated that they were indeed placed correctly. According to Mendeleev, the elements are arranged on the basis on atomic mass, but this created some setbacks. For example, Iodine has a lower atomic mass then tellurium. Based on the Mendeleev’s Periodic Table, Iodine should come before Tellurium. So, in order to place Iodine in the same group as other elements with similar properties, Mendeleev had to place it after Tellurium, and thus broke his own rules. Moseley’s concept (based on the atomic number) solved the problem faced by Mendeleev’s table. Following is the Moseley’s Periodic Table.

Reihen	Gruppe I. — R ¹ O	Gruppe II. — R ² O	Gruppe III. — R ³ O ³	Gruppe IV. RH ⁴ RO ²	Gruppe V. RH ⁵ R ² O ⁵	Gruppe VI. RH ⁶ RO ³	Gruppe VII. RH R ² O ⁷	Gruppe VIII. — R ³
1	H=1							
2	Li=7	Be=9,4	B=11	C=12	N=14	O=16	F=19	
3	Na=23	Mg=24	Al=27,3	Si=28	P=31	S=32	Cl=35,5	
4	K=39	Ca=40	—=44	Ti=48	V=51	Cr=	Mn=55	Fe=56, Co=59, Ni=59, Cu=63.
5	(Cu=63)	Zn=65	—=68	—=72	As=75	Se=78	Br=80	
6	Rb=85	Sr=87	?Yt=88	Zr=90	Nb=94	Mo=96	—=100	Ru=104, Rh=104, Pd=106, Ag=108.
7	(Ag=108)	Cd=112	In=113	Sn=118	Sb=122	Tc=125	J=127	
8	Cs=133	Ba=137	?Di=138	?Ce=140	—	—	—	—
9	(—)	—	—	—	—	—	—	—
10	—	—	?Er=173	?La=180	Ta=182	W=184	—	Os=195, Ir=197, Pt=198, Au=199.
11	(Au=199)	Hg=200	Tl=204	Pb=207	Bi=208	—	—	—
12	—	—	—	Th=231	—	U=240	—	—

missing elements
 ignore this for now

Moseley’s Periodic Table

Moseley left his research work at the University of Oxford to join the British army as a telecommunications officer during World War I. He was killed during the Battle of Gallipoli in Turkey.

Summary

- Before 1800 (34 elements): discoveries during and before the age of enlightenment.
- 1800-1849 (24 elements): impulse from Scientific Revolution and Atomic theory and Industrial



Revolution.

- 1850-1899 (26 elements): the age of classifying elements; application of spectrum analysis techniques
- 1900-1949 (13 elements): development of old quantum theory and quantum mechanics.
- 1950-1999 (16 elements): “post atomic bomb” era; synthesis of atomic numbers 98 and above
- 2000-present (5 elements): recent synthesis.

The elements in the periodic table are arranged according to their properties, and the periodic table serves as an aid in predicting chemical behavior. The periodic table arranges the elements according to their electron configurations, such that elements in the same column have the same valence electron configurations. Periodic variations in size and chemical properties are important factors in dictating the types of chemical reactions the elements undergo and the kinds of chemical compounds they form. The modern periodic table was based on empirical correlations of properties such as atomic mass; early models using limited data noted the existence of **triads** and **octaves** of elements with similar properties. The periodic table achieved its current form through the work of Dimitri Mendeleev and Julius Lothar Meyer, who both focused on the relationship between atomic mass and chemical properties. Meyer arranged the elements by their atomic volume, which today is equivalent to the **molar volume**, defined as molar mass divided by molar density. The correlation with the electronic structure of atoms was made when H. G. J. Moseley showed that the periodic arrangement of the elements was determined by atomic number, not atomic mass.

Periodic Table of the Elements

Legend: atomic number, symbol, name, atomic mass

Groups: 1 IA, 2 IIA, 3-10 IIIA-VIIIA, 11 IB, 12 IIB, 13-18 IIIA-VIIIA, 19 IA, 20 IIA, 21-28 Sc-Zn, 29-36 Cu-Zn, 37-38 Rb-Sr, 39-40 Y-Ca, 41-48 Sr-Zn, 49-50 Rb-Sr, 51-56 Ba-Lu, 57-71 Lanthanide Series, 72-79 Hf-Ta, 80-86 Rn, 87-88 Fr-Ra, 89-103 Actinide Series, 104-109 Rf-Lu, 110-118 Ds-Og

Categories: Alkali, Alkaline Earth, Transition Metal, Rare Metal, Semimetal, Nonmetal, Halogen, Noble Gas, Lanthanide

Periodic Table now....

Bibliography

1. Scerri E.R. 2006. *The Periodic Table: Its Story and Its Significance*; New York City, New York; Oxford University Press.
2. <http://www.rsc.org/education/teachers/learnnet/periodictable/pre16/develop/mendeleev.htm>
3. <http://allperiodictables.com/ClientPages/AAEpages/aaeHistory.html>
4. https://chem.libretexts.org/Ancillary_Materials/Exemplars_and_Case_Studies/Exemplars/Culture/History_of_the_Periodic_Table
5. [https://chem.libretexts.org/Bookshelves/General_Chemistry/Map%3A_Chemistry__The_Central_Science_\(Brown_et_al.\)/07._Periodic_Properties_of_the_Elements/7.3%3A_Sizes_of_Atoms_and_Ions](https://chem.libretexts.org/Bookshelves/General_Chemistry/Map%3A_Chemistry__The_Central_Science_(Brown_et_al.)/07._Periodic_Properties_of_the_Elements/7.3%3A_Sizes_of_Atoms_and_Ions)
6. http://elements.vanderkrogt.net/chemical_symbols.php
7. <https://corrosion-doctors.org/Periodic/Periodic-de-Chancourtois.htm>
8. <https://corrosion-doctors.org/Periodic/Periodic-Newlands.htm>
9. http://www.newworldencyclopedia.org/entry/History_of_the_periodic_table
10. *Traité Élémentaire de Chimie*, Cuchet, Paris, 1789, p. 192
11. Antoine Lavoisier (1743-1794) from *Elements of Chemistry*
12. *From Alchemy to Chemistry: Five Hundred Years of Rare and Interesting Books*
13. John Dalton (1766-1844): *The Father of the Chemical Atomic Theory*.



Integration of Fundamental Organic Chemistry with Green Chemistry: A Laboratory Manual

Dr Anuradha Mukherjee,
Indian Institute of Science, Bengaluru, India
Narosa Publishing House Pvt. Ltd., New Delhi,
www.narosa.com
ISBN 978-81-8487-644-4
2019, pages 244.

Green Chemistry has acquired great importance in the last few years with its emphasis on the use of environmentally friendly chemical processes involving the use of safe reagents and solvents under ambient conditions of experimentation. Green Chemistry aims at designing processes and products that minimize the use and generation of hazardous substances. Green Chemistry is now an integral component of most college and university curricula and has made inroads into the laboratory. Over the years, there has been an increasing number of publications describing novel experiments based on the principles of Green Chemistry.

Organic Chemistry is essential to all aspects of life and provides us with almost all our requirements- medicines, clothing, polymers, plastics, fertilizers, energy, fuels to name a few. Both Chemistry sub disciplines are intertwined and complement each other.

In this well written book, the author has tried to blend the conceptual understanding of Organic Chemistry with the knowledge of Green Chemistry- indeed a laudable effort!

The first chapter deals with the rules to be meticulously followed to ensure safety in the laboratory. Since, unfortunately safety norms are not followed in most laboratories, this is a must read chapter for students and researchers working in laboratories. Useful instructions have also been given for preparation of laboratory reagents used routinely in experiments. Green Chemistry terms like green solvents, atom economy and E factor have been clearly explained.

The author has discussed in detail the uses and advantages of microwave and sonication techniques vis a vis the conventional techniques of synthesis eg. in the preparation of the pain reliever drug, Ibuprofen.

Some of the topics discussed are :

- 1) Qualitative analysis of Organic compounds which gives an overview of organic functional groups followed by details of tests for nitrogen, sulphur and halogens in organic compounds and finally identification of functional groups.
- 2) Preparation of derivatives and the importance of derivatization in organic synthesis.
- 3) Principles of Thin Layer Chromatography (TLC) and its potential as a separation/purification technique.
- 4) Principles and protocols of the green syntheses of some industrially important compounds like Salicylic acid, Aspirin, Acetanilide, Benzocaine, Benzhydrol, Cyclohexanone (precursor of Nylon -6) and Methyl Orange dye.

An exhaustive list of references has been given at the end of the book which includes some latest references. At the end of each chapter, several multiple choice questions, long questions and problems have been given to enable students to reinforce their learning and understanding of the subject.

The author has taken great efforts to bring out this excellent book which amalgamates Organic Chemistry synthesis with the principles of Green Chemistry. I recommend the book to students, researchers and teachers engaged in synthesis of organic compounds and I am sure it will be beneficial to them. The book is indeed a welcome addition to the available literature on the subject of Green Chemistry.

Dr D V Prabhu
Editor in Chief,
GP Globalize Research Journal of Chemistry,
ISSN 2581 5911



Conference Alerts

- 1) International Congress on Catalysis and Chemical Science (Catalysis 2019),
March 11-13, 2019, Singapore
Website: <http://catalysiscongress.com>
- 2) 3rd Ocean, Marine and Environmental Science International Conference 2019,
March 15-17, 2019, Krabi, Thailand
Website: <http://omesic.weebly.com>
- 3) 4th International Conference on Materials Chemistry and Science,
March 18-19, 2019, Singapore City, Singapore
Enquiries: materialschemistry@annualmeetings.net
- 4) Global Chemistry and Expo2019,
March 25-27, 2019, Valencia, Spain
Website: <http://www.chemistryconference.linkinscience.com>
- 5) International Conference on Advances in Engineering, Technology and Chemical Science 2019,
March 29-30, 2019, Bangkok, Thailand
Website : <https://www.imrfedu.org/etcthailand>
- 6) 2nd Hatyai International Conference on Chemistry and Chemical Engineering 2019, (HaICCCE 2019),
April 2-3, 2019, Hatyai, Thailand
Website :<https://haicce2019.weebly.com>
- 7) 5th International Mediterranean Symposium on Medicinal and Aromatic Plants (MESMAP-5),
April 24-28, 2019, Cappadocia, Turkey
Website: <http://www.mesmap.com>
- 8) 4th Green and Sustainable Chemistry Conference,
May 5-8, 2019, Dresden, Germany
Website: <http://www.elsevier.com/events/conferences/green-and-sustainable-chemistry-conference/register>
Enquiries: conferences@mail.elsevier.com
- 9) 4th Edition of International Conference on Catalysis and Green Chemistry,
May 13-14, 2019, Tokyo, Japan
Website: <https://catalysis-conferences.com/>
Enquiries: greenchemistry@magnusmeetings.com
- 10) 2nd Molecular Medicinal Chemistry Symposium-Facing novel challenges in Drug Discovery,
May 15-17, 2019, Barcelona, Spain
Website: <http://mmcs2019.sciform.net/>

-
- 11) 2nd International Conference on Pharmaceutical Science,
May 20-21, 2019, Colombo, Sri Lanka
Website: <http://healthconference.science/pharmaceutical/>

 - 12) 6th World Congress on Natural Product and Synthetic Chemistry,
June 24-25, 2019, New York, USA
Enquiries: syntheticchemistry@insightssummits.com

 - 13) International Conference on Science and Technology Research (3rd ICSTR Singapore)
June 28-29, 2019, Singapore
Organised by Scientific and Technical Research Association (STRA)
Websites : <http://eurasiaresearch.org/contactus>
<http://straweb.org>
Enquiries: convenor@eurasiaresearch.info



ORDER FORM

I/We wish to subscribe to **G P Globalize Research Journal of Chemistry**
(Please fill in the form in **BLOCK** Letters).

Name:.....

Address:.....

.....

.....

.....Pin code:.....

Tel No:.....Email:.....

DD No.Dated.....Amount.....(a)

For Online payment:

Name of the Bank: Axis Bank

Branch Name: Tardeo, Mumbai (MH)

Account No. 916020066451552

IFSC Code: UTIB0001345

Note :

All Payments by Bank Draft/Multicity Cheque (please add a 75/- for outstation cheque) should be drawn in favour of **“Gaurang Publishing Globalize Pvt. Ltd.”** payable at Mumbai.

RNI No. MAHENG/2017/74063
ISSN No. 2581-5911



Send your orders to - - - - -

Gaurang Publishing Globalize Private Limited

1, Plot 72, Pandit Madan Mohan Malviya Marg,

Tardeo, Mumbai-400034, India

● Mobile: 9969 392 245 ● E-mail: gpglobalize@gmail.com



RNI - No. MAHENG/2017/74063

ISSN NO 2581-5911

G P GLOBALIZE RESEARCH JOURNAL OF CHEMISTRY

VOLUME 2 (Issue 2) January - June 2019

BI-ANNUAL 2019

**Abstracted in Chemical Abstracts (CAS), USA
International Scientific Indexing (ISI)
Impact Factor 0.883 (2018)**

CIN U22130MH2016PTC287238

UAN- MH19D0008178



GAURANG PUBLISHING GLOBALIZE PVT. LTD

1,PLOT-72, P. M. M. M. MARG,
TARDEO, MUMBAI-400034.

TEL. 022 23522068 (M) : +91 9969392245

Email : gpglobalize@gmail.com / publish@gpglobalize.com

Web : www.gpglobalize.com